NASA/CR—2001-211322

Exoskeletal Engine Concept: Feasibility Studies for Medium and Small Thrust Engines

Ian Halliwell
Modern Technologies Corporation, Middleburg Heights, Ohio

November 2001

The NASA STI Program Office . . . in Profile

Since its founding, NASA has been dedicated to the advancement of aeronautics and space science. The NASA Scientific and Technical Information (STI) Program Office plays a key part in helping NASA maintain this important role.

The NASA STI Program Office is operated by Langley Research Center, the Lead Center for NASA's scientific and technical information. The NASA STI Program Office provides access to the NASA STI Database, the largest collection of aeronautical and space science STI in the world. The Program Office is also NASA's institutional mechanism for disseminating the results of its research and development activities. These results are published by NASA in the NASA STI Report Series, which includes the following report types:

- TECHNICAL PUBLICATION. Reports of completed research or a major significant phase of research that present the results of NASA programs and include extensive data or theoretical analysis. Includes compilations of significant scientific and technical data and information deemed to be of continuing reference value. NASA's counterpart of peer-reviewed formal professional papers but has less stringent limitations on manuscript length and extent of graphic presentations.

- TECHNICAL MEMORANDUM. Scientific and technical findings that are preliminary or of specialized interest, e.g., quick release reports, working papers, and bibliographies that contain minimal annotation. Does not contain extensive analysis.

- CONTRACTOR REPORT. Scientific and technical findings by NASA-sponsored contractors and grantees.

- CONFERENCE PUBLICATION. Collected papers from scientific and technical conferences, symposia, seminars, or other meetings sponsored or cosponsored by NASA.

- SPECIAL PUBLICATION. Scientific, technical, or historical information from NASA programs, projects, and missions, often concerned with subjects having substantial public interest.

- TECHNICAL TRANSLATION. English-language translations of foreign scientific and technical material pertinent to NASA's mission.

Specialized services that complement the STI Program Office's diverse offerings include creating custom thesauri, building customized data bases, organizing and publishing research results . . . even providing videos.

For more information about the NASA STI Program Office, see the following:

- Access the NASA STI Program Home Page at ***http://www.sti.nasa.gov***

- E-mail your question via the Internet to help@sti.nasa.gov

- Fax your question to the NASA Access Help Desk at 301–621–0134

- Telephone the NASA Access Help Desk at 301–621–0390

- Write to:
  NASA Access Help Desk
  NASA Center for AeroSpace Information
  7121 Standard Drive
  Hanover, MD 21076

NASA/CR—2001-211322

Exoskeletal Engine Concept: Feasibility Studies for Medium and Small Thrust Engines

Ian Halliwell
Modern Technologies Corporation, Middleburg Heights, Ohio

Prepared under Contract NAS3–27326

National Aeronautics and
Space Administration

Glenn Research Center

November 2001

Available from

NASA Center for Aerospace Information
7121 Standard Drive
Hanover, MD 21076

National Technical Information Service
5285 Port Royal Road
Springfield, VA 22100

Available electronically at http://gltrs.grc.nasa.gov/GLTRS

General Summary

Since its advent, some 60 years ago, the history of the gas turbine engine has been marked by steady improvements in cycle temperatures, overall pressure ratios, reduced parts counts, thrust/weight ratio, reliability, and any number of other features by which performance may be characterized. In recent times, however, the search for improvement has become increasingly more difficult as "conventional" technologies have approached their limits. In the interests of progress, there is a clear need for a radical new approach with more scope for application of technological ingenuity. The exoskeletal engine concept is one in which the shafts and disks are eliminated and are replaced by rotating casings that support the blades in spanwise compression. Omission of the shafts and disks leads to an open channel at the engine centerline. This has immense potential for reduced jet noise and for the accommodation of an alternative form of thruster for use in a combined cycle. The use of ceramic composite materials has the potential for significantly reduced weight as well as higher working temperatures without cooling air. The exoskeletal configuration is also a natural stepping-stone to complete counter-rotating turbomachinery. Ultimately this will lead to reductions in weight, length, parts-count and improved efficiency.

Before quantitative estimates can be made of the potential improvements and advantages to specific missions, feasibility of the basic concept must be established and fundamental design rules must be determined. These issues have been the focus of the efforts described in the following document - a combination of two intermediate reports issued under the contract.

An initial feasibility study of the exoskeletal engine concept was carried out from May to December 1999, with funding from the NASA Glenn Research Center, under Contract *NAS3-27326*. A first intermediate report, entitled "*Part I – Systems & Component Requirements*", addressed the mechanical aspects of components from a functionality perspective. This effort laid the groundwork for preliminary design studies. Although important, it is not felt to be particularly original, and has therefore not been included in the current overview. Subsequent objectives were to examine some of the cycle and performance issues inherent in an exoskeletal configuration, and to identify areas of potential difficulty in the preliminary design of turbomachinery. These aims were addressed in "*Part 2"* of the program, and the relevant report appears in tact as the first portion of the current document. The program was extended to February 2001 and additional preliminary design studies were carried out. The results of that work were presented as "*Part 3*" of the program and that report makes up the remainder of the current combined document.

"*Part 2 – Preliminary Design Studies"* turned to some of the cycle and performance issues inherent in an exoskeletal configuration and some initial attempts at preliminary design of turbomachinery were described. Twin-spool and single-spool 25,800-lbf-thrust turbofans were used as reference vehicles in the mid-size commercial subsonic category in addition to a single-spool 5,000-lbf-thrust turbofan that represented a general aviation application. The exoskeletal engine, with its open centerline, has tremendous potential

for noise suppression and some preliminary analysis was done which began to quantify the benefits.

"*Part 3 – Additional Preliminary Design Studies*" revisited the design of single-spool 25,800-lbf-thrust turbofan configurations, but in addition to the original FPR = 1.6 & BPR = 5.1 reference engine, two additional configurations using FPR = 2.4 & BPR = 3.0 and FPR = 3.2 & BPR = 2.0 were investigated. The single-spool 5,000-lbf-thrust turbofan was refined and the small engine study was extended to include a 2,000-lbf-thrust turbojet. More attention was paid to optimizing the turbomachinery. Turbine cooling flows were eliminated, in keeping with the use of uncooled CMC materials in exoskeletal engines. The turbine performance parameters moved much closer to the nominal target values, demonstrating the great benefits to the cycle of uncooled turbines.

Conventional methods for stacking blade sections may need to be modified significantly because of the need to support the blades at the tips. This leads naturally to the consideration of vaneless counter-rotating turbomachinery, which is extremely attractive in exoskeletal systems. This concept offers a reduced parts-count, reduced length, reduced weight, a reduction in the loss sources of about 40% by elimination of the vanes, and "balanced" rotation within an engine.

Ian Halliwell
Modern Technologies Corporation
e-mail: ihalliwell_mtc@core.com
July 2001.

Preliminary Design Studies

Summary

This document is the second in a series of two reports describing a feasibility study of an exoskeletal engine concept. The work was carried out from May to December 1999, with funding from the NASA Glenn Research Center, under Contract *NAS3-27326*. The first report addressed the mechanical aspects of components from a functionality perspective. The objectives of the current phase of the work were to examine some of the cycle and performance issues inherent in an exoskeletal configuration, and to identify areas of potential difficulty in the preliminary design of turbomachinery.

Twin-spool and single-spool turbofan configurations producing 25,000-lbf thrust, were used as reference vehicles in the mid-size commercial subsonic category. A single-spool turbofan producing 5,000-lbf of thrust was also examined to represent a general aviation application. The design studies were only cursory examinations of the technical environment, the results were not optimized, and no quantitative conclusions were intended. Rather, the objectives were to indicate technical directions where solutions may lie and to estimate the degree of difficulty of some of the key issues.

No real problems have appeared. The performance targets proved challenging but accessible, with several aspects of turbomachinery design being of particular interest.

- Fan construction and the means of power transfer from the turbine are of obvious special relevance in an exoskeletal engine.
- Radius ratio could become especially important, particularly in the core components, depending on the area of the open centerline.
- Rotational speed is also a critical issue, particularly in a single spool configuration, where a degree of freedom is sacrificed in design and engine operation.
- It is recommended that design guidelines be established for the exoskeletal engine concept before it is applied to particular missions.

It is important to realize that these topics do not represent insurmountable obstacles but interesting technical challenges, typical of those encountered during any new engineering enterprise.

With regard to noise[1], the exhaust nozzle of the exoskeletal engine, with its open centerline, constitutes a special type of inverted velocity profile. This has tremendous potential for noise suppression and some preliminary analysis has been done which begins to quantify the benefits.

Ian Halliwell
Modern Technologies Corporation
Tel: (440) 243 8488
E-mail: *ihalliwell_mtc@stratos.net*

[1] The development of the noise prediction code, the acoustics analysis of the open centerline flow, and the results presented in *Section 8*, were all done at MTC by Jim Stone.

Contents

1. Introduction

This document is the second in a series of two reports describing a feasibility study of an exoskeletal engine concept. The first report (*Reference 1*) contains an overview of the system and component requirements, based on an examination of the functions of the relevant assemblies in current subsonic commercial engines. In *Reference 1*, the emphasis is mainly on structural features, mechanical characteristics, and construction, since it is those that specifically determine engine feasibility, as distinct from its level of performance. (i.e. "Will it work at all?", rather than "for how long?" or "how well?") Performance is determined generally by internal and external aerodynamics, and although below structural integrity on a list of priorities, it is still very important and cannot be neglected in a program to develop a marketable exoskeletal gas turbine engine. This report covers some limited preliminary design work whose objectives were firstly, to investigate engine cycles and performance characteristics for the exoskeletal concept, and secondly, to explore some of the potential difficulties likely to be encountered in the design of the engine flowpath, especially the turbomachinery.

A typical design process for a gas turbine engine is laid out in *Figure 1*, taken from *Reference 2*, with conceptual/preliminary design activities being largely confined to the boxes designated "*MISSION*", "*CYCLE*", and "*CONFIGURATION*". The thrust requirements for various segments of the aircraft mission are determined in the mission analysis, based on limited assumptions of aircraft characteristics. Cycle analysis is then carried out for each possible engine configuration, using target values of component efficiencies. This produces vast tables of thermodynamic data, containing mass flow rates and gas properties throughout the engine at each mission point. It is the task of the flowpath designer to turn the thermodynamic tables into hardware, and this occurs within the "*CONFIGURATION*" box in *Figure 1*. Here it is necessary to demonstrate the ability to design and integrate all of the components. This work also provides the first glimpse of engine layout, size and weight.

Figure 2 is a somewhat closer examination of the preliminary design process for the engine configuration. The use of take-off conditions to design a whole engine results in a solution which is non-optimum, and it is often appropriate to select an individual design point for each component or assembly (*Reference 3*). An engine is assembled from a library of generic component models, mainly characterized by non-dimensional parameters, and exemplified by the list on the left of *Figure 2*. The components are scaled according to the mass flow rates from the cycle data, and geometric continuity is also effected. As the internal features of the component models are manipulated, it is essential to ensure that the values of efficiency assumed in the cycle are at least maintained, and appropriate performance codes must be incorporated in the design process for this reason. The skill of the engine designer is tested, not only in the design and assembly of the components, but in doing so under a number of design constraints. Examples of design constraints are given in the box on the right of *Figure 2*. The constraints are both internal, such as limits on Mach numbers and stage loading coefficients, and external, such as those imposed by the FAA regarding noise and emissions. In order to be competitive, a new engine must approach the design limits in

almost all branches of technology, including aerodynamics, thermodynamics, structures, and materials. The risks are usually very high because engines are extremely complex, and the interactions between all of the above technologies preclude the possibility of anticipating completely how the system will behave. However, the level of risk may be reduced by the quality of the preliminary design work and the reliability of the results.

One obvious special feature of the exoskeletal engine is the air stream through the free centerline. This additional flow offers considerable potential for noise attenuation, and has also been investigated briefly. The results and the method of analysis are presented and discussed below in *Section 8*.

2. Approach

2.1 Engine Cycle

Early in the program it was noted that the exoskeletal engine should be comparable in weight and performance with current powerplants. Even though this objective may be rather ambitious for purposes of demonstrating feasibility, it is still quite relevant and indeed necessary, as a target for any subsequent development program. A mid-size subsonic commercial application was selected as a medium for the present feasibility study, and in order to expedite the exercise, the results of mission and cycle analyses done by the Propulsion Systems Analysis Office at the NASA Glenn Research Center were used as a starting point. This is subsequently termed *the reference engine*.

The available results constituted a model of a high bypass ratio turbofan engine for a 150-passenger commercial aircraft, cruising at Mach 0.8 and an altitude of 43,000 feet. An additional advantage was that these results were based on reasonable assumptions of typical airplane characteristics. Output from the *NEPP* cycle code provided a complete range of mission points, with gas properties, thrust levels, fuel flow rates, bypass ratios, PR splits, component efficiencies, mass flow rates, etc. This information was used both as input for our cycle spreadsheet calculations and as a check on the results. Output from the NASA *WATE* code provided component weights and dimensions for comparison purposes. Net take-off thrust for this reference engine was 25,800-lbf.

A small-scale exoskeletal engine was also considered. This was sized at a net take-off thrust of 5,000-lbf, using the same cycle spreadsheet as for the mid-size engine with values of design parameters and efficiencies typical of small engine components.

2.2 Flowpath/turbomachinery

Since the turbomachinery constitutes the working parts of any engine, it deserves special consideration, especially in regard to some of the potential difficulties posed by the exoskeletal concept. The main objective is to determine such characteristics as numbers

of stages, possible rotational speeds, compatibility between fan/compressor and turbine(s), approximate sizes, and continuity of the gas path. A secondary objective is the verification of approximate levels of efficiency.

An MTC derivative (*CDE – Compressor Design Envelopes*) of the NASA code *CSPAN* was used for the preliminary design of fans and compressors.

> *CSPAN* is a spanline analysis code that uses isentropic simple radial equilibrium to determine a compressor flowpath and its efficiency either for a given number of stages or for a given overall pressure ratio. ***CDE*** contains the design routines for axial-flow compressors and associated performance models for efficiency and stall margin. It runs on a PC under Windows 95 et seq. There is a single calculation station between blade rows. Hub radius is determined from the inlet radius ratio and the input tip radius distribution and this feature simplifies the continuity solution. The addition of energy to the stage is controlled by specification of maximum allowable values for several aerodynamic design parameters: rotor-tip and stator-hub diffusion factors, rotor-hub turning, and stator-inlet-hub Mach number. There are two internal loss models: (1) stage and rotor polytropic efficiencies as functions of stage pressure ratio, and (2) blade-row pressure-loss coefficients as a function of meanline diffusion, tip clearance, and shocks. Correlations are included for the calculation of endwall blockage (optional) and for the prediction of stall margin.
>
> *CSPAN* input includes the design requirements of flow rate and overall pressure ratio (or maximum number of stages). First-rotor tip speed, inlet radius ratio, tip-diameter variation, and aerodynamic design limits can be fixed or varied for parametric studies. Default values are available for the aerodynamic variables, as well as for geometric descriptors such as solidities, aspect ratios, and stage reaction distribution. The output includes the hub radii, velocity diagrams, a summary of blading geometry, stage and overall efficiencies, and stall margin.
>
> For the generation of design envelopes, *CDE* is run four times for combinations of two values of two basic design variables. However, the program has an option to run a single design case, and it was this mode that was used for the present exercise. A description of *CDE* is given in Reference 4.

The MTC code *TDE (Turbine Design Envelopes)* was used for the preliminary design of turbines.

> *TDE* contains the design routines for axial-flow turbines and an associated performance model. It also runs on a PC under *Windows 95 et seq*. The starting point for its application is a definition of the turbine inlet conditions and the overall work requirement, along with the number of stages and the desired work split. Minimal geometric input is required, since the general pitch of the turbine is

set via the first stage loading coefficient and the rotational design speed. The exit area is obtained from the design limit value on AN^2. The internal details are dependent on a number of generic, mostly non-dimensional, input parameters. The turbine performance is predicted from a loss model that considers the components of total pressure loss due to airfoil profile, secondary flows, trailing edge blockage, and tip clearance. The performance model is based largely on that of *Ainley & Mathieson* with up-dates from *Kacker & Okapuu*. Details are available in *Reference 5*.

3. Mid Size Engines: Cycle Studies

Using take-off conditions as the design point for the whole engine (despite the reservations expressed above!), the spreadsheet cycle routine was used to investigate possible exoskeletal configurations at this size. Matrices were run for single-spool and twin-spool designs for various combinations of fan pressure ratio (from 1.6 to 2.4) and bypass ratio (from 1 to 8), holding the overall pressure ratio at 27.45, the turbine rotor entry temperature at 2960 °R, and the net thrust at 25,800-lbf.

Values of adiabatic efficiency assumed for the various components in the cycle calculations are shown below in *Table 1*.

Parameter	Single-Spool	Twin-Spool
$\eta_{AD\ FAN}$	88.5%	88.4%
$\eta_{AD\ BOOSTER}$	85.1%	89.4%
$\eta_{AD\ HPC}$	-	87.1%
η_{COMB}	99.5%	99.5%
$\eta_{AD\ HPT}$	-	92.9%
$\eta_{AD\ LPT}$	94.2%	93.4%

Table 1. Assumed Adiabatic Efficiencies for Components in the Reference Mid-Size Engine

The values are similar to those from the reference engine cited in *Section 2.1*. It should be noted that the cycle calculations and results are identical to those for a conventional turbofan engine, since the means by which the thermodynamic conditions are generated are largely irrelevant at this stage of the work. It should also be noted that in the current

cycle calculations, the fan flow is stratified; that is, the bypass and core streams are considered separately. One implication of this is that for a single spool engine the pressure ratio through the fan hub is combined with that through the booster to give a booster pressure ratio that is identical to the overall value. Slight variations in the values of efficiency, combined with similar variations in component pressure ratios, ensure that identical values of total temperature and pressure are achieved at compressor delivery. The input variations also account for the duct losses between the booster and HP compressor in the twin-spool case.

The results discussed below are for separate bypass and core exhaust streams. The effect of mixing was investigated, and resulted in very little improvement in either engine size or performance. Thermodynamically, this is no surprise, but it should be noted that the associated penalty in terms of weight and nozzle complexity cannot be accounted for in the cycle studies.

3.1 Single Spool

For a single spool turbofan engine at constant thrust, the effects on fuel consumption of varying the bypass ratio and fan pressure ratio are shown in *Figure 3*. This is a very common scenario, demonstrated in many text books, but our interest lies mainly in the fact that the exoskeletal concept especially lends itself to a single spool configuration – an arrangement not often addressed in a turbofan. It is necessary, therefore, to ascertain whether or not there are significant differences between single and two-spool designs.

Figure 3 shows that increasing the bypass ratio has a very beneficial effect on fuel burn, especially near the lower end of the range considered. In contrast, raising the fan pressure ratio has much less of an influence, and the selection of a design value must depend on other criteria. The option of increasing bypass ratio by reducing the size of the engine core is available only if the turbine entry temperature can be increased. This alternative would rely on the use of materials significantly superior to those that exist currently. The benefits of higher bypass ratio do not come without a price, however, and the trade-off is illustrated in *Figure 4*. There, it may be seen that to maintain the required thrust, as bypass ratio is raised, the overall flow rate into the engine increases in almost a linear fashion. This means that the size and weight of the engine must increase correspondingly. For each value of fan pressure ratio in *Figure 4*, there is a limiting value of bypass ratio, above which a design solution is not possible. This because the flow through the engine core, from which power is extracted to drive the fan via the turbine, simply runs out of energy! This phenomenon causes a reduction in the core exhaust velocity as the bypass ratio limit is approached, resulting in more flow being needed to maintain the thrust. The up-sweep of the constant fan pressure lines in *Figure 4* is also a manifestation of this, as is the leveling out of the curves in *Figure 3*.

3.2 Twin Spool

The behavior of a twin-spool turbofan, as bypass ratio and fan pressure ratio are increased, is essentially the same as for a single spool device. This is shown in *Figures 5* and *6*. On the face of it, the twin spool design is not quite as good, probably because of the additional duct losses between the compressor elements. However, the operability of the single spool, exoskeletal engine - needed to make it competitive with a conventional turbofan - must still be demonstrated!

4. Mid Size, Single Spool Turbomachinery

A bypass ratio of 5.1 was selected for design of the fan, compressor and turbine. It is no coincidence that this is the same as that of the NASA reference engine in *Section 2.1*. In order to design the turbomachinery, it is necessary to have an engine layout in mind. One possible configuration for a two-spool system is shown in *Figure 7*, which is a combination of *Figures 3* and *4* from *Reference 1*. This layout is based on the mass flow rates from the NASA reference engine, and it serves chiefly to define the inlet radii and radius ratios in the case of a single spool design. Axial dimensions are approximate and more accurate values for single spool components will be derived from the preliminary design process outlined below. Some relevant cycle parameters for the compression process are given in *Table 2*.

Parameter	Fan Bypass Stream	Core Compressor
Mass flow rate (lbm/s)	654.64	128.36
Entry temperature (°R)	518.7	518.7
Entry pressure (psi)	14.7	14.7
Pressure ratio	1.6	27.17
Adiabatic efficiency	89.23 %	90.13 %
Inlet radius ratio	0.5938	0.80

Table 2. Fan and Compressor Design Parameters in a Mid-Size, Single Spool Exoskeletal Engine

Since the cycle analysis has considered a stratified flow through the fan, and the exoskeletal configuration lends itself readily to a similar treatment, it is convenient to address the fan bypass flow separately from the fan hub flow. This is combined with the remainder of the core compression system to produce the overall pressure ratio of 27.17. Note that differences exist between values of overall pressure ratios for the single and twin spool engines because of pressure losses between the components in the latter and also because of minor variations in component efficiencies.

After some iteration, an inlet radius ratio of 0.80 was selected for the core compressor. The bypass ratio of 5.1 then resulted in a value of 0.5938 for the inlet radius ratio of the core compressor. In combination, they corresponded to a fan tip radius of 33.22 inches, which matched the value from the reference engine reasonably well. The values of the design parameters from *Table 2* were used as input to *CSPAN* for the fan bypass stream and the core compressor, respectively, together with a few other basic inputs. A number of *CSPAN* internal defaults were accepted for simplicity.

The fan flowpath from *CSPAN* is shown in *Figure 8*, where it has been combined with an outline of the core compressor. Clearly, the means of accommodating the fan exit (or outlet) guide vane in the exoskeletal system needs to be addressed. However the reduction in swirl will result in lower losses in the bypass duct and improved engine performance, so the presence of the OGV is undoubtedly beneficial. A few general characteristics of the fan are given in *Table 3*.

Parameter	**Value**
Inlet radius ratio	0.5938
Rotational speed (rpm)	6,000
Specific flow rate (lbm/s/ft^2)	42.0
Tip speed (ft/s)	1739.38
Relative Mach number at blade tip	1.733
Stall margin (%)	32.76
Adiabatic efficiency (%)	74.58

Table 3. Fan (Bypass Stream) Characteristics in a Mid-Size, Single Spool Exoskeletal Engine

The value of the fan tip speed is of great interest, and is quite high. It has occurred because of the need to maintain a high rpm for the engine core. Its implications can be

evaluated better from the corresponding value of Mach number, which tells us immediately that shock losses are likely to be excessive. This is confirmed in the value of adiabatic efficiency, which, at 74.58%, falls far short of the 88.5% assumed in the cycle calculations (*Table 1*). The stall margin is much better than required, due primarily to the high blade speed. This means that while blade speed is beneficial in terms of stall margin, it is quite damaging in terms of efficiency, and a better balance needs to be struck! It is felt that *CSPAN* is capable of producing a better fan solution, with a little more work. Some of the geometric features of the current solution are listed in *Table 4*.

Parameter	**Blade**	**Vane**
Number of airfoils	33	64
Solidity	1.5665 (tip)	1.6895 (hub)
Aspect ratio	4.00	2.50
Hub slope	30.0°	9.85°

Table 4. Fan (Bypass Stream) Blade & Vane Characteristics in a Mid-Size, Single Spool Exoskeletal Engine

Some immediate thoughts on fan and compressor design occur in regard to radius ratio. The value used currently for the fan is fairly close to those used for conventional engines. This was done with the intention of minimizing the overall radial dimension. This is a valid approach if drag reduction at cruise speeds is an over-riding objective. It also is consistent with the achievement of minimum weight *in a conventional engine*, where the disk size predominates. For an exoskeletal configuration, disk weight is of course irrelevant, and so while large radii are still to be avoided for drag reasons, it is quite possible that optimum design solutions will be discovered outside of the normal design envelope. In particular, as we are now realizing, higher radius ratios are needed for both bypass and core streams in order to eliminate the huge performance gap between them. Traditional limitations on radius ratio should be discarded until new design guidelines can be established for exoskeletal engine applications. The new rules will be empirical, and will crystallize from a database resulting from a well-planned and executed series of preliminary design studies.

A more detailed flowpath for the core compressor with all its stages, also from *CSPAN*, is shown in *Figure 9*. Some overall characteristics are given in *Table 5*.

Parameter	Value
Inlet radius ratio	0.80
Rotational speed (rpm)	6,000
Specific flow rate (lbm/s/ft^2)	42.0
Number of stages	20
Tip speed (ft/s)	1032.86
Exit hub speed (ft/s)	1014.12
Exit radius ratio	0.98
Stall margin (%)	13.05
Adiabatic efficiency (%)	81.46

Table 5. Overall Characteristics for the Core Compressor in a Mid-Size, Single Spool Exoskeletal Engine

Both *Figure 9* and *Table 5* indicate that 20 compressor stages are needed to produce an overall core pressure ratio of 27.17 at the rotational speed of 6000 rpm and selected inlet radius ratio of 0.8. The choice of constant tip radius is deliberate, since this raises the average blade speed and minimizes the number of stages. A constant tip radius design also results in a very high exit radius ratio of 0.98, which corresponds to an exit Mach number of 0.36, with zero swirl. This means that the blade spans in the later stages will be extremely small. A conventional upper limit on exit radius ratio is about 0.93, and this value is normally inferred by the ability to hold manufacturing tolerances on airfoils in very large engines. Some relief could be sought in a design with either a constant mean or hub radius ratio, but this would then lead to an increase in the number of stages or a reduction in stall margin. However, the stall margin is already insufficient, evident in the value of 13.05 % in *Table 5*, since 20% would typically be mandated. These results cause the feelings expressed above regarding radius ratio to be echoed. It is possible that the original conceptual drawings of the exoskeletal engine are right on the money (See *Figure 2* of *Reference 1*), and compared with conventional engines, the radius ratios of exoskeletal systems will need to be very high! This argument applies even more so, if single spool systems are to become serious contenders.

The turbine flowpath from the *TDE* design code is presented in *Figure 10* and some characteristics of the turbine are given in *Table 6*.

Parameter	Value
Number of stages	7
Rotational speed (rpm)	6,000
Mass flow rate at entry to first vane (lbm/s)	105.12
Δh per stage (Btu/lbm)	48.6
Stage 1 $\Delta h/T$	0.016
Inlet flow function ($W\sqrt{T}/P$)	14.99
Stage 1 loading coefficient – ($\Delta h/2U_m^2$)	0.6973
AN^2	18×10^9
Exit Mach number	0.46
Exit swirl angle (°)	23.6
Exit radius ratio	0.72
Overall pressure ratio	13.079
Overall adiabatic efficiency (%)	93.46

Table 6. Overall Characteristics for the Turbine in a Mid-Size, Single Spool Exoskeletal Engine

The turbine design code was run by setting the work extraction equal to that in the cycle analysis of the reference engine. The temperature at entry to the first rotor blade (T_{41}) was duplicated by setting the mass flow rate at first nozzle inlet so that the addition of nozzle cooling flow, at an appropriate temperature, would produce the desired result. The cooling flow temperature was derived iteratively.

Seven turbine stages have been used to extract work from the engine core flow at a rate of 42,176 Btu/s, the total power needed to drive the fan and the core compressor. The mass flow rate shown in *Table 6* (105.12 lbm/s) is that entering the vane of the first turbine stage, when cooling flow extraction from the compressor and fuel addition to the combustor are accounted for. (It is realized that, eventually, cooling flow may not be required in the exoskeletal engine, but at this juncture it is convenient to maintain the

same flow rates as in the reference engine cycle.) With cooling flows added, the mass flow rate at the leading edge of the first stage blade, where work extraction begins, is 124.04 lbm/s. The inlet area was input as 70.0 in^2, resulting in an inlet Mach number at the prevailing conditions of 0.254 with zero swirl. The work was distributed equally between the stages, and in order to set the inlet radius somewhere close to that of the compressor exit, the first stage loading coefficient was input as 0.6973. Variation of flow area through the turbine is determined by interpolation between inlet and exit areas. The exit area is defined indirectly via an input value of AN^2, where A is the exit area in square inches and N is the maximum rotational speed in rpm. This is both convenient and useful for a conventional turbine, because AN^2 is a measure of the rim stress in the last turbine disk and provides a strong link between the aerodynamics and the structural design (See *Reference 6*). In an exoskeletal design, the significance of AN^2 is as yet undetermined, but its value enables comparisons to be made with traditional designs.

The flowpath of the 7-stage turbine is shown in *Figure 10*. A constant tip radius was intended and the observable departure from this occurs because the flowpath was squeezed at stage 2, with a non-linear distribution of flow area, in order to accelerate the flow locally in an attempt to increase the flow coefficient, C_x/U. A full output of the preliminary design code run is available. A value of AN^2 of 18×10^9 results in an exit Mach number of 0.46 and an exit swirl angle of 23.6°. These are both somewhat below the conventional design limits of 0.6 and 30° respectively, which suggests that the annulus could have been smaller. The exit radius ratio of 0.72 is greater than the typical limiting value of 0.6 used for conventional turbines. In the latter, a lower limit on radius ratio is set in order to accommodate the turbine disks and certain accessories within the flowpath hub line. Unless other restrictions become apparent, there is greater flexibility in an exoskeletal design. The turbine stage loading coefficients ($\Delta h/2U_m^2$) increase slightly through the machine, with values of 0.6973 on the first stage and 0.8558 on the last. This means that if a more aggressive loading level had been chosen, fewer stages could possibly have been used. All of the above results imply that weight reduction may be possible in this turbine design. The effect on efficiency is debatable, however.

Adiabatic efficiency is calculated between the leading edge of the first rotor blade and the mixed-out turbine exit plane. An adiabatic efficiency of 94.25% was assumed in the initial cycle calculations, which echoed the reference engine. For the required work output, this corresponds to an overall turbine pressure ratio of 12.565. The degree of success in our design is reflected in an overall pressure ratio of 13.079 for an adiabatic efficiency of 93.46%, when tip clearance losses are neglected. This is a valid comparison with the cycle value, since the cycle knows nothing about tip clearance! If tip clearance losses are considered, an adiabatic efficiency of 92.33% is achieved in the turbine design. This means that a slight improvement is needed if the cycle requirements are to be met. However, the cycle is very optimistic and a more realistic approach might be to lower the turbine efficiency in the cycle, accepting that a somewhat larger engine is needed to produce the thrust.

5. Mid Size, Twin-Spool Turbomachinery

Preliminary designs of the fan, core booster, and HP compressor were generated using *CSPAN*. Some results are shown in *Table 7* and *Figure 11*. As for the single spool configuration, a stratified flow was used through the fan, so that the bypass stream (given in the first column of *Table 7*) is considered separately from the core stream through the fan hub. The fan hub is combined with the booster to form the LP compressor (Second column of *Table 7*), which acts on the core flow. The same inlet radius ratios and specific flow rate were used for the twin spool engine as were used for the single spool configuration.

Parameter	Fan Bypass Stream	FanHub/Booster Core Stream	HP Compressor
Mass flow rate (lbm/s)	654.64	128.36	128.36
Entry temperature (°R)	518.7	518.7	777.3
Entry pressure (psi)	14.7	14.7	52.2
Pressure ratio	1.6	3.65	7.65
Inlet radius ratio	0.5938	0.80	0.92
Exit radius ratio	-	0.92	0.98
Inlet specific flow rate (lbm/s/ft^2)	42.0	42.0	111.16
Rotational speed (rpm)	5,200	5,200	10,000
Number of stages	1	4	7
Tip speed (ft/s)	1507	895	1631
Stall margin (%)	30.36	2.86	17.77
Adiabatic efficiency (%)	89.23	85.9	81.3

Table 7. Fan, Booster and Compressor Design Parameters in a Mid-Size, Twin Spool Exoskeletal Engine

On the fan and booster (the LP spool) the rotational speed was determined partly by consideration of the fan performance and partly with blade speed of the LP core compressor in mind. The adiabatic efficiency of 89.23% is slightly greater than the target value of 88.4% given in *Table 1*. The stall margin of 30.36% is rather excessive in comparison with the 20 or 25% that normally would be acceptable for a modern fan design. The fan hub/booster performance is hardly stellar, with the adiabatic efficiency being 3.5% lower than the target value (Design value = 85.9% in *Table 7* vs. Cycle value = 89.4% in *Table 1*). The stall margin predicted by CSPAN is only 2.86% and is clearly inadequate. Stall margin is not usually quoted for a fan hub in isolation, however, so this result, while of concern, may not be particularly relevant. The performance is a reflection of the lack of blade speed in the LP core machine and some improvement may be possible by increasing the number of stages. Optimization is outside the scope of this study.

The radius ratio of the HP compressor was given by the exit value of the booster. A five-inch axial gap was used between the two components to accommodate the compressor mid frame. The compressor design has seven stages and a constant tip radius, which maximizes the blade speeds. This results in an exit radius ratio of 0.98, an extremely high value, which makes the airfoils in the rear stages very small. In conventional engines an upper limit on HP compressor exit radius ratio might be 0.93, a value that ensures reasonable control of manufacturing tolerances. The rotational speed was chosen on the basis of high radius ratio and the generation of a CSPAN solution with seven stages. The resulting stall margin, at 17.8%, is somewhat short of the preferred value and could be improved with more rpm. The adiabatic efficiency is lower than the target value assumed in the cycle by a significant amount (Design value = 81.3% in *Table 7* vs. Cycle value = 87.1% in *Table 1*), although it is thought that this too could be improved by increased rpm and additional stages. Aerodynamically, the HPC does not pose too much of a problem. Frequently, in conventional designs, the rear stages of a compressor are challenged by high temperature, with this also governing the overall pressure ratio of the engine. In the exoskeletal context, it will be interesting to see the interplay between the high radius ratios, high temperatures, the application of new materials, and the evolution of construction methods.

Comparison of the single spool compression system in *Figure 8* with that of the twin spool equivalent in *Figure 11* shows that, overall, the latter is more compact, despite the insertion of the compressor mid frame. Most of the length savings accrue from the ability to use a high rotational speed for the HPC in the two-spool arrangement. Weight is still an open issue!

The HP turbine design is summarized below in *Table 8* and its flowpath is shown in *Figures 12*. The mass flow rate at entry was obtained from the cycle data. The rotational speed was taken directly from the HP compressor, since both components are designed at sea-level take-off conditions. In the *TDE* design code, the mean radius of the first turbine stage is set by the value selected for the stage loading coefficient. A stage loading coefficient of 0.77 locates the HP turbine just 0.3 inches outboard of the HP compressor

Parameter	HP Turbine	3-Stage LP Turbine	4-Stage LP Turbine
Number of stages	1	3	4
Rotational speed (rpm)	10,000	5,200	5,200
Mass flow rate at entry to first vane (lbm/s)	107.03	126.30	126.30
Δh per stage (Btu/lbm)	163.1	55.2	41.4
Stage 1 $\Delta h/T$	0.055	0.025	0.019
Inlet flow function ($W\sqrt{T}/P$)	15.27	42.25	42.25
Stage 1 loading coefficient ($\Delta h/2U_m^2$)	0.77	1.00	0.74
AN^2	12.0×10^9	12.0×10^9	10.0×10^9
Exit Mach number	0.50	0.55	0.59
Exit swirl angle (°)	30.8	31.8	15.3
Exit radius ratio	*n/a*	0.78	0.82
Overall pressure ratio	2.722	4.35	4.27
Overall adiabatic efficiency (%)	87.55	90.53	91.01

Table 8. Overall Characteristics for the Turbines in a Mid-Size, Twin Spool Exoskeletal Engine

exit and ensures that very little cant is required through the combustor. By modern standards this loading coefficient is quite modest and corresponds to high efficiency potential. The exit area was set, via AN^2, to produce fairly low values of exit velocity and swirl angle (Mach 0.5 and 30.8° respectively). A linear distribution of annulus area was used with a meanline slope of 5° inwards. In retrospect, a constant radius blade tip should have been chosen, but this is a minor issue in the current context. The predicted value of isentropic efficiency is 87.55%, which includes the effects of tip clearance losses. A value of 92.9% was assumed in the cycle calculations, but this did not consider the 2.4 % adjustment for tip clearance. The output file shows that both the vane and blade of the turbine are choked (barely) and it is this that has contributed to the relatively low level of performance because of high profile losses. It is important to avoid choking

at a turbine design point, partly because it leads to poor performance at those conditions, and partly because it can lead to more severe choking at off-design. Significant choking reduces the gas flow, not only through the turbine but also through the rest of the engine. This will result in the engine having to be scaled up to meet the thrust requirements. It is quite possible that the flow area (gas speed), blade speed (loading coefficient), and stage reaction can be manipulated to alleviate the choking phenomenon, but this has not been pursued here. We could also resort to two stages! No attempt has been made to optimize the turbine design in terms of airfoil numbers, aspect ratios, Zweifel coefficients, etc.

Initially, a 3-stage LP turbine was designed but in the quest for improved efficiency, a 4-stage version was also considered. In both cases an equal inter-stage work split was used and the inlet radius ratio was matched to that of the HP turbine exit by adjustment of the first stage loading coefficient. Some characteristics of the two LP turbine candidates are given in *Table 8*, and their flowpaths are shown in *Figures 13* and *14*. A constant tip radius was maintained.

The relatively low work extraction per stage in both the 3-stage and 4-stage designs, enabled choke-free conditions to be established fairly easily. Higher levels of swirl angle are generated in the 3-stage machine, and it is this that results in higher velocities, higher losses and hence a lower overall efficiency. A smaller exit area has been chosen for the 4-stage turbine, and this has resulted in a greater exit velocity and smaller exit swirl than in its 3-stage counter-part. The hub radius of the 3-stage turbine could be moved outwards, possibly leaving more volume open for the centerline stream. Both combinations are within conventional limits for exhaust system inlet conditions. For the same work extraction, the values of overall pressure ratio inversely reflect the adiabatic efficiencies. Both efficiencies have been adjusted for tip clearance effects. Both efficiencies listed in *Table 8* fall short of the value assumed in the cycle (*Table 1*). As in the case of the HP turbine design, no real attempt has been made at optimization, and it is felt that the performance target set by the cycle is achievable. The only aerodynamic challenge posed by the exoskeletal configuration seems to be the requirement for relatively high radius ratios. This compromises the relationship between blade speed and the axial component of gas velocity, making the design task somewhat harder.

6. Small Engines: Cycle Studies

Cycle data was generated for a small, single spool turbofan engine to produce a thrust of 5000 lbf at take-off. Some of the quantitative assumptions input to the cycle calculations are given in *Table 9*. The values are fairly typical of those encountered in such powerplants, although they do not represent any particular engine. The mass flow rate was determined by the cycle program, based on the assumed component efficiencies and the net thrust required. In the cycle analysis, the fan flow is stratified, with the overall pressure ratio being generated through the fan hub followed by the remainder of the core compressor. The values in *Table 9* correspond to a specific fuel consumption of 0.507.

The exhaust streams are unmixed and emerge with velocities of 916 ft/s (fan) and 1837 ft/s (core).

Parameter	Value
Flow rate through engine core (lb/s)	34.54
Bypass ratio	3.0
Fan pressure ratio	1.6
Overall pressure ratio	10.0
T_{41} (°R)	2600
$\eta_{AD\ FAN}$ (%)	88.5
$\eta_{AD\ CORE\ COMPRESSOR}$ (%)	90.1
$\eta_{AD\ TURBINE}$ (%)	91.6

Table 9. Cycle Assumptions for a 5000 lbf Thrust Single Spool Exoskeletal Engine

7. Small Engines: Turbomachinery

The same construction was assumed as for the mid-size, single spool exoskeletal engine discussed in *Sections 3* and *4*. An inlet radius ratio of 0.8 was selected for the fan hub or core stream, which led to a corresponding value of 0.6934 for the fan bypass stream.

The flowpath for the fan bypass stream is shown in *Figure 15* and some design and performance data is given in *Table 10*. A rotational speed of 12,000 rpm was selected as input to *CSPAN* and this resulted in as adiabatic efficiency of 77.9% and a stall margin of 34.1%. In retrospect, a lower rpm would have been preferred, since the chosen value is responsible for both the low efficiency and the excessively generous stall margin. Clearly the 10% shortfall in adiabatic efficiency is not acceptable, although improvement should not be too difficult. However, the exercise serves to show the size and geometry of the fan blade.

The core compressor is shown in *Figure 16*, and some of its characteristics are given in the right hand column of *Table 10*. A constant tip radius has been maintained, and a 9-stage compressor has been designed. The resulting adiabatic efficiency of 84.3% is significantly less than the cycle target value of 90.1% in *Table 9*, and the stall margin of

Parameter	Fan Bypass Stream	Core Compressor
Mass flow rate (lbm/s)	103.62	34.54
Inlet specific flow (lbm/s/ft^2)	42.0	42.0
Entry temperature (°R)	518.7	518.7
Entry pressure (psi)	14.7	14.7
Pressure ratio	1.6	10.00
Inlet radius ratio	0.6934	0.80
Number of stages	1	9
Rotational speed (rpm)	12,000	12,000
Tip speed (ft/s)	1545	1072
Relative tip Mach number	1.568	1.179
Adiabatic efficiency (%)	77.9	84.3
Stall margin (%)	34.1	5.8

Table 10. Fan and Compressor Design Parameters in a Small-Size, Single Spool Exoskeletal Engine

5.8% is also very low. As for the fan, however, no optimization has been attempted, and it is felt that this situation can be rectified. Again the primary objective was to generate an overall geometry for the single-spool compression system.

A 3-stage, constant tip radius turbine was designed to drive the fan/compressor combination, and this is shown in *Figure 17* with some design details being listed in *Table 11*. The stage 1 loading coefficient was chosen to locate the mean radius of the turbine entry reasonably close to that of the compressor exit, with a few degrees of cant angle on the combustor. The relative locations of the fan, core compressor and turbine have been laid out in *Figure 18*, showing the approximate overall size of the turbomachinery.

Parameter	Value
Number of stages	3
Rotational speed (rpm)	12,000
Mass flow rate at entry to first vane (lbm/s)	29.38
Δh per stage (Btu/lbm)	78.0
Stage 1 $\Delta h/T$	0.030
Inlet flow function ($W\sqrt{T}/P$)	10.99
Stage 1 loading coefficient ($\Delta h/2U_m^2$)	0.9
AN^2	20.0×10^9
Exit Mach number	0.68
Exit swirl angle (°)	26.2
Exit radius ratio	0.77
Overall pressure ratio	6.04
Overall adiabatic efficiency (%)	94.9

Table 11. Overall Characteristics for the Turbine in a Small-Size, Single Spool Exoskeletal Engine

The adiabatic efficiency has been expressed in terms of total conditions between the leading edge of the first blade row and the mixed-out exit plane of the final blade row. The inclusion of the cooling flow at the start of the expansion process lowers the initial temperature relative to the corresponding pressure, and raises the value of the numerator in the expression for efficiency. However, the predicted high value in *Table 11* is only partly due to the bookkeeping! The design was able to take advantage of the beneficial combinations of blade speed and axial gas velocity (C_z/U is close to unity throughout), using them to minimize the values of absolute and relative velocities in the velocity diagrams, thus keeping profile losses small. The relatively large radius ratios have aided greatly in this. The design is fairly moderate and a more aggressive approach might well have led to a two-stage solution. An overall conclusion is that no difficulty should be encountered in matching the turbine efficiency in the cycle in this small engine.

8. Noise Advantages of the Open Centerline

There are potential noise advantages inherent in the exoskeletal engine concept and these are extremely attractive in view of the current interest in minimizing environmental impact, especially at take-off. The benefits are quantifiable using a simple approach to noise prediction, recently developed by *MTC* as part of their contribution to the Supersonic Business Jet program at NASA Glenn (*References 7, 8, & 9*).

An inverted velocity profile (IVP) jet is one in which the central flow has a lower velocity than that of the surrounding flow field. The exoskeletal engine creates a naturally inverted velocity profile at the nozzle exit and this is shown schematically in *Figure 19*. Here, the take-off conditions from the reference engine in *Section 2.1* are assumed. This results in a mixed engine exhaust velocity of 1000 ft/s and an effective ambient velocity, due to the flight speed, of about 300 ft/s. For convenience, the free central stream is assumed to emerge with the same velocity as it had on entry, although there is scope to change this by manipulation of the central area at its exit plane.

IVP jets were investigated extensively in the late 1970s and early 1980s, in conjunction with NASA's Variable Cycle Engine program, where they were shown to have significant noise benefits (*Reference 10*). The reductions in noise are due primarily to the increased mixing perimeter and shortened shear layer, but shielding of the inner shear layer reinforces the effects. The overall acoustic benefits are quantified by comparing the measured noise to a hypothetical fully-mixed jet from an untreated conic nozzle. Typical results are shown in *Figure 20*, where the experimental overall sound pressure level relative to the fully-mixed datum case is plotted against outer-stream to inner-stream velocity ratio for four different nozzle configurations, as described in *Reference 11*. Of course, what really matters is the reduction in "effective perceived noise level" (EPNL), and it has been pointed out in *Reference 12* that the IVP benefit has two components – a radius ratio effect and a velocity ratio effect. Each of these can contribute as much as 3 EPNdB noise suppression, so that a total net benefit as much as 6 EPNdB relative to a hypothetical fully-mixed case can be obtained.

MTC's simple analytical approach may be applied to the exoskeletal configuration as follows. The noise from the exoskeletal engine exhaust relative to the equivalent flow through a conical nozzle is correlated as the sum of three effects:

- the hypothetical mixing that will always produce a noise reduction
- the radius ratio effect that produces between 0 and 3 EPNdB noise reduction
- the IVP effect that ranges from a noise reduction of up to 3 EPNdB to a large noise increase.

The results are shown in *Figure 21*. For the baseline case depicted in *Figure 19*, where the velocity ratio is about 3, there is a benefit of about 6 EPNdB relative to an untreated conic nozzle. This corresponds top the left-hand end of the solid curve in *Figure 21*. By

comparing the left-hand ends of each of the curves, it may be deduced that the larger the central passage in the exhaust system, the greater the noise benefit! However, the velocity ratio is far from optimum. If the induced central exhaust velocity were to be increased by reducing the exit area or perhaps pressurizing the flow from the engine core, the jet velocity ratio would be decreased and this would enable an acoustic optimum to be attained. Beyond that point, the noise would increase.

The results indicate clearly that this phenomenon is worthy of further study.

9. Conclusions & Recommendations

The very limited amount of investigative preliminary design work has provided the following information.

- There is a need to determine acceptable methods of construction for exoskeletal engine systems and components. The fan configuration suggested for the mid-size engine, with torque being provided by a mid-span shroud, seems reasonable both aerodynamically and structurally. The tip shroud that connects two rows of blades in the initial conceptual drawing (*Reference 1, Figure 2*) is impractical, at least for a subsonic engine with a bypass ratio significantly higher than unity. A two-stage fan is unnecessary for a fan pressure ratio typical of a subsonic commercial engine and would pose operability problems. Additional fan stages only become necessary for high specific thrust engines, with higher fan pressure ratios and lower bypass ratios. It should be noted, however, that turbine power would still be transmitted to the fan through a mid-span shroud attached to the last row of fan blades!

- There is a clear shortage of design guidelines for exoskeletal engine systems. The current studies indicate that radius ratios will probably be greater than those encountered in current conventional engines. This issue is compounded by its obvious association with levels of blade speed needed for efficient operation of turbomachinery. For fans and compressors, pressure ratio is related to blade speed, and there is a dichotomy in single spool configurations, where the rpm is limited by the fan tip, leaving the core compressor chronically short of blade speed. In compression systems, blade speed is also linked to the ability to maintain required stall margins.

- For turbines, a large body of knowledge exists on the correlation between stage loading coefficients and efficiency. This is all based on "conventional" radius ratios, so while we can continue to rely on basic aerodynamic theories, their application to exoskeletal turbomachinery must be re-cast in the light of increased radius ratios. The radius ratio in turbomachinery establishes critical relations between blade speed and gas velocity (flow factor, C_z/U), which in turn determines stage loading and attainable efficiency. Radius ratios also influence blade spans. Extremely high radius ratios and exceedingly small airfoils have been encountered in the HP compressors

(*Section 4*, *Tables 5* & *7*). This was because constant tip designs were chosen for these specific HPCs. Great care will be needed in the manufacture of such airfoils. The maintenance of very tight tip clearances also poses performance problems.

- An important design parameter used in turbines as a link between aerodynamics and structural integrity, is AN^2. In conventional systems, this is a measure of rim stress, which is irrelevant in an exoskeletal configuration. Can it be re-interpreted in a useful manner, or can an exoskeletal equivalent be generated? This question can only be answered by the results of structural analysis of either the steady state behavior or perhaps the dynamic behavior of the airfoils.

- Limits on rpm and tip speed need to be firmly established and related to the use of materials. This is especially relevant to fans, whose relative tip speeds constitute rpm limits on an engine. We need to know how fast we can spin the relatively heavy casings, which carry the blade sets in compression. This depends on the material properties and determines the casing thickness, since the casing must also support itself.

- Knowledge of such factors will enable generic models of the turbomachinery components to be constructed, the objectives being

  - their inclusion in a library of component models shown in *Figure 2*,

  - their use in the construction of an engine model, and

  - the prediction of component weights within a realistic engine build.

- It is believed that at least some of the above work should be carried out before studies are made of the specific application of the exoskeletal concept to subsonic missions, supersonic missions, hypersonic missions, etc. We already have extensive knowledge of the general requirements of propulsion systems for the aforementioned applications. General, rather than specific, preliminary design work will provide useful data regarding the wisdom of their pursuit, without premature commitment to any one of them.

- The very limited resources spent so far on consideration of noise implications have generated some very promising results. This field of research could yield data of interest to all branches of aeronautics, and produce rewards that would offset some of the possible negative aspects of the exoskeltal concept.

- There almost certainly will be drawbacks as well as benefits to the exoskeletal concept, and only a well-planned program of systems studies will discover optimum solutions within the maze of aircraft/engine noise, weight, and performance.

References

1. *"Feasibility Study of an Exoskeletal Engine Concept. Part 1. System & Component Requirements."*
   NASA Contract *NAS3-27326*.
   Ian Halliwell. December 1999.

2. *"Preliminary Engine Design – A Practical Overview for the NASA Glenn Research Center."*
   A Lecture Course presented periodically by Ian Halliwell.

3. "*The Selection & Use of Individual Component Design Points in Preliminary Engine Design.*"
   NASA Contract NAS3-27377.
   Ian Halliwell. December 1998.

4. "*A User Guide for CDE. A Preliminary Design Code to Generate Compressor Design Envelopes.*"
   NASA Contract NAS3-27377.
   Ian Halliwell. September 1997.

5. "*A User Guide for TDE. A Preliminary Design Code to Generate Turbine Design Envelopes. Volume I: The Turbine Design Code*"
   NASA Contract NAS3-27377.
   Ian Halliwell. September 1997.

6. "*A User Guide for TDE. A Preliminary Design Code to Generate Turbine Design Envelopes. Volume II: Turbine Design Envelopes*"
   NASA Contract NAS3-27377.
   Ian Halliwell. September 1997.

7. "*Preliminary Engine Design for the Supersonic Business Jet*"
   NASA Contract C-70321-J.
   Ian Halliwell. May 17, 1999.

8. "*Preliminary Engine Noise Assessment for the Supersonic Business Jet Subtask 1 Report: Noise Suppression Technology Survey*"

NASA Contract C-70321-J.
James R.Stone, Ian Halliwell, Eugene A. Krejsa, Bruce J. Clark. September 1, 1999.

9. "*Preliminary Engine Noise Assessment for the Supersonic Business Jet Subtask 2 Report: Acoustic Sensitivity Studies*"
NASA Contract C-70321-J.
James R.Stone, Ian Halliwell, Eugene A. Krejsa, Bruce J. Clark. September 1, 1999.

10. "*NASA Research in Supersonic Propulsion – A Decade of Progress*"
AIAA-82-1048, June 1982. (NASA TM-82862).
L.H. Fishbach, L.E. Stitt, J.R. Stone, & J.B. Whitlow

11. "*Effects of Geometric and Flow Field Variables on Inverted-Velocity-Profile Coaxial Jet Noise and Source Distributions*"
AIAA-79-0635, March 1979. (NASA TM-79095)
J.R. Stone, J.H. Goodykoontz, O.A. Gutierrez.

12. "*Supersonic Jet Noise and the High Speed Civil Transport*"
AIAA-89-2358, 1989.
J.M. Seiner & E.A. Krejsa.

Figures

14. Mid-Size Twin Spool Exoskeletal Engine – 4-Stage LP Turbine

15. Small-Size Single Spool Exoskeletal Engine – Fan

16. Small-Size Single Spool Exoskeletal Engine – Core Compressor

17. Small-Size Single Spool Exoskeletal Engine – Turbine

18. Small-Size Single Spool Exoskeletal Engine – Layout

19. The Exoskeletal Engine Exhaust – a Naturally Inverted Velocity Profile

20. Effect of Velocity Ratio on Noise Relative to Mixed Flow Conical Nozzle Prediction at $\theta = 139°$ (*Reference 11*)

21. Preliminary Results for Natural Noise Reduction in an Exoskeletal Engine

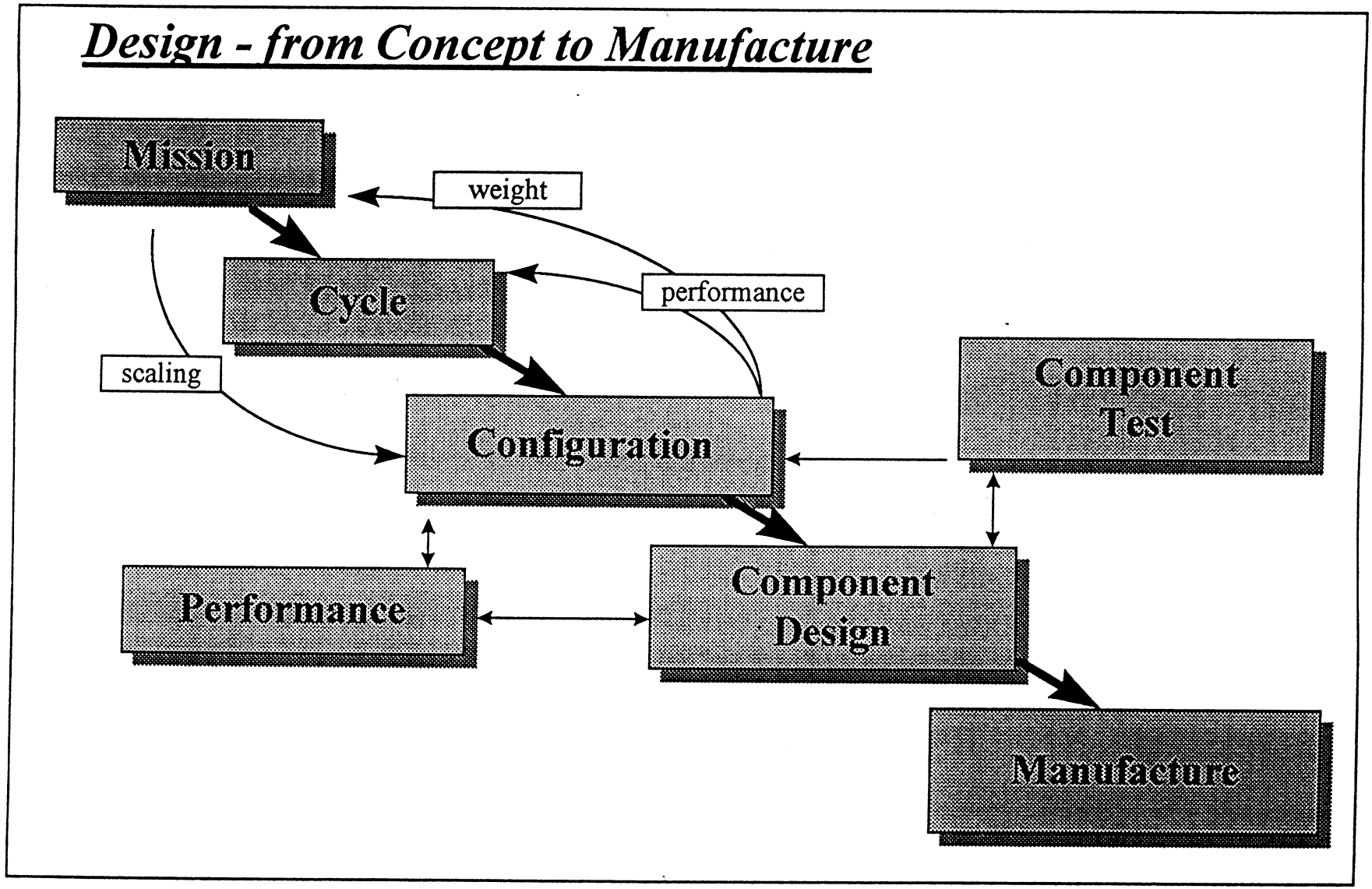

Figure 1. Typical Design Process for a Gas Turbine Engine

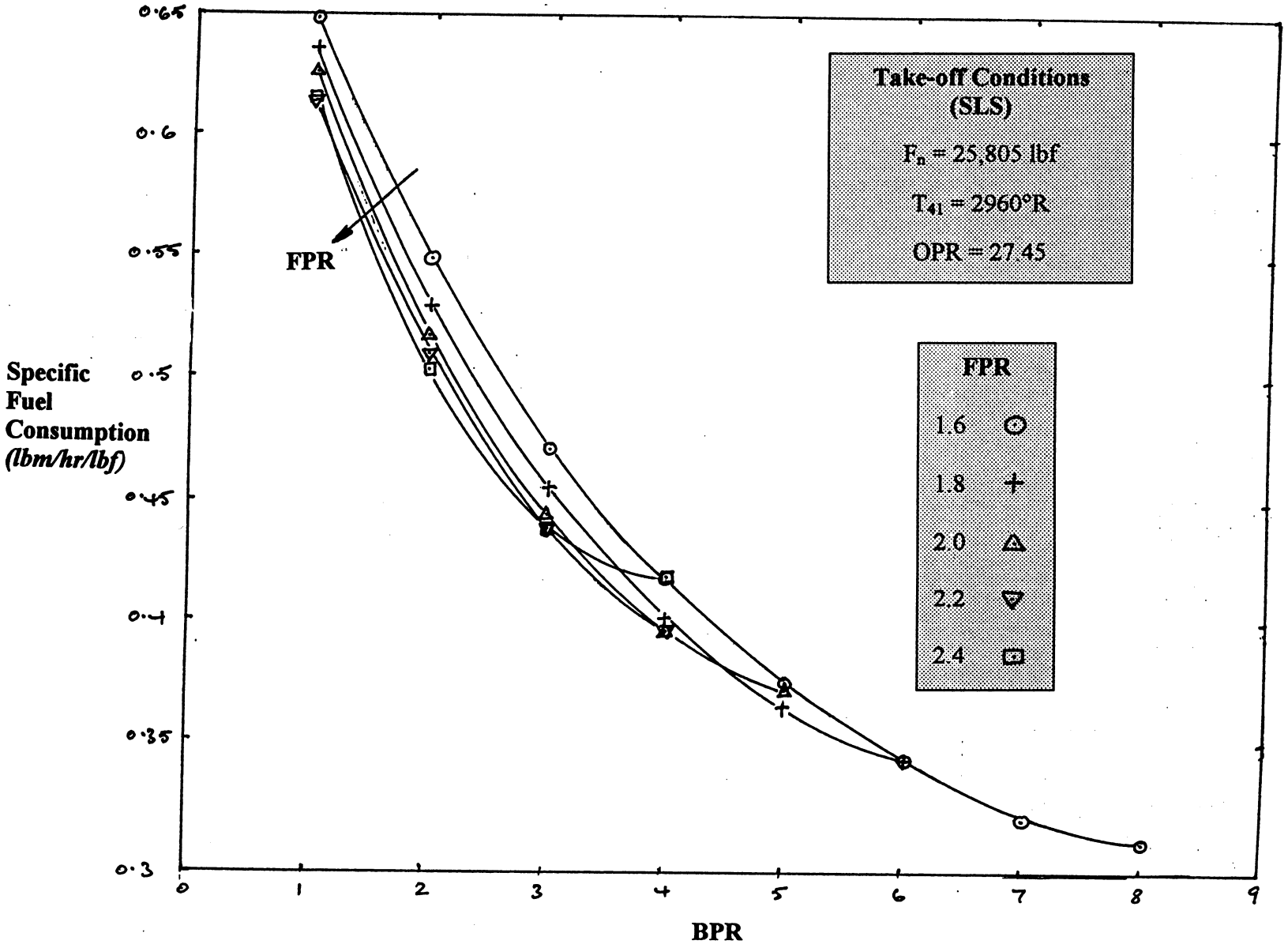

Figure 3. The Effects of Bypass Ratio and Fan Pressure Ratio on Specific Fuel Consumption for a Mid-Size Single-Spool Engine with Separate Exhaust Streams

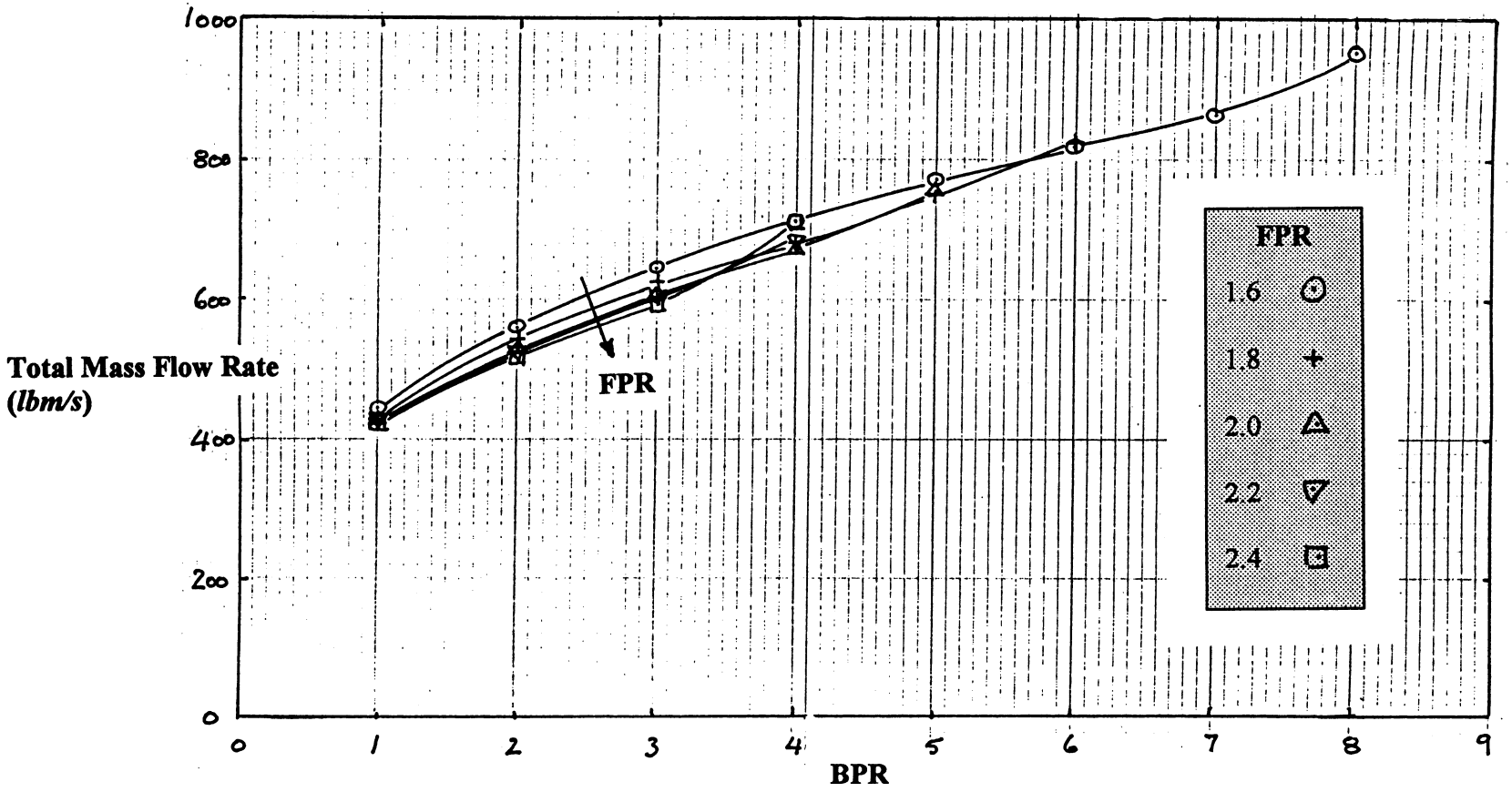

Figure 4. The Effects of Bypass Ratio and Fan Pressure Ratio on Total Mass Flow Rate Required to Produce 25,805 lbf Thrust for a Mid-Size Single-Spool Engine with Separate Exhaust Streams

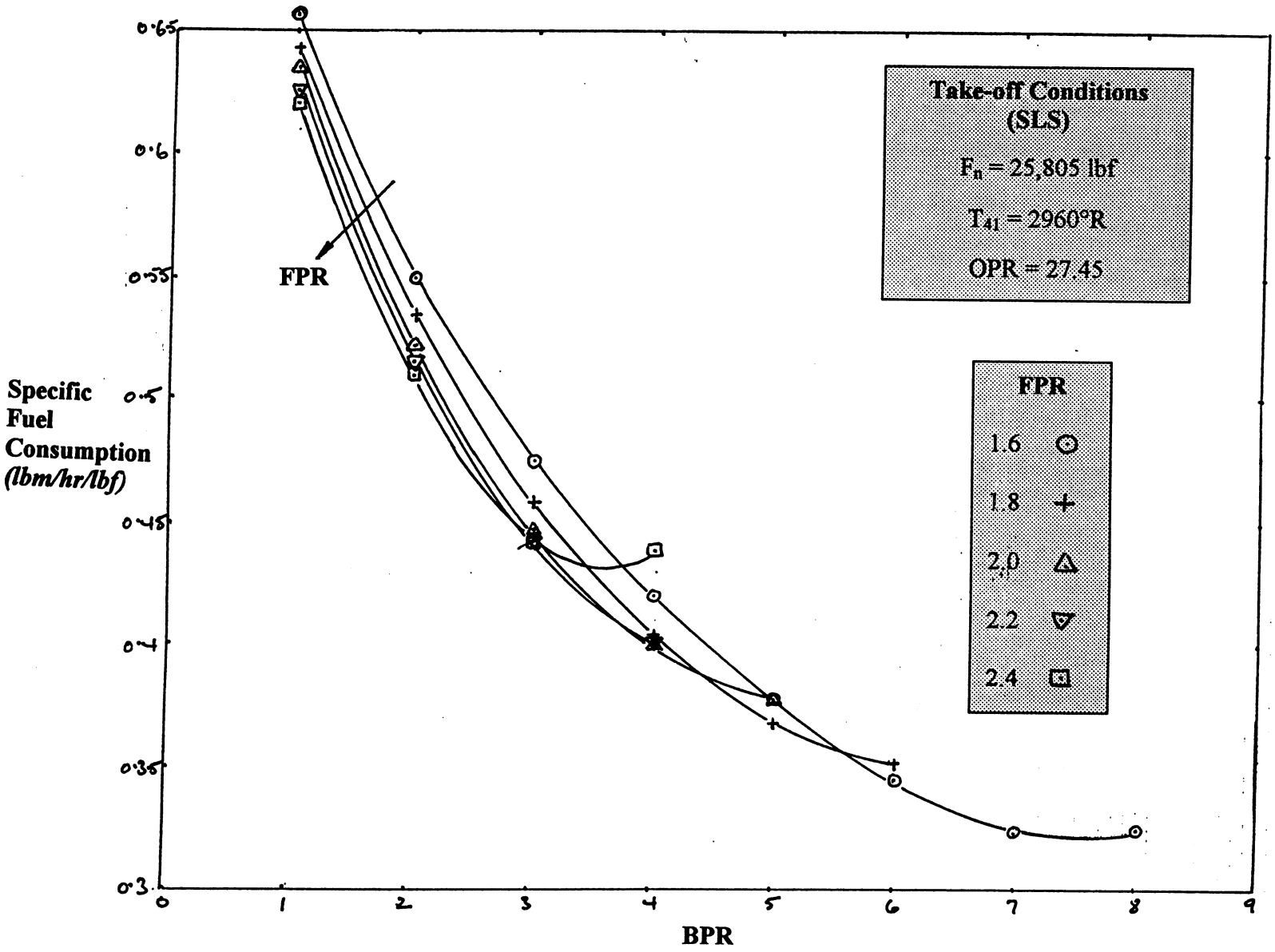

Figure 5. The Effects of Bypass Ratio and Fan Pressure Ratio on Specific Fuel Consumption for a Mid-Size Twin-Spool Engine with ~~Separate~~ mixed Exhaust Streams

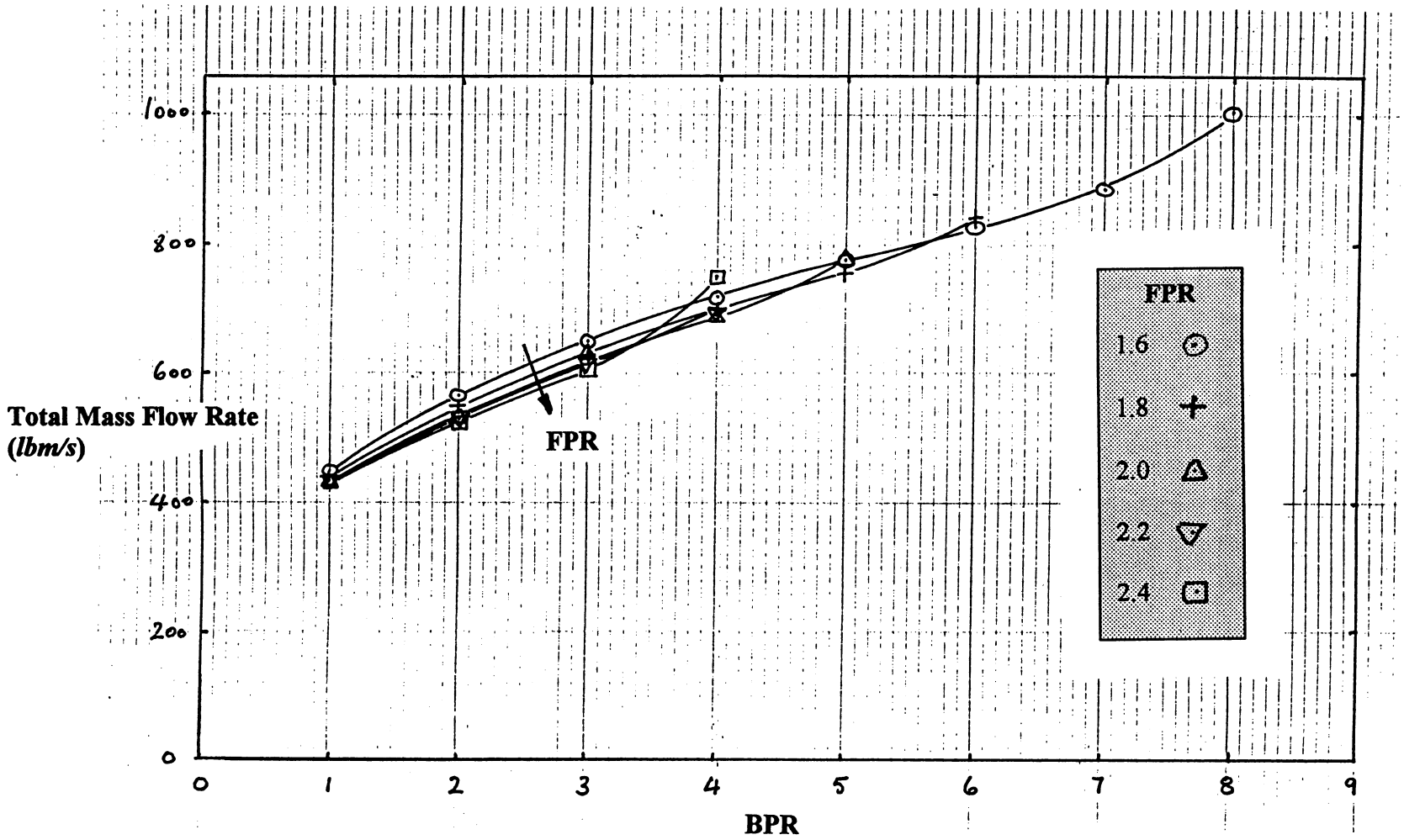

Figure 6. The Effects of Bypass Ratio and Fan Pressure Ratio on Total Mass Flow Rate Required to Produce 25,805 lbf Thrust for a Mid-Size Twin-Spool Engine with Separate Exhaust Streams

mixed

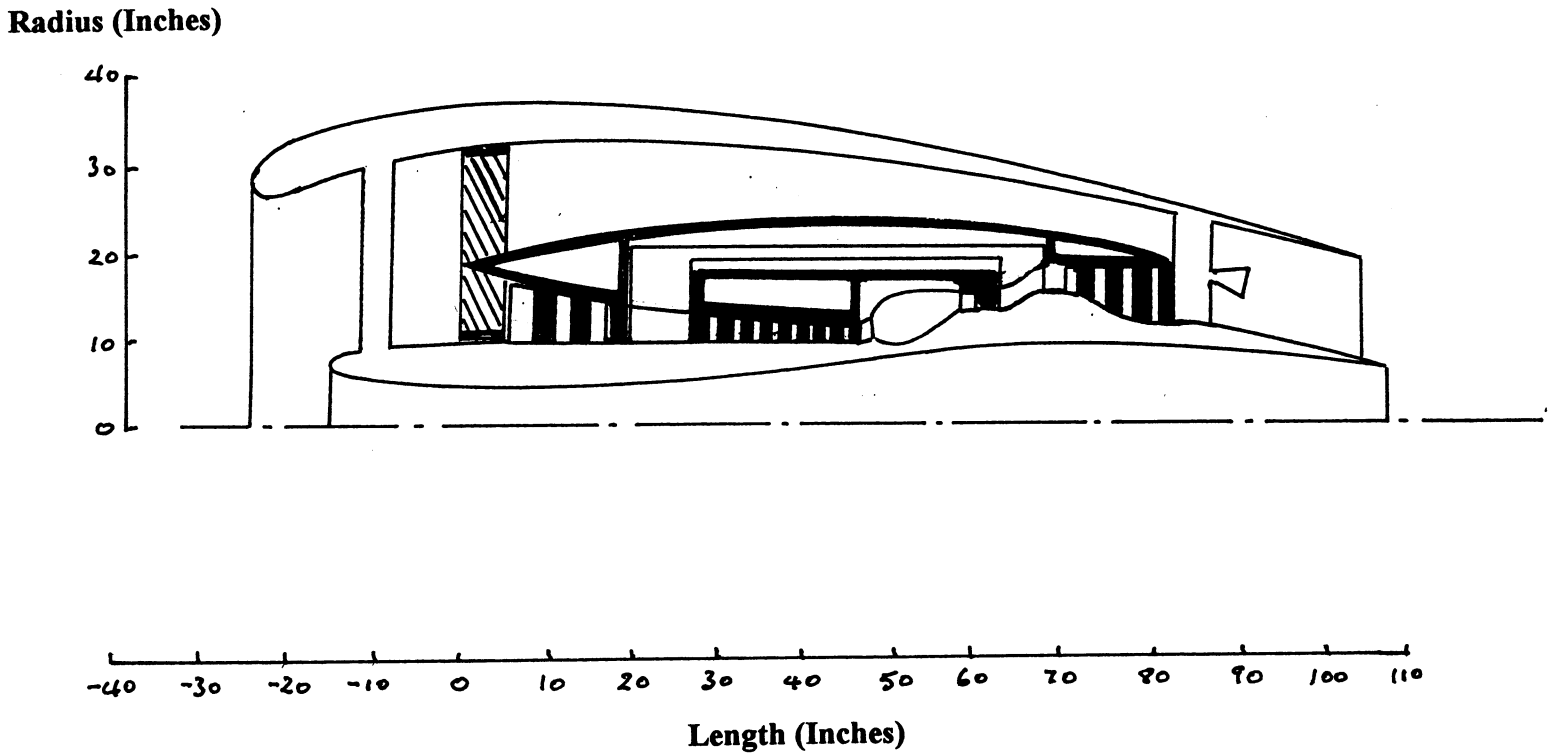

Figure 7. A Possible Twin Spool Configuration for an Exoskeletal Engine

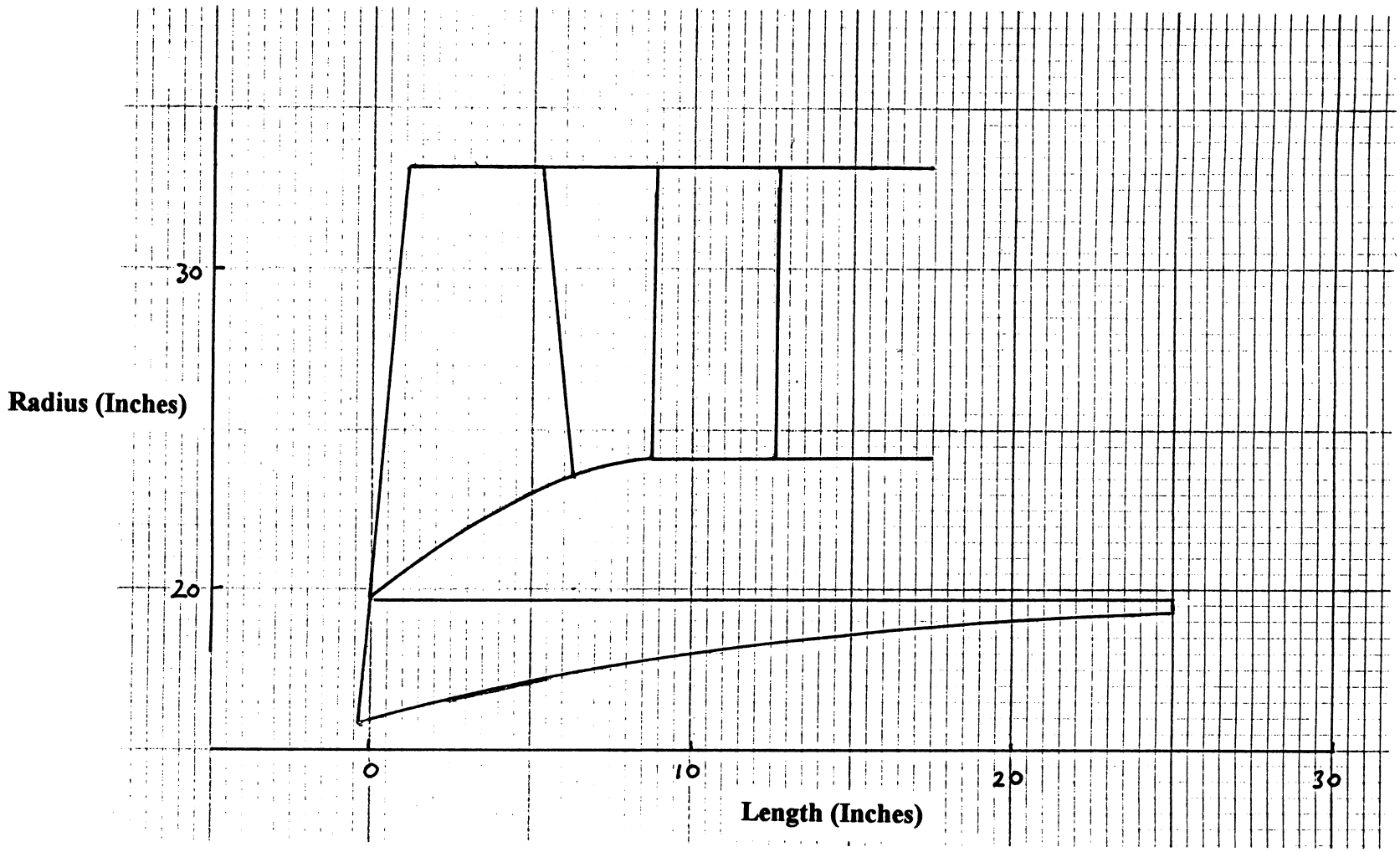

Figure 8. Mid-Size Single Spool Exoskeletal Engine – Fan & Core Compressor

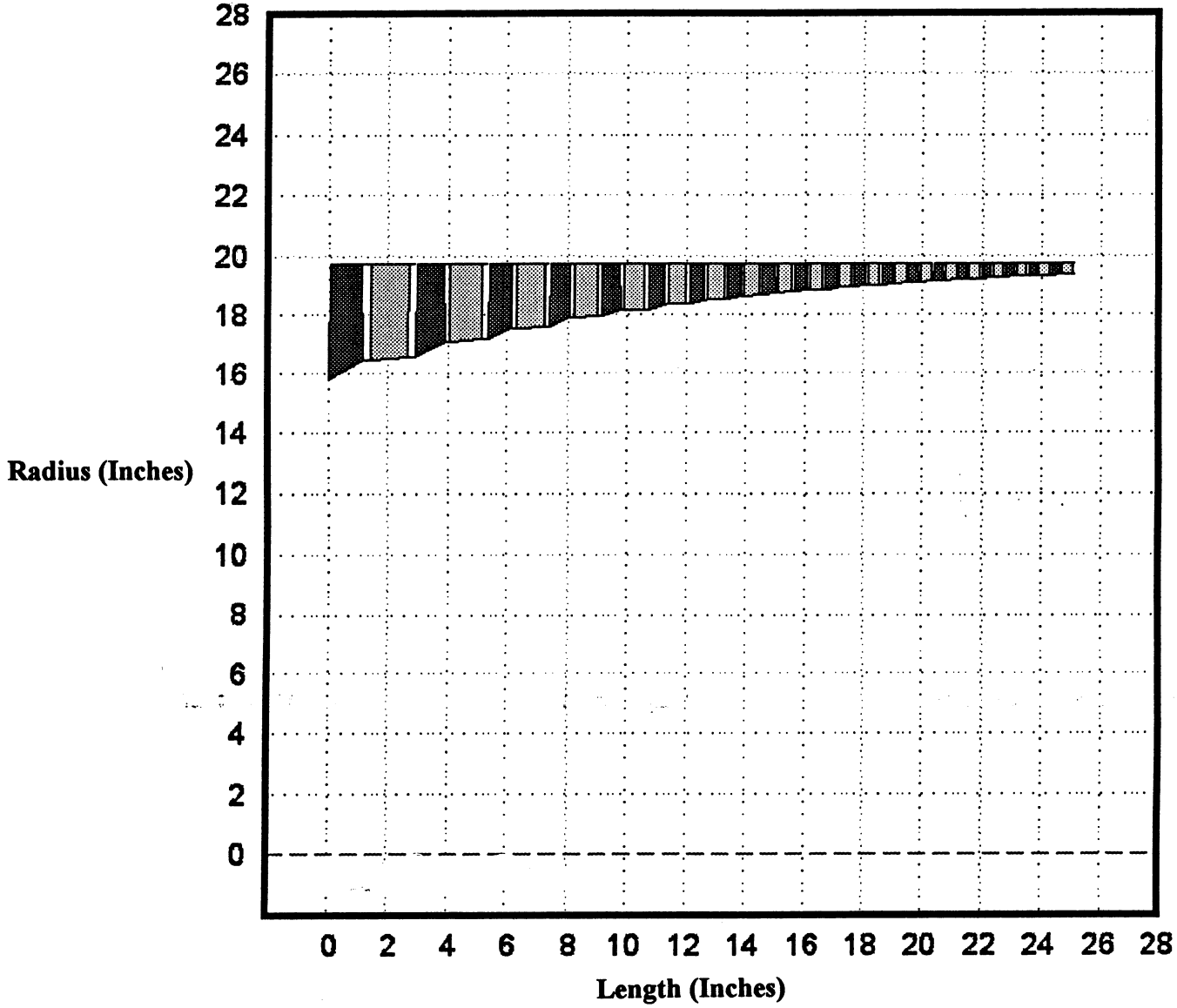

Figure 9. Mid-Size Single Spool Exoskeletal Engine – Core Compressor

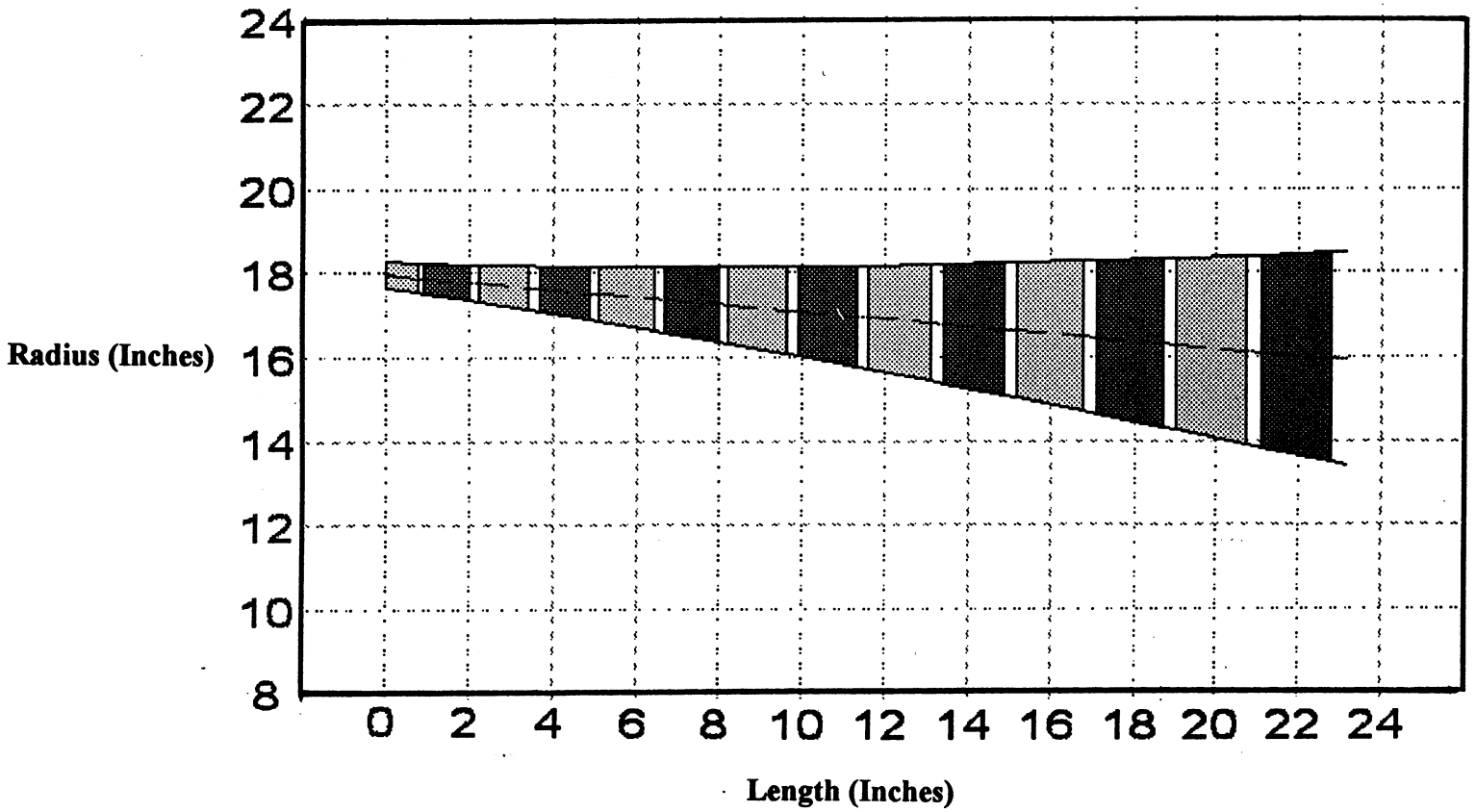

Figure 10. Mid-Size Single Spool Exoskeletal Engine - Turbine

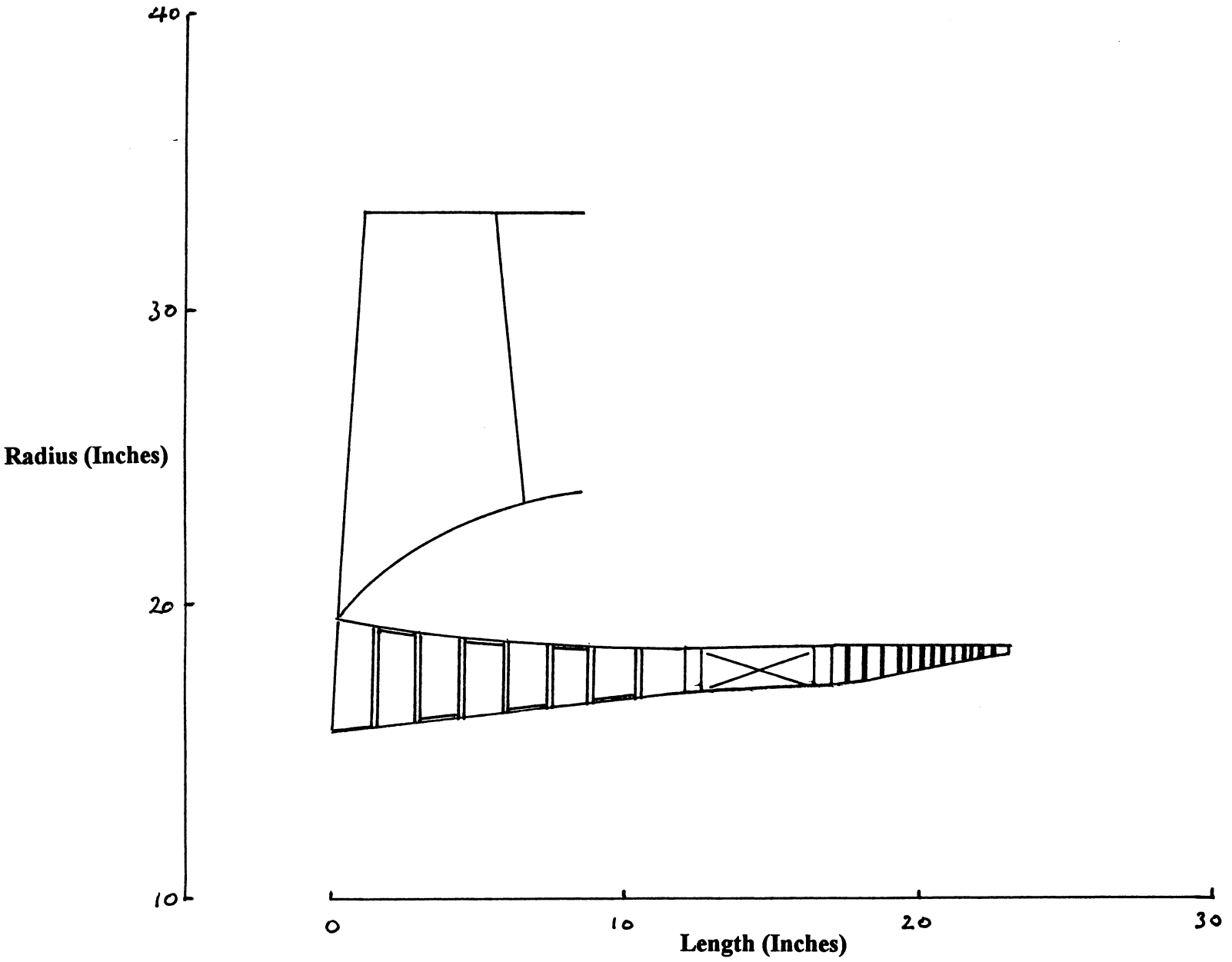

Figure 11. Mid-Size Twin Spool Exoskeletal Engine – Fan, Booster & HP Compressor

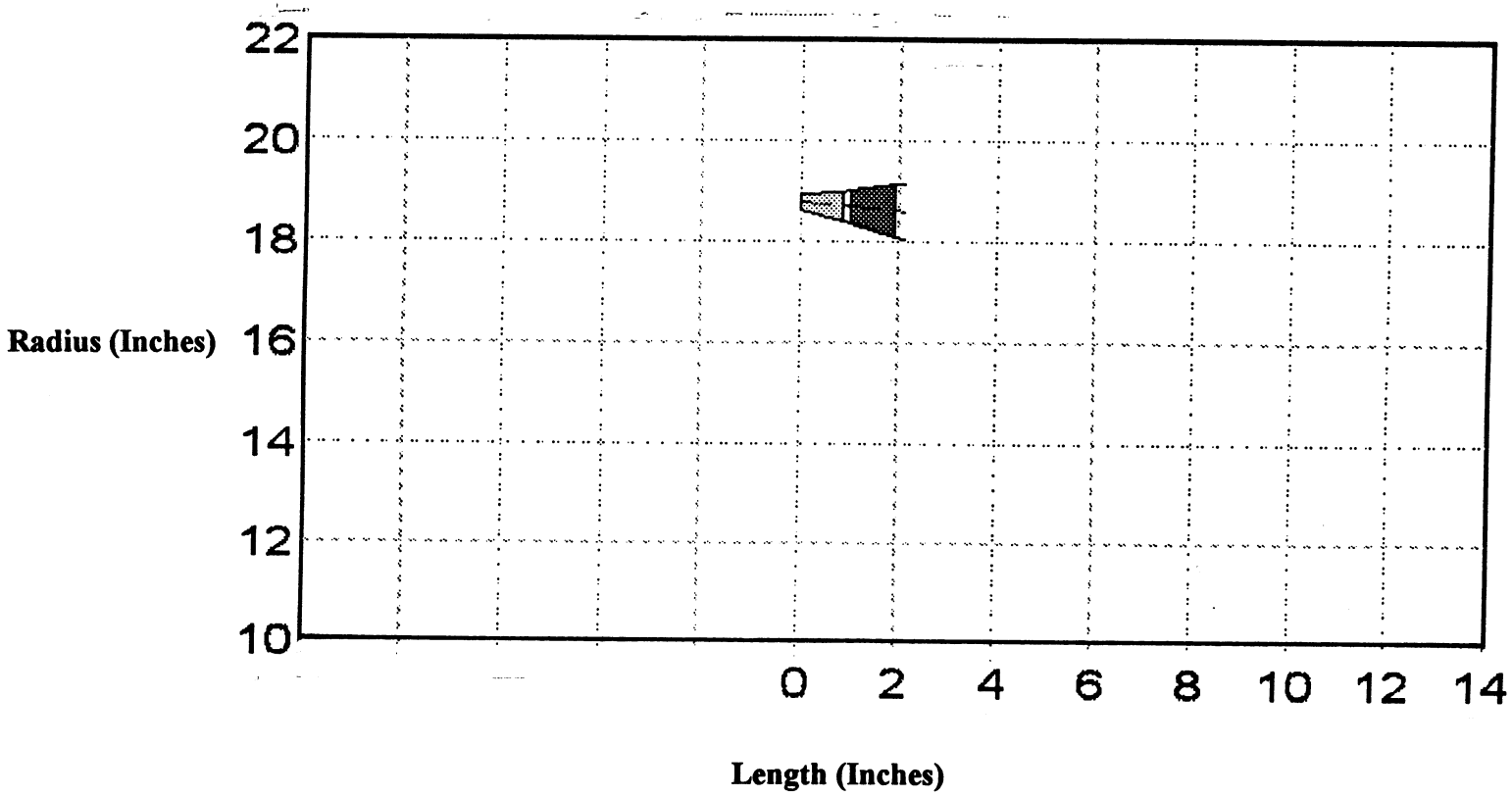

Figure 12. Mid-Size Twin Spool Exoskeletal Engine – HP Turbine

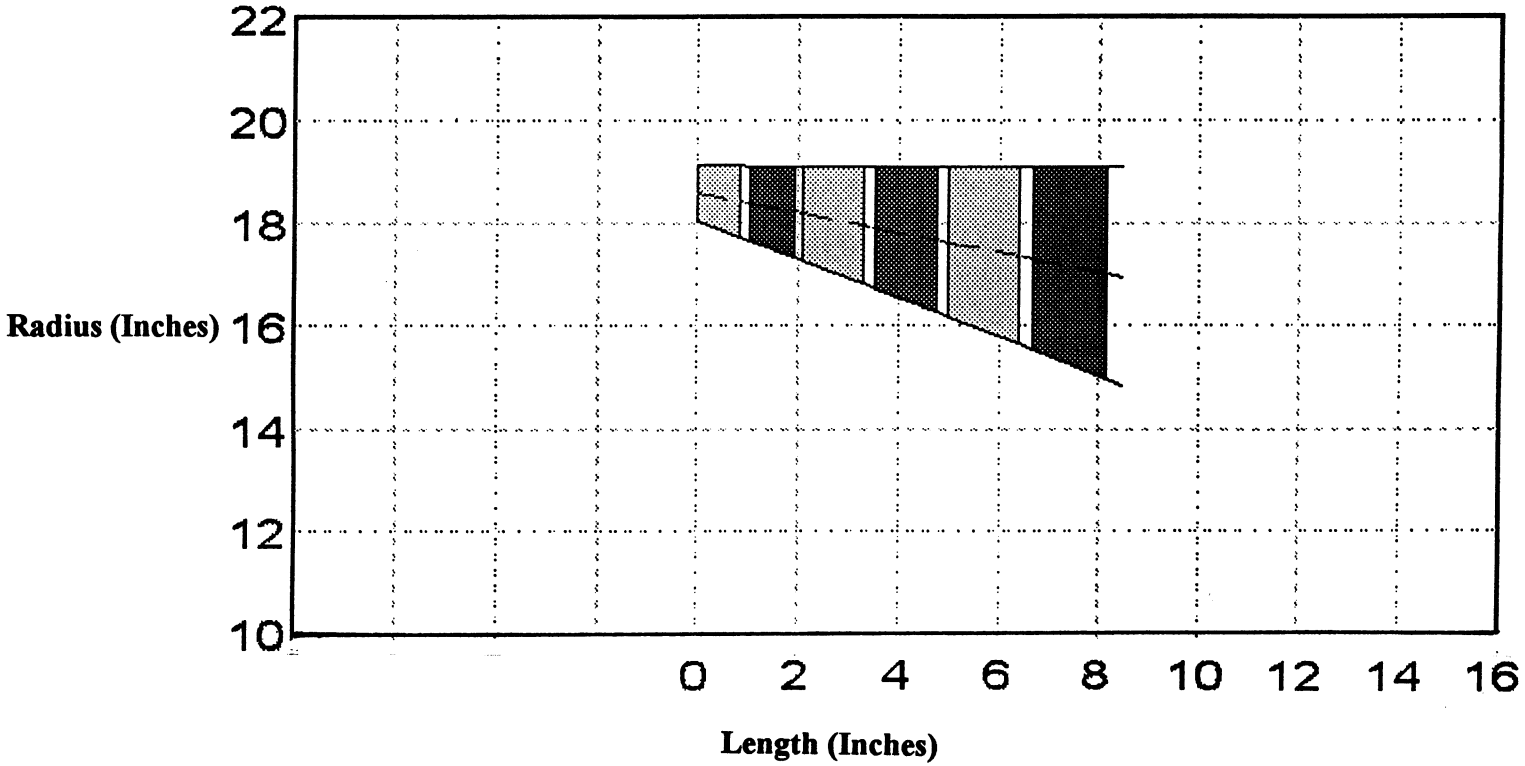

Figure 13. Mid-Size Twin Spool Exoskeletal Engine – 3-Stage LP Turbine

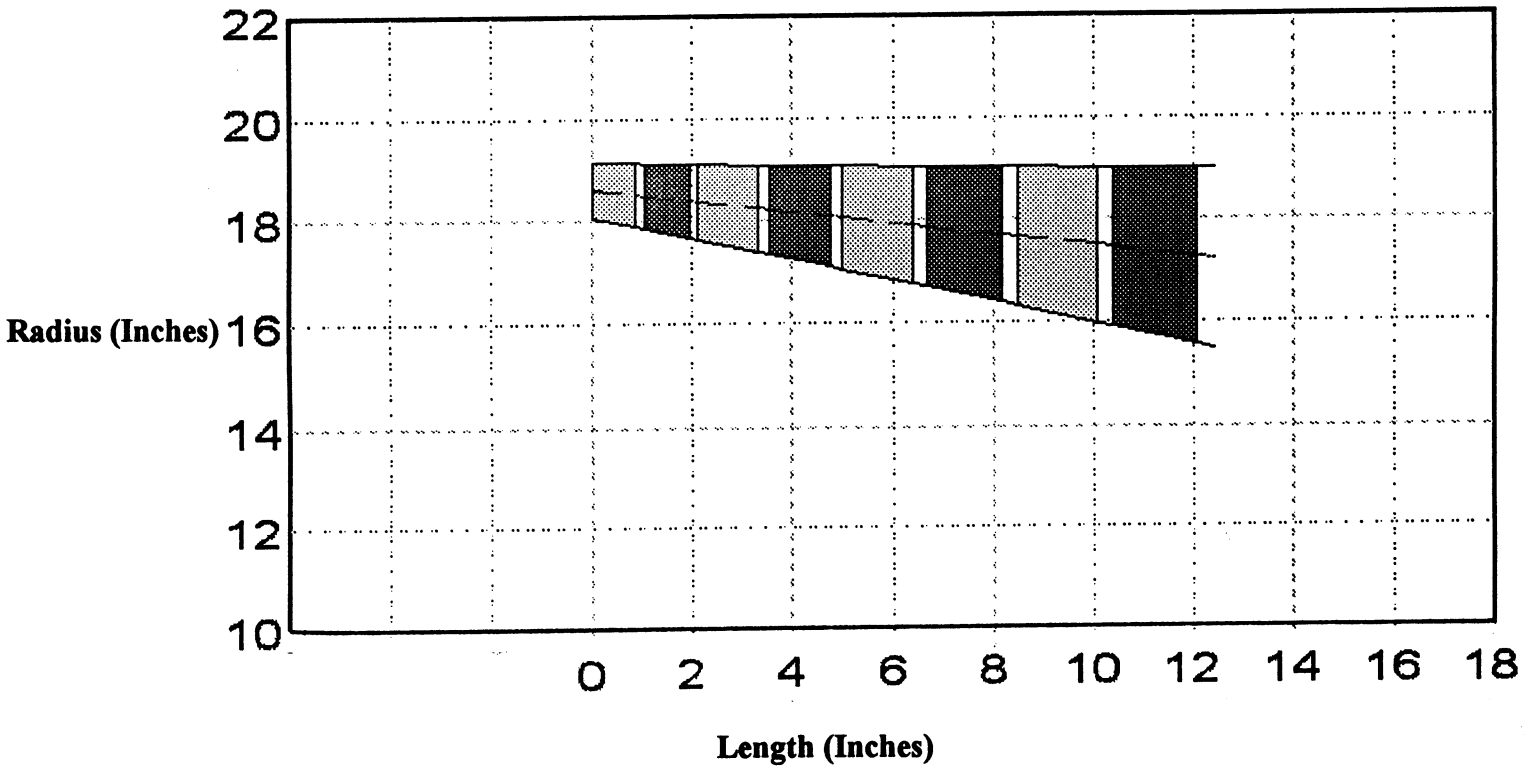

Figure 14. Mid-Size Twin Spool Exoskeletal Engine – 4-Stage LP Turbine

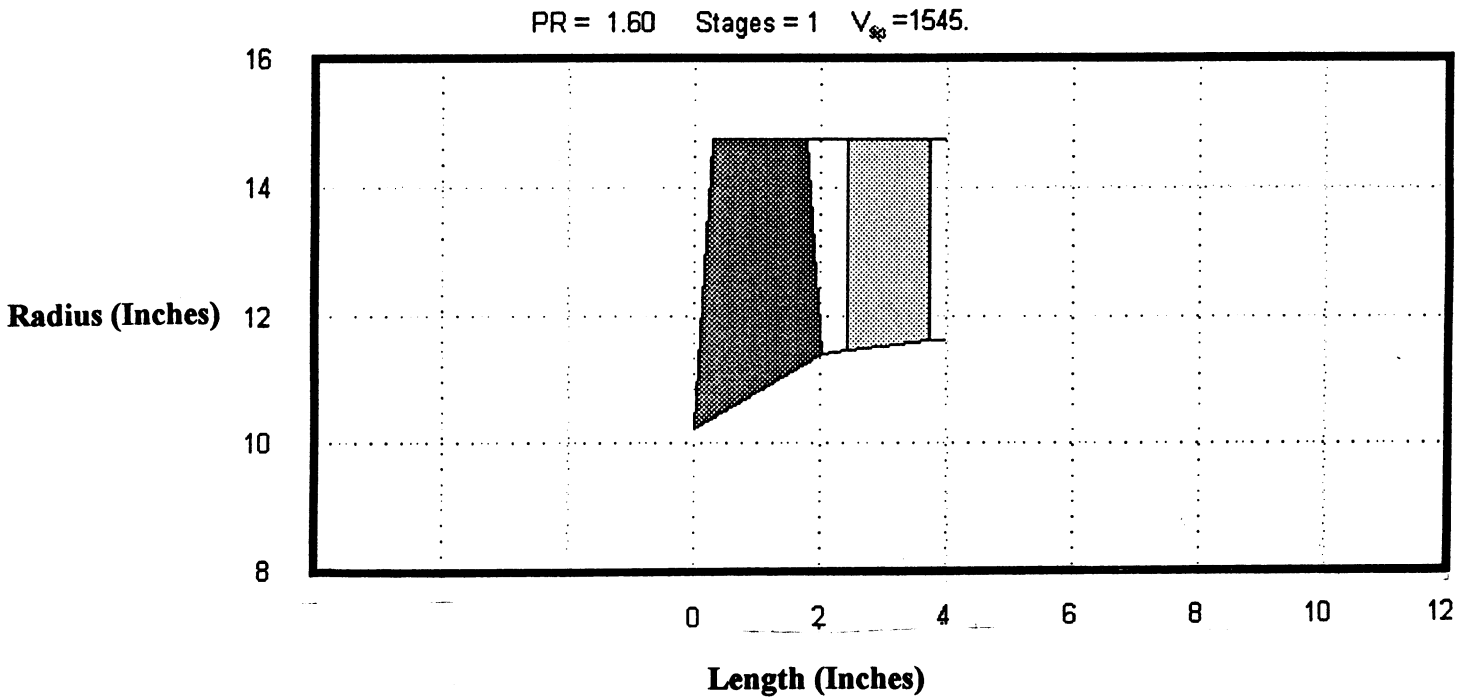

Figure 15. Small-Size Single Spool Exoskeletal Engine – Fan

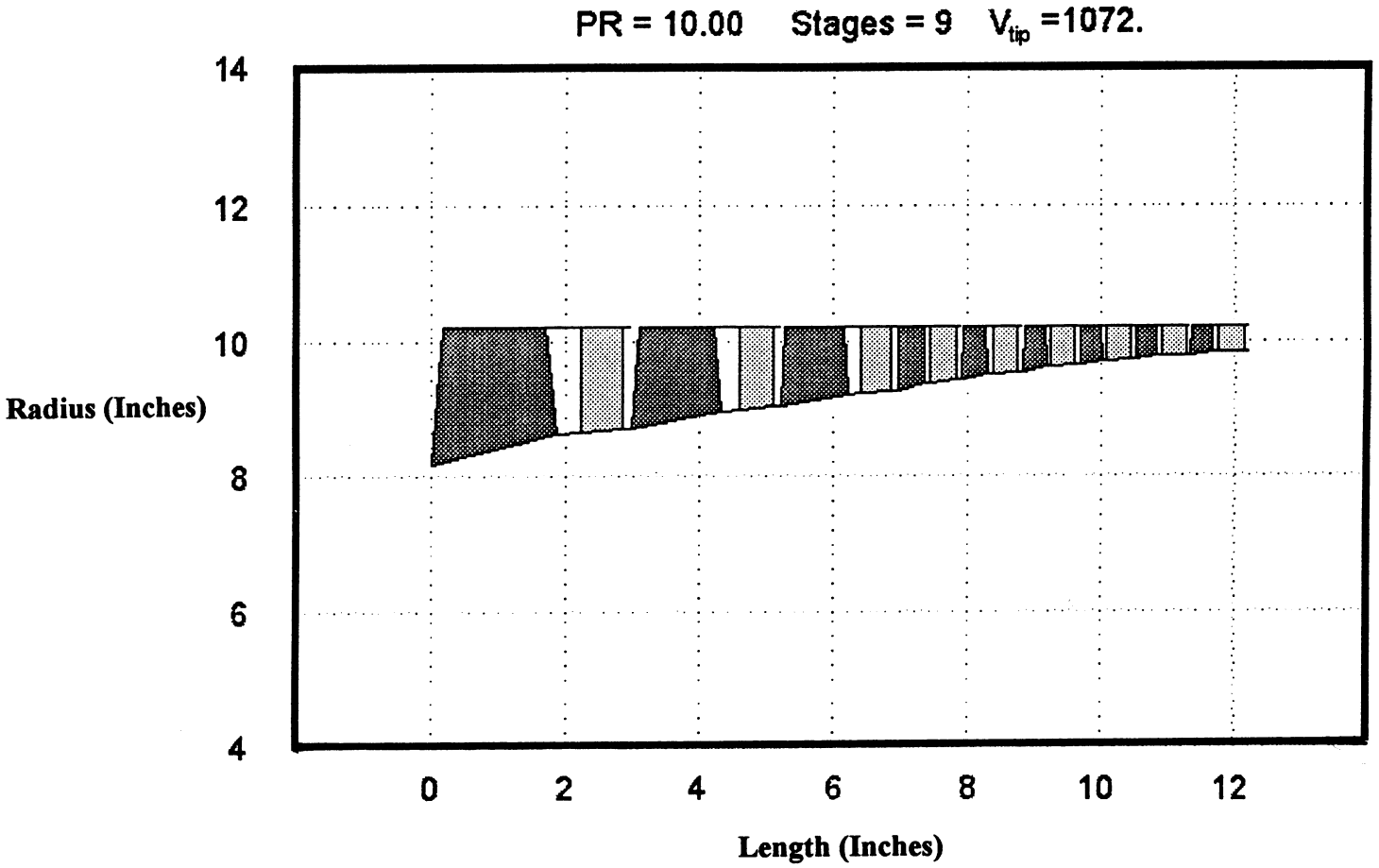

Figure 16. Small-Size Single Spool Exoskeletal Engine – Core Compressor

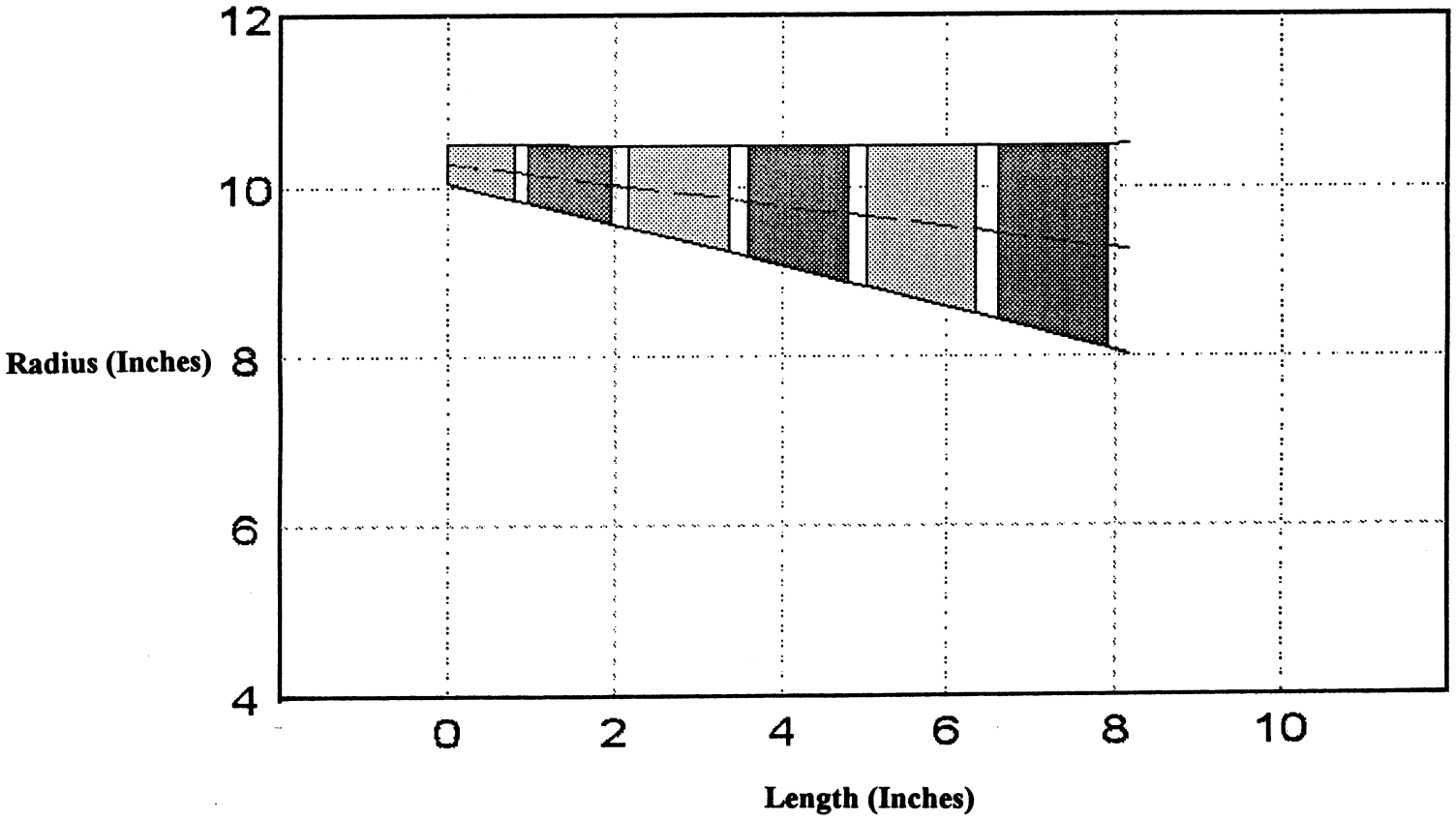

Figure 17. Small-Size Single Spool Exoskeletal Engine – Turbine

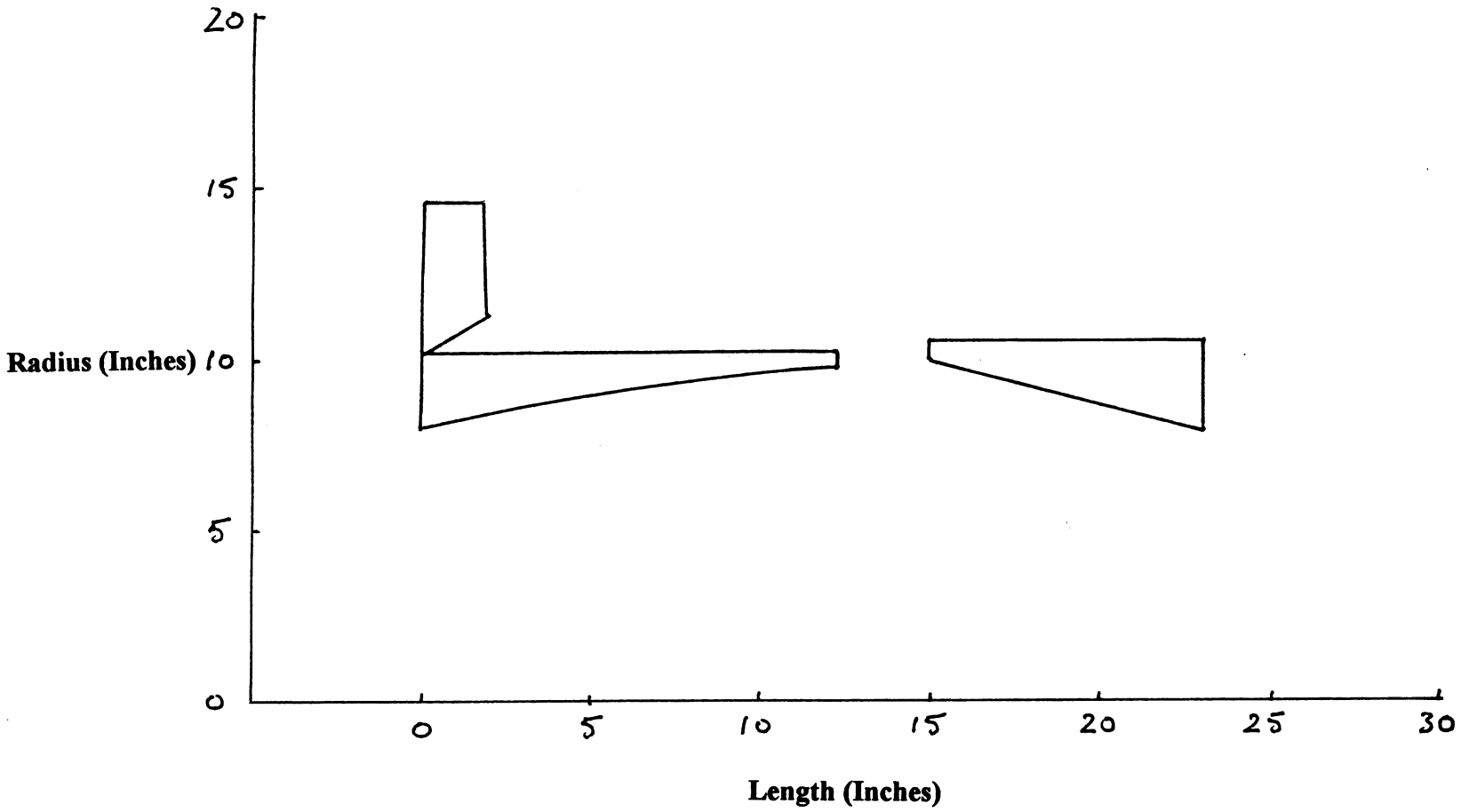

Figure 18. Small-Size Single Spool Exoskeletal Engine - Layout

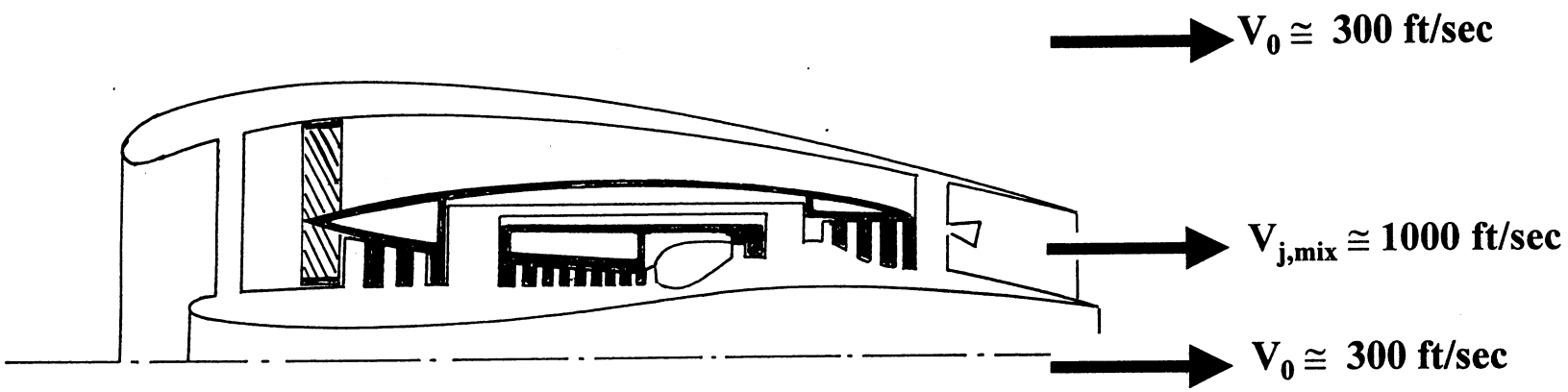

Figure 19. The Exoskeletal Engine Exhaust – a Naturally Inverted Velocity Profile

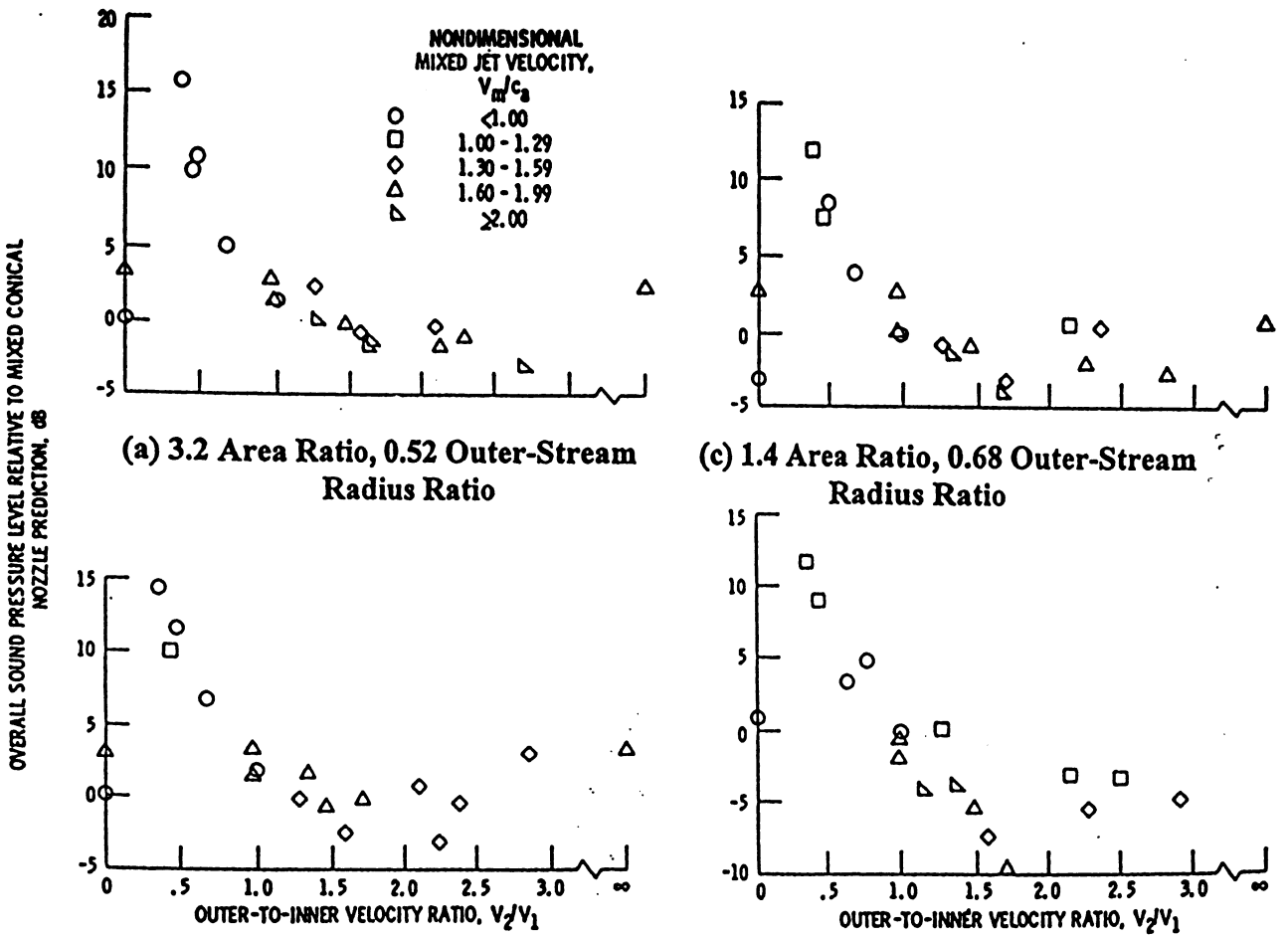

(a) 3.2 Area Ratio, 0.52 Outer-Stream Radius Ratio

(c) 1.4 Area Ratio, 0.68 Outer-Stream Radius Ratio

(b) 1.9 Area Ratio, 0.62 Outer-Stream Radius Ratio

(d) 1.2 Area Ratio, 0.95 Outer-Stream Radius Ratio (Non-Coplanar)

Figure 20. Effect of Velocity Ratio on Noise Relative to Mixed Flow Conical Nozzle Prediction at θ = 139° (*Reference 11*)

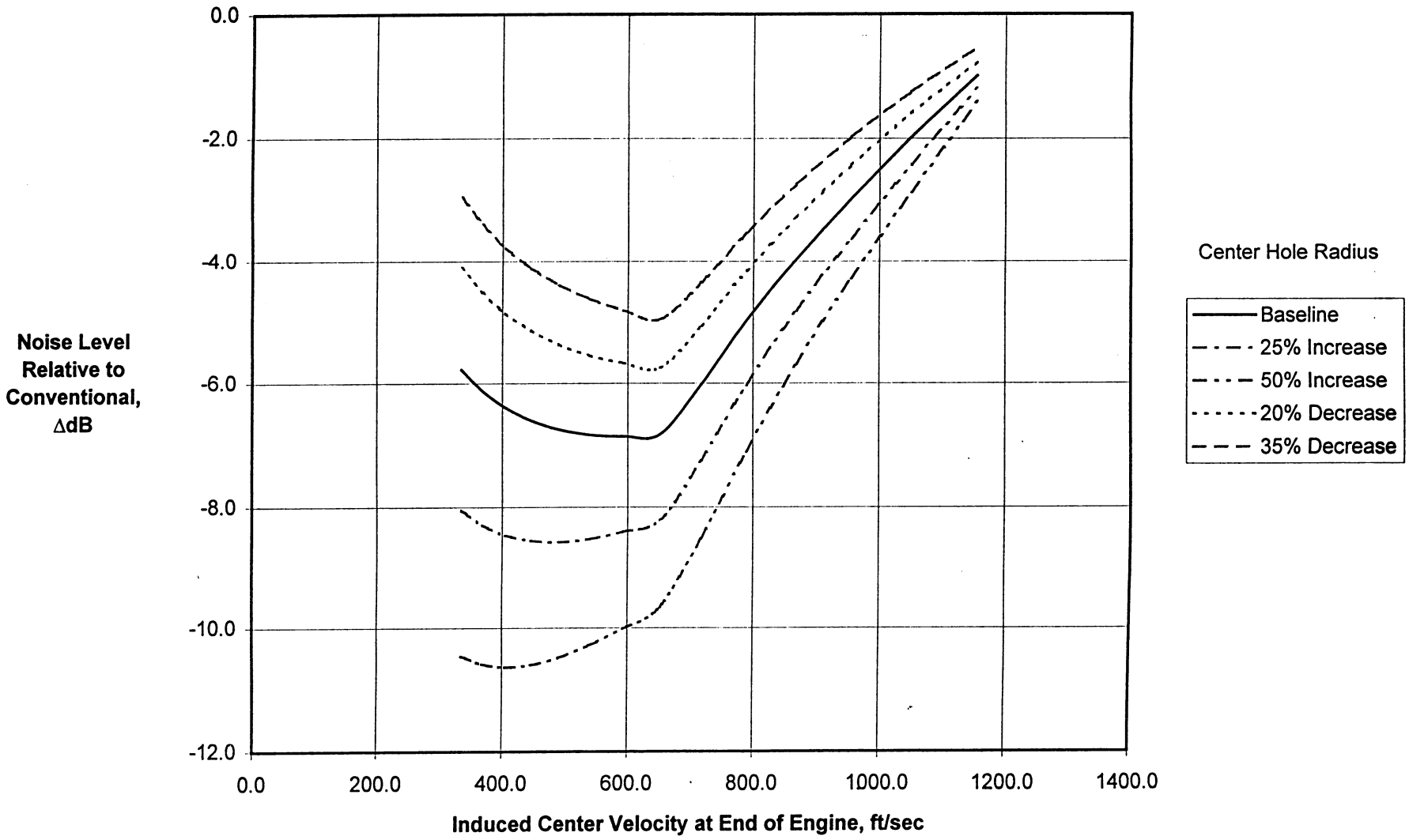

Figure 21. Preliminary Results for Natural Noise Reduction in an Exoskeletal Engine

Feasibility Study of an Exoskeletal Engine Concept

Addendum to "Conclusions & Recommendations in Part 2 – Preliminary Design Studies"

Preface

Following the issue of the above report, it was realized that some of the findings had been misrepresented, with specific results being presented as general conclusions and potential benefits being omitted or understated. It is intended that this amendment should correct any misinterpretations and clarify the conclusions and recommendations.

Ian Halliwell
Modern Technologies Corporation
Tel: (440) 243 8488
e-mail: ihalliwell_mtc@stratos.net

March 6, 2000.

Conclusions

"*Part 2 – Preliminary Design Studies*" is the second in a series of two reports describing a feasibility study of an exoskeletal engine concept. The work was carried out from May to December 1999, with funding from the NASA Glenn Research Center, under Contract *NAS3-27326*. The first report addressed the mechanical aspects of components from a functionality perspective. The objectives of the current report were to examine some of the cycle and performance issues inherent in an exoskeletal configuration and to identify areas of potential difficulty in the preliminary design of turbomachinery.

- The design studies were only cursory examinations of the technical environment, the results were not optimized, and no quantitative conclusions were intended. Rather, the objectives were to indicate technical directions where solutions may lie and to estimate the degree of difficulty of some of the key issues. Twin-spool and single-spool turbofan configurations producing 25,000-lbf thrust, were used as reference vehicles in the mid-size commercial subsonic category. A single-spool turbofan producing 5,000-lbf of thrust was also examined to represent a general aviation application.

- No real problems have appeared. The performance targets proved challenging but attainable, with several aspects of turbomachinery design being of particular interest. It is important to realize that the recommendations for further work do not represent insurmountable obstacles but interesting technical challenges, typical of those encountered in any new engineering enterprise.

- The current initial evaluation has served to reinforce the positive conclusions stated in *Reference 1*, which expressed a belief that that the potential advantages of the exoskeletal engine can be realized and exploited.

- No major problems or obstacles were encountered in the preliminary analysis of the turbomachinery. A number of questions were raised, just as might be expected for any new type of technology, and these will pose interesting challenges for researchers in many branches of propulsion technology over the next few years. It is stressed that none of the challenges appear to be insurmountable.

- The general objective of the flowpath analyses was to assess the difficulty of the design task by applying rudimentary tools and techniques to three possible configurations of the exoskeletal engine: a single-spool mid size engine, a twin-spool mid size engine, and a single spool small engine. No attempt was made to optimize the designs and therefore quantitative interpretation should be made with caution and the limited results from the examples should not be interpreted too broadly. A

number of tentative conclusions may be drawn, with certain qualifying statements, as follows:

- The performance targets, set typically by levels of component efficiency in current conventional engines, are within reach.

- Single-spool, mid size engine.

  - The combination of a high bypass ratio and a high overall pressure ratio is an extreme test of the single-spool exoskeletal configuration. In this 25,000 lbf-thrust system, the choice of 6,000 rpm as the rotational speed is a compromise between the requirements of the fan bypass stream and the core compressor stream. A reduction in rpm would balance out the excessive stall margin and the low adiabatic efficiency in the fan bypass flow, but force an increase in the number of stages in the core because of the lower blade speeds that would occur there. An alternative to the latter action would be to increase the radii of the later core stages, although this would cause radius ratios to increase and blades to become smaller. This result suggests that the single-spool exoskeletal configuration is immediately suited to low bypass ratio, high fan pressure ratio engine cycles found in high speed civil or military missions.

  - The use of a single spool exoskeletal configuration for low speed commercial applications is still extremely attractive, and worthy of further investigation. The examples discussed here have not considered combinations of low radius ratios and high rotational speeds in the search for a design solution, and these should be addressed. In fact there is no real reason why conventional radius ratios cannot be used with an exoskeletal engine, unless the centerline opening needs to be inordinately large. A mid-span shroud that provides torque to the fan also serves as a flow splitter between the bypass and core streams. This means that different blades with variable pitch could be employed in the core to enhance performance and operability, or different amounts of variable blade pitch could be used in each stream. Additionally, further research into the effects of high radius ratios on turbomachinery performance would assist in reducing the disparity between fan and core speeds in a single spool configuration and broaden the range of application.

  - The design of high performance multi-stage turbines for single-spool use does not pose any problems.

- Twin-spool, mid size engine.

  - For the same fan inlet radius ratio, the two-spool engine is considerably shorter than its single-spool equivalent (*Figures 8 & 10* vs. *Figures*

11, 12, & 13). This is due mainly to the ability to use a higher rotational speed on the engine core. In the example discussed in *Section 5*, the high radius ratios were chosen, not mandated, and lower values could have been incorporated just as easily. The HP compressor has been designed at the same mean radius as the booster, but a converging goose-neck duct through the compressor mid-frame could have been used to reduce the inlet radius of the HPC. The tip speeds are acceptable and these could have been maintained by adopting even higher rotational values. Center flow notwithstanding, the design of the turbomachinery in a twin spool exoskeletal engine can follow that of a conventional system. The only new challenge is the determination of the frame configurations.

- The modest values of stage loading coefficient in both the HP and LP turbines (*Table 8*) indicate that smaller mean radii could be achieved, and subsequent optimization would also not only maintain, but would raise the values of efficiency.

- Single-spool, small engine.

  - The discussion in *Section 7* indicates that a small turbofan engine is an ideal first application for a single-spool exoskeletal configuration. With the benefit of hindsight, a significantly higher rotational speed (20,000 rpm or more) could be used in its design along with much smaller radii. These adjustments, together with some optimization, would overcome all of the performance deficiencies of the compression system listed in *Table 10*. As far as the turbine goes, there is no shortage of design options to provide a corresponding superior level of efficiency.

- Noise

The preliminary analysis of the effects of the open centerline on jet noise in *Section 8* indicates huge potential benefits. The situation may be even more rewarding acoustically by tailoring the center exhaust nozzle and pressurizing the flow with air diverted from the core compressor.

- The Future

We are just scratching the surface of exoskeletal potential. The exoskeletal engine is an ideal vehicle for NASA to demonstrate its technical leadership. It has great promise for the future, and if we do not take the initiative, someone else surely will!

Short-term Recommendations

Over the next twelve months or so it is recommended that the following actions be taken.

- The three sample engines above should be optimized in terms of performance and geometry using the design codes currently available. This exercise should resolve many of the issues of radius ratio.

- For a datum engine the minimum diameter should be determined for the centerline duct in relation to a selected level of acoustic benefits. This will provide important guidelines for radius ratio limits in the turbomachinery.

- For the same datum engine the maximum diameter should be determined for the centerline duct in terms of acoustic benefits and overall nacelle diameter.

- Collaborative efforts should be undertaken between the engine designer(s) and materials/structural engineers to generate exoskeletal component models for use in preliminary design. This would enable weight estimates to be made in addition to exploring potential difficulties in manufacture and design.

- An initial set of design guidelines should be compiled for exoskeletal engines to enable equable comparisons to be made during subsequent design studies. Just as for conventional engines, various levels of technology could be established (c.f. *GEN 5, 6, 7*, etc.). This action item would include the definition of rotational speed limits for the casings, material properties and casing thicknesses for the new (ceramic) composites likely to be used, and a possible new design parameter to replace AN^2 in exoskeletal turbines.

    - The free power turbine used to drive the fan in the *GE 36 (UDF)* engine is effectively an exoskeletal construction, albeit with counter-rotating stages. A review should be made of any relevant design issues in order to capitalize where possible. Successful demonstration of exoskeletal technology opens the door to full counter-rotational turbomachinery, in which, by eliminating the "non-working" stators, greater efficiencies and lower weights can be achieved.

- In view of its importance to the end product and of its promise so far, additional acoustics work should be undertaken to further assess the benefits of the IVP nozzle and to refine the prediction code if it is deemed appropriate.

Long-term Recommendations

After the first year, the program should be opened up to include the following.

- Specific application of the exoskeletal engine concept to subsonic, supersonic, and hypersonic missions in both large and small sizes, as appropriate. This will be made easier by the earlier generation of general design guidelines.

    - Collaborative work should be started with the Propulsion Systems Analysis Office at NASA Glenn on systems studies. This organization is the focus of preliminary engine design at the Center, with much necessary expertise and software. NEPP and WATE are the codes that will be used for cycle analysis and for the determination of geometry and weights, either in their existing forms or after the addition of new component models.

    These efforts would eventually include trade studies using cycle, mission, and engine weights and flowpaths in order to identify optimum solutions for selected applications.

    - Cycle & mission studies should be done for turbo-ramjet applications

- Component research is needed in the following areas.

Mechanical design/Structures

- The application of ceramic composites to the construction of exoskeletal hardware; rotating casings, fans with mid-span shrouds, turbines with tip shrouds, etc.

- Structural dynamics of exoskeletal blades, failure modes, etc.

- Containment. The rotating casing has three roles – blade support, bearing support, and containment. Their successful integration is critical.

- Bearings. Oil-free bearings are very attractive, and the use of magnetic bearings to start the engine is even more so.

- Component lives

Aerodynamics

- Fans. In a stratified fan, the use of different blade designs is possible, with different degrees of variable pitch in inner and outer streams.

- Hub leakage characteristics. The effect of reduced blade speed in the clearance region should be investigated. Also the means of hub sealing, in the form of hub shrouds, trenches, etc is well worth studying in both compressors and turbines.

- If radius ratios should prove to be significantly different from those we currently encounter, their effect on the design of turbomachinery will become extremely important.

- The effects of the centerline flow area on the overall aerodynamics of the engine should be determined. This work would also address optimization of the exit area, mixing the three exhaust streams, and pressurizing the center stream using compressor bleed. These impact noise attenuation primarily, but also affect installation and engine/airframe integration.

- Industrial participation should be invited as well as input from the Wright Laboratory.

    - The costs of exoskeletal systems should be studied.

Additional Preliminary Design Studies

Summary

This document is the last in a series of three reports describing a feasibility study of the exoskeletal engine concept. The study has been active since May 1999, with funding from the NASA Glenn Research Center, under Contract *NAS3-27326*. The contents of the three reports are as follows.

- "*Part 1 - System & Component Requirements*" (*Reference 1*) addressed the mechanical aspects of components from a functionality perspective. Since any new exoskeletal engine would have to compete with existing devices, the subsystems must fulfill the same functions. The report identifies those functions and how their demands might be met in an exoskeletal configuration.

- "*Part 2 – Preliminary Design Studies*" (*Reference 2*) turned to some of the cycle and performance issues inherent in an exoskeletal configuration and some initial attempts at preliminary design of turbomachinery were described. Twin-spool and single-spool 25,800-lbf-thrust turbofans were used as reference vehicles in the mid-size commercial subsonic category in addition to a single-spool 5,000-lbf-thrust turbofan that represented a general aviation application. The exoskeletal engine, with its open centerline, has tremendous potential for noise suppression and some preliminary analysis was done which begins to quantify the benefits.

- "*Part 3 – Additional Preliminary Design Studies*", the current document, revisits the design of single-spool 25,800-lbf-thrust turbofan configurations, but in addition to the original FPR = 1.6 & BPR = 5.1 reference engine, two additional configurations using FPR = 2.4 & BPR = 3.0 and FPR = 3.2 & BPR = 2.0 are investigated. The single-spool 5,000-lbf-thrust turbofan has been refined and the small engine study has been extended to include a 2,000-lbf-thrust turbojet. This time, more attention was paid to optimizing the turbomachinery. Turbine cooling flows were eliminated, in keeping with the use of uncooled CMC materials in exoskeletal engines. The turbine performance parameters moved much closer to the nominal target values, demonstrating the great benefits to the cycle of uncooled turbines

  Conventional methods for stacking blade sections may need to be modified significantly because of the need to support the blades at the tips. This leads naturally to the consideration of vaneless counter-rotating turbomachinery, which is extremely attractive in exoskeletal systems. This concept offers a reduced parts-count, reduced length, reduced weight, a reduction in the loss sources of about 40% by elimination of the vanes, and "balanced" rotation within an engine.

Ian Halliwell
Modern Technologies Corporation
Tel: (440) 243 8488
E-mail: ihalliwell_mtc@core.com

Contents

1. Introduction

Previous work (*Reference 2*) has indicated that, at relatively high values of bypass ratio, specific challenges arise in the design of single-spool exoskeletal engine configurations because of large differences between the blade speeds of the fan and core compressor. Even though it is felt that a single-spool exoskeletal engine may not be competitive with current large versions of civil twin- or triple-spool powerplants on the merits of sfc and operability, the attraction of a single rotor assembly warrants further exploration. There is further incentive for addressing the single-spool option in the pursuit of acceptable turbomachinery efficiencies. The efficiencies used in the cycle analysis both here and in *Reference 2* were obtained from the twin-spool NASA model, and although they represented no absolute standard, our initial failure to match them in our compressor and turbine designs was a source of dissatisfaction. Since unconventionally high numbers of stages are often required, the efficiency issue was felt to be worthy of more investigation. The mid-size engine studies are covered in *Sections 3 & 4*.

Since the 5,000 lbf-thrust turboshaft in *Reference 2* had appeared to be much more amenable to the exoskeletal approach than the larger mid-size engines, it was decided to examine a 2,000 lbf-thrust turbojet, naturally using a single spool. The 5,000 lbf-thrust-turbofan is discussed in *Section 5*. The examination of the 2,000 lbf-thrust-turbojet is contained in *Section 6*.

Finally, for exoskeletal engine blades fixed at the tip, the free-vortex flow distribution (used in preliminary design to achieve radial equilibrium and define tip and hub characteristics) appears to be unsatisfactory. Although free-vortex designs are normally not carried over into the detailed design stages, some semblance often remains, with more turning being present at the blade hub than at the tip in order to produce constant work across the blade span. This issue has been addressed in *Section 7*, and some suggestions for an alternative approach have been made. The question of radial equilibrium and work variation provides an obvious link between the exoskeletal concept and counter-rotating turbomachinery stages. The merits of counter-rotation are therefore discussed briefly in *Section 8*.

2. Approach

2.1 Engine Cycle - Assumptions

The same reference engine cycle cited in Part 2 of the study (*Reference 2*) has been used to explore potential design improvements in the single-spool exoskeletal configuration. The principal characteristics of this mid-size, subsonic, commercial engine are

- Bypass ratio (BPR) = 5.1, fan pressure ratio (FPR) = 1.6, overall pressure ratio (OPR) = 27.45, turbine entry temperature (T_{41}) = 2960°R.

- Net thrust at take-off = 25,800 lbf.

With the reference values of component efficiencies (*Table 1* below), the mass flow rate required through the engine core is 129.14 lbm/s for a total mass flow rate of 783.0 lbm/s. Only unmixed exhaust streams are considered in the current phase of the study.

In order to examine the effects on an exoskeletal engine configuration of reduced bypass ratios and increased fan pressure ratios at constant thrust, two other combinations are considered for the same level of thrust. These are

- BPR = 3.0, FPR = 2.4
- BPR = 2.0, FPR = 3.2.

In view of previous findings, it was expected that there would be less conflict between the fan and core blade speeds for the latter two configurations using a single spool, since the values of the respective radial dimensions converge as bypass ratio is reduced.

A small, single-spool, exoskeletal, turbofan engine producing 5,000-lbf-thrust was also examined in Part 2. This study has been continued in the current report, where improved efficiency has been pursued. This interesting avenue is explored further, with the preliminary design of a 2,000-lbf-thrust turbojet being undertaken. With the elimination of blade speed differences, it is felt that the installation of such a small exoskeletal engine in a missile could offer an immediate potential application for the new technology in a relatively simple form, with the open centerline being used to accommodate a ramjet.

2.2 Flowpath/turbomachinery

Preliminary designs were generated for the compressor and turbine systems corresponding to the above cycles. When reasonable designs had been achieved, the resulting values of efficiency were substituted back into the cycle to examine the effects. For the turbines, it became clear that the penalties associated with blade cooling were the major cause of a shortfall in performance. Since it is hoped that ceramic matrix composites will be used in the exoskeletal engines to save weight, it was decided to exploit their thermal properties also and eliminate turbine cooling. Consequently, another round of preliminary turbine design was carried out. This resulted in some remarkable, although not entirely surprising, improvements.

3. Mid Size, Single-Spool Engines: Cycles

Using take-off conditions as the design point for the whole engine, a spreadsheet was used to investigate possible exoskeletal configurations at a thrust level of 25,805-lbf. In *Part 2*, matrices were run for various combinations of fan pressure ratio (from 1.6 to 2.4)

and bypass ratio (from 1 to 8), holding the overall pressure ratio at 27.45, the turbine rotor entry temperature (T_{41}) at 2960 °R, and the net thrust at 25,805-lbf. The cycle analysis outputs corresponding to the three cases outlined in *Section 2.1* will be discussed subsequently.

Efficiencies	
$\eta_{AD\ FAN}$	88.5%
$\eta_{POLY\ FAN}$	89.2%
$\eta_{AD\ CORE}$	85.1%
$\eta_{POLY\ CORE}$	90.1%
$\eta_{\ COMB}$	99.5%
$\eta_{AD\ TURBINE}$	94.2%
$\eta_{POLY\ TURBINE}$	92.3%

Table 1. Assumed Efficiencies for Components in the Reference Mid-Size Engine

Values of efficiency assumed for the various components in the cycle calculations are shown above in *Table 1*.

The values are the same as those from the reference engine cited in *Reference 2, Section 2.1*. It should be noted that the cycle calculations and results are no different from those of a conventional turbofan engine, since the means by which the thermodynamic conditions are generated are largely irrelevant at this stage of the work. It should also be noted that in the current cycle calculations, the fan flow is stratified; that is, the bypass and core streams are considered separately. This means that for a single spool engine the pressure ratio through the fan hub is combined with that through the core so that the core pressure ratio becomes identical to the overall value.

Figure 1, originally presented in *Reference 2*, shows that a thrust level of 25,805 lbf may be maintained in a turbofan engine by changing the combination of bypass ratio and fan pressure ratio, and adjusting the engine scale or core flow rate. Substantial improvements in specific fuel consumption may be achieved by increasing the bypass ratio, especially starting from a low value. Increasing the fan pressure ratio has a much smaller impact. However, the useful range of bypass ratio is limited because the core flow simply runs out of energy as the demands of the fan become excessive. *Figure 2* indicates the effect of bypass ratio on total mass flow rate or engine size.

Table 2 shows a few interesting relationships between the core and bypass flow characteristics as the bypass ratio is increased. The core flow is reduced as bypass ratio rises, but this reduction is overshadowed by the bypass ratio. The total inlet flow – core plus bypass - leads to larger engine sizes. In going from a bypass ratio of 2.0 to one of 3.0, the core thrust falls and the bypass thrust increases. Both of these trends are reversed before a BPR of 5.1 is reached, but it should be noted that this behavior is a result of specific combinations of BPR and FPR, and is not necessarily a general conclusion. The total turbine work, extracted from the core flow, must always match that required by the fan and core compressor. The core nozzle pressure ratio varies inversely with the LP turbine specific work - in other words, it is directly related to the energy of the flowfield at the turbine exit. Expansion of the flow to ambient conditions, resulting in the

Parameter	***BPR = 2.0***	***BPR = 3.0***	***BPR = 5.1***
Fan Pressure Ratio	3.2	2.4	1.6
Core Flow (lbm/s)	174.73	153.34	129.14
Bypass Flow (lbm/s)	349.47	460.04	658.63
Core Thrust (lbf)	8,662	6,850	7,462
Core Specific Thrust (lbf/lbm/s)	49.57	44.67	57.78
Bypass Thrust (lbf)	17,143	18,955	18,343
Bypass Specific Thrust (lbf/lbm/s)	98.11	123.61	142.03
Core Nozzle Pressure Ratio	1.673	1.525	2.001
Bypass Nozzle Pressure Ratio	3.086	2.314	1.511
Core Jet Velocity (ft/s)	1594	1436	1857
Bypass Jet Velocity (ft/s)	1578	1326	896
Specific Work from LP Turbine (Btu/lbm)	344.9	353.5	333.7
Specific Fuel Consumption (lbm/hr/lbf)	0.377	0.447	0.510

Table 2. Variations with Bypass Ratio in a Mid-Size, Single Spool, Exoskeletal Turbofan Engine

corresponding jet velocity, is a measure of thrust potential, and total thrust is obtained by scaling the engine core until the combined hot and cold thrust components match the 25,805 lbf requirement.

Note that the overall pressure ratio (27.45) and turbine entry temperature (2860 °R) are held constant. The compressor delivery temperature (1439 °R) is related directly to the overall pressure ratio, and is therefore constant also. It should also be noted that none of the cycle analysis is unique to the exoskeletal engine configuration.

4. Mid Size, Single Spool Engines: Turbomachinery

4.1 Bypass ratio = 5.1, Fan Pressure Ratio = 1.6

In a conventional high bypass fan, the inlet hub radius is limited by the need to have sufficient material in the hub region to hold onto the large fan blades. In an exoskeletal configuration, where the structural integrity of the fan depends on the blades being carried either by the tip casing or by a mid-span shroud, it is possible that the hub radius could be made smaller, thus reducing the overall fan diameter. The blade speeds required to generate acceptable levels of stage pressure ratio and stall margin can be obtained by increasing the rotational speed. The geometric changes to the compression system would also help to reduce the incompatibilities between the tip speed of the fan and the blade speeds encountered in the core compressor. In this second major design iteration, the rotational speed of the single-spool, exoskeletal engine was increased to 6300 rpm with a view to reducing the radius ratios and overall radial dimensions. It was felt that this could be done without affecting the intended function of the free central duct. A possible layout for a single-spool exoskeletal engine is shown in *Figure 3*.

Table 3 shows the fixed design parameters for the turbomachinery components, based on the reference engine cycle. At this point in the exercise, having wrestled already with the efficiency targets in *Reference 2*, it is felt that the performance figures may be slightly over-ambitious!

Table 4 shows some of the design features of the bypass fan and core compressor reached in our attempt to achieve the design targets. The compressor and fan flowpaths are presented in *Figures 4* and *5* respectively.

Compared with the earlier designs in *Reference 2*, both fan and compressor modules have been shifted inward, a difference made possible by the increased rotational speed. The overall hub/tip ratio is 0.282, which is significantly lower than conventional values. The fan tip speed has also been held at a lower value, and it is this that is at least partly responsible for the slightly higher adiabatic efficiency. The value of 80.7% is still 7.8%

Parameter	Fan Bypass	Core Compressor	Turbine
Mass flow rate (lbm/s)	654.64	128.36	105.12
Entry temperature (°R)	518.7	518.7	2960.0[3]
Entry pressure (psi)	14.7	14.7	381.4
Pressure ratio	1.6	27.17[2]	12.56
Adiabatic efficiency	88.5 %	85.1 %	94.2%

Table 3. Target Values for Fan and Compressor Design Parameters in a Mid-Size, Single Spool Exoskeletal Engine, BPR = 5.1

short of the target, and while it is felt that the design could be improved quite substantially, it is by no means certain that 88.5% could be reached while maintaining the rpm. The design barrier is caused by the geometric connection of the fan with the core compressor, which needs to run fast to provide sufficient blade speed to meet its obligations. The HP compressor also falls short of its efficiency target, although only by 0.8% - a deficit that could probably be reduced. The core compressor has a negative stall margin, which is indicative of too low a design speed for this component. The very high value of exit radius ratio implies extremely small airfoils, for which manufacturing tolerances would be hard to maintain. The absolute value of blade span is 0.443 inches, which is probably not impossible by today's manufacturing standards. Shifting the flow path inward could alleviate this, but the consequent loss of blade speed could only be recovered by raising the rpm - at some cost to performance.

The fan and core compressor were designed using *CSPAN*. The number of stages in the core compressor, as well as axial chord lengths, has been driven by the acceptance of a number of default values within the code. Examples of such restrictions are diffusion factors at blade hub and vane tip, aspect ratios, and solidities. The code is also dependent upon the assumption of free vortex conditions to attain radial equilibrium of the flowfield. All of reservations above are quite common in preliminary design and do not detract from the results. Improved efficiencies, a reduced stage count, and shorter overall length are quite possible in the course of continued design efforts.

The reference cycle for the BPR = 5 engine had cooled turbines, and this feature was maintained in the current design. In order to reconcile our cycle results (where T_{41}, the temperature at first blade entry, is specified in the input) with those from the original

[2] The overall pressure ratio is less than the value of 27.45 previously quoted because the inter-compressor ducts have now been eliminated.
[3] T_{41}, the blade entry temperature.

NEPP/WATE reference (where T_4, the temperature at first vane entry, is used as a principal characteristic) some adjustments were made to T_4 and the cooling flow values in order to achieve the required value of T_{41} (2960°R). The total amount of cooling air entering through the vane is 18.92 lbm/s, which is 14.64% of the engine core entry flow, W_2, or 18.0% of the turbine vane entry flow, W_4. Progress in the design of the cooled

Parameter	Fan Bypass	Core Compressor
Number of stages	1	20
Inlet radius ratio	0.48	.59
Rotational speed (rpm)	6,300	6,300
Specific flow rate (lbm/s/ft^2)	42.0	42.0
Tip speed (ft/s)	1669	801
Relative Mach number at blade tip	1.67	0.98
Exit hub speed (ft/s)	n/a	778
Exit radius ratio	n/a	0.97
Adiabatic efficiency (%)	80.7	84.3
Stall margin (%)	27.8	-3.9

Table 4. Design Characteristics for the Fan (Bypass Stream) and Core Compressor in a Mid-Size, Single Spool, Exoskeletal Engine, BPR = 5.1

turbine is shown in *Figure 6*, where an early configuration of the 7-stage turbine is contrasted with the final edition. The table shows a summary of the final results. A general reduction in axial chord lengths combined with an increase in exit area led to an improved adiabatic efficiency, even though that value (85.7%) still fell well short of the design target of 94.2%. The target value had been derived from a combination of an HP- and an LP-turbine from a twin-shaft configuration. Since each of these two separate units was able to be designed at an rpm close to optimum, it is hardly surprising that our combined machine is inadequate by comparison, although we were not penalized for the inter-turbine duct loss. Improvements to the current design could arise from a general reduction in stage loading coefficient due to either an increased number of stages or an outward radial shift. The mean radius at entry was chosen to roughly match the upstream core compressor, and therefore is not particularly amenable to change. More stages may well lead to improved efficiency but it should be borne in mind that there comes a point

at which the benefits of reduced stage loading are outweighed by the friction losses due to many more airfoils. The appearance in a single turbine of many more stages than those to which we are accustomed is a point of special interest in exoskeletal engine technology.

Since it is expected that ceramic matrix composites will be used to a greater extent in exoskeletal engines than in existing powerplants, and this material will be able to withstand high temperatures, it is interesting to consider the effects of eliminating the cooling air from the turbine design. The cooling air has been added to the previous inlet flow, with the assumption that it has passed through the combustor and a T_{41} value of 1960°R has been generated. The results are summarized in *Figure 7*.

Because of the increased flow rate, the specific enthalpy drop per stage is reduced in inverse proportion. If the values stage loading coefficient had been retained, the turbine would have moved inward quite significantly, leading to a reduction in weight. For constant flow areas, the gas velocities would have risen only slightly in the first stage. We have chosen to increase the stage loading from 0.8 to 0.94 in order to hold the mean inlet radius somewhere near the corresponding compressor dimension. We have increased the exit are, via AN^2, to lower the flow Mach numbers and the associated losses. In fact the exit Mach number has become quite low and it would be possible to squeeze the flow more to reduce the flow area and the turbine weight. Since there is no longer a hard limit on exit radius ratio, that too could be reduced, although with a resultant increase in loading values and possible performance penalty. The benefit of coolant elimination is measured most dramatically by the overall turbine pressure ratio and adiabatic efficiency. The pressure ratio has dropped from a value of 13.521 to one of 10.87 and this is reflected in an improvement in efficiency from 85.7% to 91.57%. The latter is much closer to the design target, and is of great value provided the (uncooled) materials can still deliver the component life. A sketch of the engine layout is given in *Figure 8*.

In the original reference cycle the specific fuel consumption was 0.38 lbm/hr/lbf. If the resulting values of component efficiencies are substituted back into the cycle, and the cooling flows are also eliminated the specific fuel consumption becomes 0.42 lbm/hr/lbf. Clearly this is a retrograde step, but elimination of the cooling flows has changed the cycle significantly – the core flow rate has become 121.0 lbm/s so the engine has also been reduced in size. Not all the effects are bad, but the cycle now requires re-balancing in order to make meaningful comparisons. Such an exercise would be a departure from the objectives of the current efforts.

4.2 Bypass ratio = 3.0, Fan Pressure Ratio = 2.4

In any turbofan engine cycle, a reduction in bypass ratio accompanied by an increase in fan pressure ratio results in two significant changes to the geometry. Namely, the differences in radii between the fan and core compressor become less and additional fan stages are required. One way of configuring the compression system is shown in *Figure*

9. The flow enters the fan through a front frame, which provides structural support and routing for fuel and engine services, and may or may not be variable. The total flow then passes through stage 1 of the fan, after which it is split into bypass and core streams. In an exoskeletal engine, the splitter also acts as a mid-span shroud on the second fan blade through which torque is provided from the turbine. The first fan stage is driven via the outer casing, supported by suitable bearings. With this division, the compression system can be analyzed in three parts, as indicated in the figure:

- the complete stage-1 fan
- the bypass stage-2 fan
- the core compressor.

An alternative configuration could have been derived in which the mid-span shroud is carried forward to the first fan stage, leading to complete stratification and separation of the flows. In such a system, different schedules could be contrived for variable stators to give semi-independent control and operation of the two streams.

Parameter	**Fan Bypass**	**Core Compressor**	**Turbine**
Mass flow rate (lbm/s)	460.0	153.3	110.7
Entry temperature (°R)	518.7	518.7	2960.0[6]
Entry pressure (psi)	14.7	14.7	381.4
Pressure ratio	2.4[4]	27.45[5]	16.54
Adiabatic efficiency	86.4 %	85.1 %	92.7%

Table 5. Target Values for Fan and Compressor Design Parameters in a Mid-Size, Single Spool Exoskeletal Engine, BPR = 3.0

Target values for major design parameters are given in *Table 5* above. The pressure ratio and adiabatic efficiency for the core compressor includes the contribution of the fan hub in each case.

Results of the compression systems design exercise are summarized in *Table 6* and *Figures 10 & 11*. In the bypass stream of the 2-stage fan, the required pressure ratio of

[4] Includes stage 1 fan tip
[5] Includes stage 1 fan hub
[6] T_{41}, the blade entry temperature

2.4 is made up of 1.7 through the first stage followed by a second-stage pressure ratio of 1.41 in the outer stream. The pressure ratio of 1.7 across the fan hub also contributes to the core stream, leaving a pressure ratio of 16.54 to be provided by the remainder of the core compressor when adjustments are made for duct losses. This has been achieved in an additional 14 stages. The inlet radius ratio of 0.282 for the first stage was retained from the previous engine, and this led to values of 0.728 and 0.839 for the bypass stream and core stream respectively when the flow was divided according to the bypass ratio. The increased values of specific flow are due, of course, to the density increase through stage 1. Although the tip speed[7] does not change much through the fan, the relative tip Mach number has been influenced by the change in sonic velocity due to an increase in static temperature. Although the fan and compressor components are different from those for which the target efficiencies are quoted, examination of the values in *Table 6* suggests that the required performance has been reached. A combination of 90.04% for the stage 1 fan tip with 79.99% for the second stage fan bypass compares quite well with the value of 86.4% intended, while the overall core performance, made up of 90.04% through the fan hub (we know this is not correct but it is unlikely to be worse!) plus 85.05% for the remainder, should exceed the 85.1% requirement. The only figure of concern is the core stall margin, which at 5% is lower than would be comfortable, but in pursuing this operability feature, additional more sophisticated analysis would be recommended, since the *CSPN* stall margin model is only used as an indicator rather than an accurate prediction.

The cooled turbine design from the original engine cycle is summarized in *Figure 12*. As for the previous engine, the mass flow rates of the mainstream gas at first vane entry and cooling air have been manipulated and reconciled with the value of T_{41} used in the cycle. This has resulted in a value of vane cooling flow that is almost 16% of the vane entry flow. The remaining coolant, amounting to 20.3% of the vane inlet value, is introduced via the first stage blade. The stage 1 loading coefficient (0.82) was selected in order to align the mean turbine radius with that of the compressor exit, and is a fairly modest value by modern standards. An overall inward slope of 9° means that, for an equal work split, the turbine stage loading coefficients would increase gradually with stage number for a constant value of mass flow rate. However, because of the introduction of cooling air, the increased mass flow rate results in reduced values of stage loading coefficient, with a value of 0.80 occurring on stage 6. The average stage loading levels augurs well for efficiency, so the estimated value of 88.18%, falling short of the 92.7% target, is somewhat disappointing. The overall efficiency correlates with the overall predicted turbine pressure ratio of 17.06, which exceeds the intended value of 15.07. It should be emphasized that little optimization has been carried out, and that a fair proportion of the performance deficit could be recovered by more careful selection of blade numbers, aspect ratios, Zweifel coefficients, stage work split, and reactions. These could be used to control the distribution of Mach numbers, flow areas, gas angles, and ultimately, loss components. In comparing target values of turbine efficiency from the engine cycle

[7] It was noticed in the *CSPAN* output file that the effective tip and hub radii are printed, as are the associated velocities. This is an error and should be corrected. The use of effective radii is necessary to calculate flow characteristics, but they have no place in the definition of the hardware, where actual dimensions must be used!

analysis with design accomplishments, it should also be borne in mind that the cycle values are based on first blade entry conditions whereas the design code covers the turbine from the leading edge of the first vane. The cycle does not care what happens between the point of combustion (plane 36) and the first blade entry (plane 41); in the current exercise the distribution of vane cooling air has been chosen to reconcile the mass flow balance and T_{41} with the cycle values.

Parameter	Fan – Stage 1 (Total Flow)	Fan - Stage 2 (Bypass)	Core Compressor
Mass flow rate (lbm/s)	619.6	464.7	154.9
Number of stages	1	1	14
Pressure ratio	1.7	1.41	16.15
Inlet radius ratio	0.282	0.728	0.839
Rotational speed (rpm)	6,300	6,300	6,300
Specific flow rate (lbm/s/ft^2)	42.0	62.3	62.3
Tip speed (ft/s)	1485	1480	1078
Relative Mach number at blade tip	1.52	1.38	1.08
Exit hub speed (ft/s)	n/a	n/a	1054
Exit radius ratio	n/a	n/a	0.98
Adiabatic efficiency (%)	90.04	79.99	85.05
Stall margin (%)	18.8	36.6	5.0

Table 6. Design Characteristics for the Fan (Bypass Stream) and Core Compressor in a Mid-Size, Single Spool, Exoskeletal Engine, BPR = 3.0

The impact of cooling flows on the overall performance may be investigated by allowing all of the turbine flow to enter through the first stage vane, with an appropriate adjustment of the inlet temperature. The results are given in *Figure 13*, where we see a 4.63% improvement in adiabatic efficiency, enabling the design target to be attained. The change in mass flow rate is reflected in many of the other turbine characteristics shown in the table. For example the specific stage work extraction (Δh) is reduced from

70.9 to 60.3 Btu/lbm, and turbine inlet flow function ($W\sqrt{T}/P$) is increased from 16.14 to 21.11. The value of the first stage loading-coefficient has been retained, and this has resulted in a significant reduction in mean radius, caused by a reduction in the required value of mean blade speed. This in turn, implies a reduction in turbine weight, albeit with an inward cant of the combustor. The most dramatic measure of efficiency is seen in the huge reduction in overall pressure ratio – down from 17.06 to 12.65. This is because the greater flow rate means that reduced swirl angles and turning angles (and hence local values of Mach number) are now needed to produce the overall work. Although the current analysis method does not account completely for the beneficial effects of reductions in cooling flow rates, these secondary flows are chargeable to the engine cycle and manifest themselves ultimately as fuel savings or weight reductions.

The sketch in *Figure 14* gives some idea of sizes and dimensions of the BPR = 3 engine. It is shown with the cooled turbine, whose maximum diameter was chosen to be within the inner dimension of the fan bypass duct.

4.3 Bypass ratio = 2.0, Fan Pressure Ratio = 3.2

The bypass ratio was further reduced to a value of 2.0 in order to investigate the possibility of bringing the fan and compressor blade speeds closer to one another. A fan pressure ratio of 3.2 was selected. Cycle analysis resulted in mass flow rates and target values of adiabatic efficiency for the turbomachinery as shown in *Table 7*.

Parameter	Fan Bypass	Core Compressor	Turbine
Mass flow rate (lbm/s)	352.9	176.5	126.0
Entry temperature (°R)	518.7	518.7	2960.0[8]
Entry pressure (psi)	14.7	14.7	387.8
Pressure ratio	3.2	27.45	15.07
Adiabatic efficiency	85.9 %	85.1 %	92.7%

Table 7. Target Values for Fan and Compressor Design Parameters in a Mid-Size, Single Spool Exoskeletal Engine, BPR = 2.0

[8] T_{41}, the blade entry temperature.

A three-stage fan was considered but deemed unnecessary, and a two-stage device was retained. For design purposes, using *CSPAN*, the compression system was divided in a similar manner to the previous engine, namely:

- the complete stage-1 fan
- the bypass stage-2 fan
- the core compressor.

Parameter	Fan Stage 1 (Total Flow)	Fan Stage 2 (Bypass)	Core Compressor
Mass Flow rate (lb/s)	529.5	352.9	176.5
Number of stages	1	1	11
Pressure Ratio	2.05	1.55	13.32
Inlet radius ratio	0.30	0.78	0.82
Rotational speed (rpm)	7,400	7,400	7,400
Specific flow rate (lbm/s/ft^2)	42.0	65.78	65.78
Tip speed (ft/s)	1619	1617	1262
Relative Mach number at blade tip	1.63	1.13	0.84
Exit hub speed (ft/s)	n/a	n/a	1235
Exit radius ratio	n/a	n/a	0.98
Adiabatic efficiency (%)	90.3	90.1	84.1
Stall margin (%)	20.9	6.5	7.0

Table 8. Design Characteristics for the Fan (Bypass Stream) and Core Compressor in a Mid-Size, Single Spool, Exoskeletal Engine, BPR = 2.0

Table 8 indicates that the fan pressure ratio is realized via 2.05 across the stage 1, which applies to the whole flow, followed by a second bypass stage that produces a pressure ratio of 1.55. The overall core pressure ratio (27.45) is obtained from the product of 2.05 through the fan hub and 13.32 through the inner flowpath. The rotational speed has been

increased to 7,400 rpm and this complements the tip radius, leading to a blade tip speed of 1619 ft/s and a relative tip Mach number of 1.63. Both of these values are higher than their equivalents in the BPR = 3 engine, but some justification may be sought from the improved values of efficiency. If the comments made in *Section 4.2* regarding configuration differences are borne in mind, the combination of 90.3% for stage 1 of the fan with 90.1% for the second stage fan bypass would seem to meet the targets expressed in *Table 7* quite easily. In a similar vein, if the stage-1"whole-fan" efficiency of 90.3% can be extended to the fan hub, the combination of 90.3% and 84.1% for the remainder of the core compares fairly well with the overall core target efficiency of 85.1%.

The corresponding flowpath geometries are given in *Figures 15* and *16*. The selection of a 2.05 pressure ratio for the first fan stage has led to a large axial chord for the blade in order to reduce the flow area to the required value - within the limits imposed on inner wall slope and solidity. In retrospect, a three-stage fan with higher aspect ratios on the first two stages might have been more suitable and would have offered more options in regard to forward extension of the splitter/mid-span shroud.

The cooled turbine solution is presented in *Figure 17*. Six stages have been retained, but with the more favorable bypass ratio, it is possible that a 5-stage turbine may have been possible but was not pursued. However, since the resulting efficiency is rather dismal, falling short of the target by almost ten points, it seems that 5-stages would not have been the way to go although some relief could have been obtained by increasing the radius slightly. However, the picture is not as bleak as it might appear because the comments made in *Section 4.2* regarding differences in the entry plane between the cycle and design calculations also apply here.

As for the previous design case, a significant improvement in performance is obtained by eliminating the cooling flow. This is illustrated in *Figure 18*, where an "uncooled" efficiency value of 94.45% is obtained. As for the previous BPR = 3 engine, the resulting increase in flow rate for a constant value of stage 1 loading coefficient has caused an inward shift of the flowpath, and it is this which is responsible for the increase in the height of the exit plane; the exit area has not changed. Once again, the improvement in performance is due to reductions in turning angles required of the increased flow to produce the same overall work.

4.4 Design Envelopes

This is a convenient point in the study to introduce the concept of *design envelopes*. A design envelope is a simple graphical representation of several aerodynamic and mechanical limits within which the designer must work to meet the requirements of the engine cycle. The value of a design envelope is that it assists the design engineer in the simultaneous consideration of all relevant design limits. Design choices are restricted to manageable ranges based on an appropriate level of technology. The technique thereby alleviates an onerous burden for a designer who is relatively inexperienced and improves the rate of convergence to an acceptable, realistic solution for any user. An overall

benefit is that the design cycle time may be reduced considerably. Compressor design envelopes are based on *CSPAN* and are implemented in the code *CDE*. Turbine design envelopes are based on an MTC design code and are applied within the program *TDE*. The background and application of the method are discussed in *References 3, 4 & 5*.

The choice of parameters and specific limiting values is important, indeed critical, to successful application. *Figure 19* contains the design envelope for the fan in the previous example constructed with rpm and first-stage inlet hub/tip ratio as primary variables. As long as the design point falls within the open area (and an open area exists!), all of the design requirements will automatically be satisfied. The four reference design points, used to construct the envelope, are indicated by asterisks although one of them is masked by the final design point, corresponding to a hub/tip radius ratio of 0.3 and rotational speed of 7400 rpm. The open area available to us is triangular, except the small portion on the right, cut off by the upper hub/tip ratio limit line (*hub/tip < 0.6*). Clearly the selected hub/tip ratio is comfortably within the lower limit of 0.2, while the maximum tip radius of 30 inches is also not influential. The maximum tip speed (V_{tip} < 1700 ft/s) and maximum blade turning angle *($\Delta\beta < 40°$)*form the upper and lower borders respectively. The lower limit on adiabatic efficiency (*Eff > 0.85*) falls outside of the envelope and therefore does not restrict us. The design point corresponds to the value of 90.3% given in *Table 8*. Other design limits imposed on *Figure 19* are a minimum stall margin (*Stall > 10%*), a maximum rotor tip diffusion factor ($DR_{tip} < 0.4$), and a maximum stator hub diffusion factor ($DS_{hub} < 0.8$). It is partly fortuitous that the nominal selections of limiting values have resulted in a feasible design space. Current values may need to be changed as we learn more about exoskeletal engine technology. Whether or not a structural limit on exoskeletal fans exists that might over-ride tip speed is of great interest. The appropriate analysis needs to be done to enable any such limit to be considered on the envelope plot.

Figure 20 shows the design envelope for the core compressor. Many of the same design parameters are plotted as in *Figure 19* for the fan. Their limit values have been changed according to their different application. It may be seen that rotor tip diffusion is the major obstacle to size reduction, as the inlet hub/tip radius ratio cannot be reduced without crossing the "$DR_{tip} < 0.4$" limit line. The layout and orientation of the limit lines is completely different from the pattern in *Figure 19*. Careful review and analysis of a design envelope will invariably reveal the reasons for the location and slope of the boundaries. Such examination will often teach us much about the behavior of the particular turbomachine under a given set of circumstances, especially when exploring advanced design concepts.

The design envelope for the last stage of the 6-stage uncooled turbine is given in *Figure 21*. The first stage loading coefficient, another key design variable, is used as the ordinate. For a fixed value of stage work and a fixed rpm, this sets the mean inlet radius, as well as being correlated empirically with efficiency. The scale of the abscissa is now specified by AN^2_{exit}, the product of annulus area at the final stage exit in square inches and rotational speed in rpm. This value is a measure of rim stress in a turbine disk and provides an important link between aerodynamics and structural integrity. AN^2 has been

used here for convenience since it can still be quantified, however it has very little physical meaning in the exoskeletal context.

The envelope in *Figure 21* has been constructed from four reference design points corresponding to the points of intersection of stage-1 loading coefficient values of 0.9 & 0.6 and AN^2_{exit} values of 30×10^9 & 32×10^9. The selected design point coincides with the fourth reference point. The permitted design space is defined by the limits on maximum flow coefficient ($C_x/U < 1.0$), maximum blade turning angle ($Beta < 134°$), and the minimum flow coefficient ($C_x/U > 0.5$). The other visible limits on leading and trailing edge Mach numbers and AN^2 are not of direct influence. The limiting value of AN^2 is 45×10^9. This is set by the level of technology assumed for the engine program and depends on material strength, value of exit temperature, and the overall pressure ratio in the engine. However, a replacement should be sought for use in exoskeletal engine design studies, preferably some combination of characteristics that links the aerodynamics (*Area is driven by Mach numbers, blade spans, swirl angles, and radius ratios. Rotational speed relates to relative Mach numbers and radii*) to structural behavior. (*How does a blade in spanwise compression fail and can this be related to easily defined geometric characteristics?*)

The *CDE* and *TDE* codes permit design envelopes to be constructed for every stage of a multi-stage compressor or turbine, and this facility may be useful in a case of special difficulty. Usually only one stage will be critical to the designer's objectives. In the case of a turbine it is usually the last stage, because he/she has had more options open in the preceding stages and, having used them, may be hard-pressed to achieve overall objectives with a solution to the demands of the final stage. In order that envelopes from different stages are compatible they must be able to be super-imposed. It is for that reason that they must be plotted on common co-ordinates. The first stage loading coefficient and last-stage AN^2 are used as co-ordinates in the construction of design envelopes for all turbine stages therefore. A similar philosophy applies to compressor design envelopes, although quite different variables are used in their implementation.

5. Small Engines: A 5,000 lbf Thrust Turbofan

Progress on the single-spool 5,000-lbf-thrust exoskeletal engine was made mainly on the turbine. The design work from the study in *Reference 2* was not repeated, but some of the results are duplicated here for further discussion and comparison purposes.

Table 9 contains the values of the major design variables and performance targets, including polytropic expressions of efficiency. (It should be noted that the "adiabatic efficiency" of the core compressor given in *Table 9* of *Reference 2* was in fact the polytropic value, and this error has now been corrected.) For completeness, the bypass fan and core compressor designs are shown in *Figures 22 & 23*, with values of some design variables and performance parameters given in *Table 10*. The value of adiabatic efficiency achieved for the core compressor (84.3%) now compares much better with the

revised target value (86.6%). Regrettably, no errors were found in the fan parameters and the 10% short fall still exists between design and target. The fan designs in other systems presented in this report all have better efficiencies despite having similar levels of inlet tip Mach numbers and pressure ratios. It is felt therefore that improvements would result from adjustments to internal details such as wall slope, diffusion factors, aspect ratios, and solidities.

Progress in the turbine design is indicated in *Figure 24*. The configuration shown in the background, with an overall length of about 8 inches, is the cooled turbine from *Reference 2*, *Figure 17*. This may be contrasted with the improved version in the foreground. The adiabatic efficiency stated in *Reference 2* (94.9%) was obtained by calculating performance between the first blade leading edge (*Plane 41*) and the last blade trailing edge (*Plane 48*). This corresponds to the value that appears in the cycle analysis; the cycle does not recognize the first vane. Since the first vane must exist and is accounted for in our turbine design code, it is important to reconcile the differences caused by "book-keeping". These are comprised of losses due to the first vane itself and losses due to the presence of cooling air. Both of these are included in the value shown in *Figure 24*, namely 85.98%.

Parameter	**Value**
Flow rate through engine core (lbm/s)	34.54
Bypass ratio	3.0
Fan pressure ratio	1.6
Overall pressure ratio	10.0
T_{41} (°R)	2600
$\eta_{AD\ FAN}$ (%)	88.5
$\eta_{POLY\ FAN}$ (%)	89.2
$\eta_{AD\ CORE\ COMPRESSOR}$ (%)	86.6
$\eta_{POLY\ CORE\ COMPRESSOR}$ (%)	90.1
$\eta_{AD\ TURBINE}$ (%)	91.6
$\eta_{POLY\ TURBINE}$ (%)	90.0

Table 9. Target Values for a 5000 lbf Thrust, Single Spool, Exoskeletal Engine

Physical improvements are evident in the final turbine design in *Figure 24*. The axial chords have been reduced and this has led to lower values of both profile and secondary losses. The improved overall efficiency is also due to an increase in the input value of AN^2 (from 20×10^9 to 25×10^9) that has resulted in lower exit Mach numbers (from 0.68 to 0.52) and a lower exit radius ratio (from 0.77 to 0.74). All of these contribute to reduced length, a reduced outer diameter, and reduced weight.

Parameter	Fan Bypass Stream	Core Compressor
Mass flow rate (lbm/s)	103.62	34.54
Inlet specific flow (lbm/s/ft^2)	42.0	42.0
Entry temperature (°R)	518.7	518.7
Entry pressure (psi)	14.7	14.7
Pressure ratio	1.6	10.0
Inlet radius ratio	0.6934	0.80
Number of stages	1	9
Rotational speed (rpm)	12,000	12,000
Tip speed (ft/s)	1542	1070
Relative tip Mach number	1.568	1.179
Exit radius ratio	n/a	0.96
Exit hub speed (ft/s)	n/a	1031
Adiabatic efficiency (%)	77.9	84.3
Stall margin (%)	34.1	5.8

Table 10. Design Characteristics for the Fan and Compressor in a 5000 lbf Thrust Single Spool Exoskeletal Turbofan Engine

As in previous engines, it is informative to examine the effect of eliminating the cooling air. This was done by routing all of the mass flow through the combustor and the first

vane. The vane entry temperature, T_4, was also modified so that it matched the value of T_{41} used in the cycle. The design solution for the uncooled turbine is shown in *Figure 25*.

Parameter	Cooled	Uncooled
Number of stages	3	3
Rotational speed (rpm)	12,000	12,000
Mass flow rate at entry to first vane (lbm/s)	29.38	33.22
Δh per stage (Btu/lbm)	80.8	78.6
Stage 1 Δh/T	0.029	0.030
Inlet flow function ($W\sqrt{T}/P$)	11.09	12.19
Stage 1 loading coefficient ($\Delta h/2U_m^2$)	0.9	0.9
AN^2_{exit}	25.0×10^9	25.0×10^9
Exit Mach number	0.51	0.51
Exit swirl angle (°)	30.9	32.3
Exit radius ratio	0.74	0.73
Overall pressure ratio	6.01	5.78
Overall adiabatic efficiency (%)	90.5	91.36

Table 11. Design Characteristics for the Turbine in a 5000 lbf Thrust Single Spool Exoskeletal Turbofan Engine

Table 11 shows a direct comparison of the features of the cooled and uncooled turbines. Except for the increased mass flow rate at entry, no input variables were changed. Compared with the mid-size engine, relatively little cooling air has been used – $10\%W_2$ being introduced through the first stage vane and an additional 3% through the blade. The slightly higher mass flow rate resulted in marginally improved efficiencies for the first two stages of the uncooled turbine (90.61% & 90.56% vs. 90.58% & 90.51% if tip leakage losses are neglected) The last stage of the cooled machine performs somewhat better than the uncooled (91.56% vs. 91.21%) due to specifics of the flowfield, but the overall effect leaves the uncooled turbine ahead . This is reflected in the overall pressure

ratios of 6.01 for the cooled turbine and 5.78 for its uncooled counterpart. The lower losses are due to the need for lower turning angles, lower swirl angles and lower internal velocities in the case of the higher mass flow rate.

Note that, in practice, the effect of reduced cooling air would be an increase in T_4 and T_{41} because of improved material properties.

6. Small Engines: A 2,000 lbf-Thrust Turbojet

Parameter	Value
Inlet flow rate (lbm/s)	24.59
Overall pressure ratio	15.0
Entry temperature (°R)	518.7
Entry pressure (psi)	14.7
T_{41} (°R)	2400
$\eta_{AD\ COMPRESSOR}$ (%)	83.3%
$\eta_{POLY\ COMPRESSOR}$	88.2%
η_{COMB}	99.5%
$\eta_{AD\ TURBINE}$	88.5%
$\eta_{POLY\ TURBINE}$	86.7%

Table 12. Target Values for a 2000 lbf Thrust, Single Spool, Exoskeletal Turbojet Engine

A 2000-lbf-thrust exoskeletal turbojet engine was examined because such a device appears suitable for missile propulsion, when combined with the installation of a ramjet in the free central core. Such a small powerplant is also attractive because of previous results that indicate more immediate potential for a single-spool exoskeletal concept. Primary requirements for a missile application are small size and low cost, with fuel consumption being of secondary importance. Cycle studies were run for turbine entry temperatures from 1400 °R to 3000 °R and overall pressure ratios from 6 to 26. Assumed values of polytropic efficiencies for the compressor and turbine were 88.2% and 88.5% respectively. The selected design point at sea level static conditions had the following

characteristics: T_{41} = 2400 °R, OPR = 15, sfc = 0.83 lbm/hr/lbf, with a mass flow rate of 24.6 lbm/s being required to produce the 2000-lbf thrust at sea level take-off. The performance figures constitute the design target values that are specified above in *Table 12*.

The compressor and turbine designs are shown in *Figures 26 & 27* respectively, with further details being listed in *Tables 13 & 14*.

Parameter	Value
Mass flow rate (lbm/s)	23.49
Inlet specific flow (lbm/s/ft^2)	41.0
Inlet radius ratio	0.50
Number of stages	12
Rotational speed (rpm)	25,000
Tip speed (ft/s)	1286
Relative tip Mach number	1.34
Adiabatic efficiency (%)	83.2
Stall margin (%)	14.9

Table 13. Design Characteristics for the Compressor in a 2000 lbf Thrust Exoskeletal Turbojet Engine

For the compressor, the overall pressure ratio of 15 was achieved with 12 stages and a rotational speed of 25,000 rpm. An inlet radius ratio of 0.5 was chosen, which resulted in a tip radius of 5.92 inches and a tip speed of 1291 ft/s - a relative Mach number of 1.34, which is fairly modest by previous standards. The modest relative tip Mach number is indicative of the ease by which the target value of efficiency was met since it reflects the overall low level of relative air velocities and associated losses. The moderate stall margin is felt to be adequate for a missile operation.

No cooling was used in the turbine design. It is expected that ceramic matrix composites will be used for construction to achieve low weight and low manufacturing costs. Turbine life is not an issue. A two-stage design was selected and a first-stage loading coefficient of 0.8 resulted in mean radius at inlet that was fairly close to the compressor exit value, with a small negative cant angle being required of the combustor. The design

adiabatic efficiency of 88.5% matches the target exactly. The overall diameter of the engine is less than one foot, and if as much as two inches are allowed axially to accommodate the combustor, the overall length will be about two feet, assuming two inches each for the front and rear frames. The inlet and exhaust nozzle must still be added of course. The results of the turbine design suggest that radial dimensions could certainly be reduced, and although this may be somewhat more challenging for the compressor, an outer diameter of less than ten inches appears feasible. This would leave a free center passage with a minimum diameter of almost four inches.

Parameter	Value
Number of stages	2
Rotational speed (rpm)	25,000
Mass flow rate at entry to first vane (lbm/s)	23.94
Δh per stage (Btu/lbm)	84.3
Stage 1 $\Delta h/T$	0.035
Inlet flow function ($W\sqrt{T}/P$)	5.63
Stage 1 loading coefficient ($\Delta h/2U_m^2$)	0.8
AN^2_{EXIT}	28.0×10^9
Exit Mach number	0.62
Exit swirl angle (°)	21.8
Exit radius ratio	0.76
Overall pressure ratio	3.82
Overall adiabatic efficiency (%)	88.5

Table 14. Design Characteristics for the Turbine in a 2000 lbf Thrust Single Spool Exoskeletal Turbojet Engine

7. Forced Vortex Blade Design

7.1 Radial Equilibrium and Associated Blade Characteristics

In conventional turbomachinery, a high stage pressure ratio (in the case of a compressor) or a high stage work extraction (in the case of a turbine) demands high blade speed, high axial flow velocity, and high turning in the blade row. Between the vane and blade rows, the flowfield can be described by the vortex energy equation

$$\frac{dh_0}{dr} = C_a \frac{dC_a}{dr} + C_w \frac{dC_w}{dr} + \frac{C_w^2}{r}$$

Normally we proceed by prescribing a constant distribution of work across the blade span, which sets the left-hand side of the equation to zero. Usually, for preliminary design purposes, we also require radial equilibrium between vane and blade rows, whereby the inertia forces balance the static pressure field. Radial equilibrium may be described somewhat simplistically by

$$\frac{1}{\rho}\frac{dp}{dr} = \frac{C_w^2}{r}$$

It is also convenient to assume constant axial velocity, so that substitution in the vortex energy equation ultimately results in a free vortex flow, that is

$$C_w r = \text{constant}$$

In other words, we achieve radial equilibrium via

- Constant specific work
- Constant axial velocity
- Free vortex distribution of C_w

This is a simple and convenient way of being able to evaluate flow properties across the annulus in the preliminary design phase of a program. (It is important to be able to assess such parameters as hub reaction and relative tip Mach number even though the design has been based on mid-height values.) Mass flow rate and stage work are also easily calculated. A disadvantage of a free vortex flow is that there are extreme spanwise variations of stage reaction and relative exit angle.

7.2 Application to an Exoskeletal System

The increase in stagnation temperature corresponding to the stage specific work may be expressed as

$$\Delta T_{0s} = \frac{UC_a}{gJc_p}\left(\tan\beta_1 - \tan\beta_2\right)$$

For constant axial velocity, C_a, constant specific work across the blade span is achieved at the tip by combining the relatively high blade speed with relatively little turning. The latter leads to airfoil sections with low camber. This works out well in a conventional turbomachine, with the blade fixed at the hub because the airfoil is secured by the highly cambered, large-chord root section and tapering the blade towards the tip alleviates the root stresses. The small tip chord accommodates the reduced camber quite conveniently.

In an exoskeletal configuration, with the rotor blade attached at the tip, low camber together with a small chord and cross-sectional area may result in inadequate strength at the fixture. Increasing the tip camber, and hence the turning angle would compromise the conventional design criterion of radial equilibrium via constant specific work, constant axial velocity and free vortex flow, but may be essential for successful operation of an exoskeletal compressor or turbine. It should be remembered that radial equilibrium might be reached via other combinations of radial distributions. In practice, radial equilibrium can become a burdensome academic exercise where the difficulties outweigh the benefits. Radial equilibrium ensures that design incidence is achieved by reducing the likelihood of radial excursions by fluid particles affecting the intended flow angles. However, how much radial movement can there be in a real turbomachine as the flow crosses a quarter-inch gap at a velocity of 500 ft/s or higher? Moreover, the effect on performance (i.e. stage efficiency) is likely to be negligible.

It is reasonable to conclude that our approach to the detailed design of turbomachinery for exoskeletal engines should be reconsidered. Constant specific work across the blade span may need to be relinquished, although it may still be possible to retain radial equilibrium if it proves convenient.

8. Vaneless, Counter-Rotating Turbomachinery

Exoskeletal configurations offer a number of potential advantages in terms of engine weight and performance. These are effected by means of a stationary inner assembly and a rotating outer assembly. If the means can be found to rotate both assemblies simultaneously, the stationary, non-working, vanes can be eliminated and the same overall work can be achieved in both compressor and turbines via vaneless, counter-rotating (VCR) systems. VCR is a natural progression of exoskeletal technology and offers the following benefits, with quite substantial advantages compared to current standards.

- Reduced parts counts
- Reduced length
- Reduced weight
- A reduction in the loss sources of about 40%, by elimination of the non-working airfoils, namely the vanes
- "Balanced" rotation within an engine

In the medium term, preliminary design codes should be generated for vaneless counter-rotating compressors and turbines. These codes should include options to select a suitable *forced vortex* flow field. To quantify the potential performance improvements, consider typical compressor and turbine designs, for which efficiency expectations might be 90% and 92% respectively. If we assume, quite reasonably, that 40% of the losses in a turbine are due to the vane rows and these can be eliminated, the loss deficit compared with the ideal situation now becomes, not 8% but 4.8%. If the exercise is repeated for the compressor, we arrive at typical efficiency targets of 94% and 95.2% for compressors and turbines, respectively.

A final thought, if we anticipate the adoption of counter-rotating vaneless systems – a variation for which exoskeletal design seems destined – is that the customary *constant work* characteristic could be maintained quite easily across two adjacent stages. This would avoid the development of extreme differences in temperature between hub and tip locations through multi-stage machines.

9. Conclusions

9.1 General

- No insurmountable problems have appeared. The performance targets, set typically by levels of component efficiency in current conventional engines, proved challenging but attainable, with several aspects of turbomachinery design being of particular interest. These are discussed in subsequent sub-sections.
- It is important to realize that the recommendations for further work do not represent formidable obstacles but interesting technical challenges, typical of those encountered in any new engineering enterprise.
- The current evaluations reinforce the positive conclusions stated in *References 1 & 2*, which expressed a belief that that the potential advantages of the exoskeletal engine can be realized and exploited.

- The general objective of the flowpath analyses was to assess the difficulty of the design task by applying rudimentary tools and techniques to three possible configurations of the exoskeletal engine: a single-spool mid size engine, a twin-spool mid size engine, and single-spool small engines. Because of current limitations of the design tools, limited attempts were made to optimize the design solutions and therefore they do not indicate the complete potential of the exoskeletal concept. Therefore quantitative interpretation should be made with appropriate reservation, within the limits and spirit of the study, and preferably by those with relevant experience.

9.2 Single-Spool, Mid -Size Turbofan

- The combination of a high bypass ratio and a high overall pressure ratio is an extreme test of the single-spool exoskeletal configuration. In this 25,000 lbf-thrust system, the choice of 6,000 rpm as the rotational speed is a compromise between the requirements of the fan bypass stream and the core compressor stream. A reduction in rpm would balance out the excessive stall margin and the low adiabatic efficiency in the fan bypass flow, but force an increase in the number of stages in the core because of the lower blade speeds that would occur there. An alternative to the latter action would be to increase the radii of the later core stages, although this would cause radius ratios to increase and blades to become smaller. This result suggests that the single-spool exoskeletal configuration is immediately suited to low bypass ratio, high fan pressure ratio engine cycles found in high speed civil or military missions.

- The use of a single spool exoskeletal configuration for low speed commercial applications is still extremely attractive, and worthy of further investigation. The examples discussed here have not considered combinations of low radius ratios and high rotational speeds in the search for a design solution, and these should be addressed. In fact there is no real reason why conventional radius ratios cannot be used with an exoskeletal engine, unless the centerline opening needs to be inordinately large. A mid-span shroud that provides torque to the fan also serves as a flow splitter between the bypass and core streams. This means that different blades with variable pitch could be employed in the core to enhance performance and operability, or different amounts of variable blade pitch could be used in each stream. Additionally, further research into the effects of high radius ratios on turbomachinery performance would assist in reducing the disparity between fan and core speeds in a single spool configuration and broaden the range of application.

- The design of high performance multi-stage turbines for single-spool use does not pose any problems. The results from *Section 4.3* show that dramatic improvements in performance may be obtained by the elimination of cooling flows. An increase in efficiency of 11.5% was achieved in the current example, although this should not be viewed as typical.

9.3 Twin-Spool, Mid-Size Turbofan

- For the same fan inlet radius ratio, the two-spool engine is considerably shorter than its single-spool equivalent (*Reference 2 - Figures 8 & 10* vs. *Figures 11, 12, & 13*). This is due mainly to the ability to use a higher rotational speed on the engine core. In the example discussed in *Reference 2, Section 5*, the high radius ratios were chosen, not mandated, and lower values could have been incorporated just as easily. The HP compressor has been designed at the same mean radius as the booster, but a converging goose-neck duct through the compressor mid-frame could have been used to reduce the inlet radius of the HPC. The tip speeds are acceptable and these could have been maintained by adopting even higher rotational values. Center flow notwithstanding, the design of the turbomachinery in a twin spool exoskeletal engine can follow that of a conventional system. The only new challenge is the determination of the frame configurations and the location of bearings.

- The modest values of stage loading coefficient in both the HP and LP turbines (*Reference 2, Table 8*) indicate that smaller mean radii could be achieved, and subsequent optimization would also not only maintain, but could raise the values of efficiency.

9.4 Single-Spool, 5000 lbf Thrust Turbofan

- The discussion in *Reference 2, Section 7* indicated that a small turbofan engine is an ideal first application for a single-spool exoskeletal configuration. With the benefit of hindsight, a significantly higher rotational speed (20,000 rpm or more if permitted by the rotating casing and blade assembly) could be used in its design along with much smaller radii. These adjustments, together with some optimization, would overcome all of the performance deficiencies of the compression system listed in *Table 10*. As far as the turbine goes, there is no shortage of design options to provide a corresponding superior level of efficiency. The analyses done in *Section 5* indicate that elimination of cooling flows produces substantially lower levels of improvement in turbine efficiency than for the mid-size engines largely because much smaller amounts of cooling air were involved in this specific example. An additional 0.86% of adiabatic efficiency was obtained – a worthwhile contribution to sfc.

9.5 Single-Spool, 2000 lbf Thrust Turbojet

- Design of the single-spool 2,000-lbf-thrust turbojet was relatively easy, with all of the performance targets being met. It appears that such a small device offers an immediate application for an exoskeletal engine once the mechanical, material and manufacturing issues can be settled.

9.6 Noise

- The preliminary analysis of the effects of the open centerline on jet noise in *Section 8* of *Reference 2* indicates huge potential benefits, ranging from 4 to 10dB of noise suppression when compared with a conventional untreated round nozzle (*Reference 2, Figure 21*). The situation may be made even more rewarding acoustically by pressurizing the flow with air diverted from the core compressor and tailoring the center exhaust nozzle to optimize the jet velocity.

10. Recommendations

10.1 Near-term Recommendations

Over the next twelve months or so it is recommended that the following actions be taken.

10.1.1 Design Guidelines

- For a datum engine the minimum diameter should be determined for the centerline duct in relation to a selected level of acoustic benefits. This will provide important guidelines for radius ratio limits in the turbomachinery.

- For the same datum engine the maximum diameter should be determined for the centerline duct in terms of acoustic benefits and overall nacelle diameter.

- Collaborative efforts should be undertaken between the engine designer(s) and materials/structural engineers to generate exoskeletal component models for use in preliminary design. This would enable weight estimates to be made in addition to exploring potential difficulties in manufacture and design.

- An initial set of design guidelines should be compiled for exoskeletal engines to enable equable comparisons to be made during subsequent design studies. Just as for conventional engines, various levels of technology could be established (c.f. *GEN 5, 6, 7*, etc.). This action item would include the definition of rotational speed limits for the casings, material properties and casing thicknesses for the new (ceramic) composites likely to be used, and a possible new design parameter to replace AN^2 in exoskeletal turbines and be considered in fan & compressor design, should it become necessary.

10.1.2 Acoustics

- In view of its importance to the end product and of its promise so far, additional acoustics work should be undertaken to further assess the benefits of the IVP nozzle and to refine the prediction code if that is deemed appropriate.

10.1.3 Structural/Mechanical

- In selecting the rotational speeds for the current studies, the lack of solid information regarding the appropriate limits for CMC casings and blades was encountered once again. This emphasizes the need for attention before these uncertainties become impediments to the exoskeletal engine program at an inconvenient time.

10.1.4 Materials & Manufacturing

- Knowledge of the temperature capabilities of CMC materials with respect to cooling needs is especially important.

- Since large rotating casings are a special unique feature of exoskeletal engines, the feasibility of cost-effective manufacture should be established as soon as is practically possible.

- The establishment of limits on trailing edge thickness, surface finish, fillet radii, blade dimensions, etc are all necessary to the cost-effective manufacture of an exoskeletal system that meets performance demands.

- The blades in vaned exoskeletal engines will be rotating under compression and may be constructed from new materials. In addition to the unique operational environment, this in turn may instigate new methods of blade manufacture or original uses of CMC materials, all of which should be investigated sooner rather than later in the exoskeletal engine program.

- It is an appropriate time for the generation of a new materials database with variations in properties with temperature. This would be made available to the systems designers so that weight predictions could be made quickly and reliably once a selection had been made for any particular component.

10.2 Far-term Recommendations

After the first year or so, the program should be expanded to include the following.

10.2.1 Design Tools & Methods

Component models. New methods of application, metrics?

10.2.2 Cycles & Systems Studies

- Collaborative work should be started with the Propulsion Systems Analysis Office at NASA Glenn on systems studies. This organization is the focus of preliminary engine design at the Center, with much necessary expertise and software. NEPP and WATE are the codes that will be used for cycle analysis and for the determination of geometry and weights, either in their existing forms or after the addition of new component models.

- These efforts would eventually include trade studies using cycle, mission, and engine weights and flowpaths in order to identify optimum solutions for selected applications.

10.2.3 Specific Applications

- Specific application of the exoskeletal engine concept to subsonic, supersonic, and hypersonic missions in both large and small sizes, as appropriate. This will be made easier by the earlier generation of general design guidelines.

- Cycle & mission studies should be done for an exoskeletal turbo-ramjet and other hybrid applications. A pulse detonation engine could also be considered in the central core.

10.2.4 Advances in Basic Technologies

Component research is needed in the following areas.

Mechanical Design/Structures

- The application of ceramic composites to the construction of exoskeletal hardware; rotating casings, fans with mid-span shrouds, turbines with tip shrouds, etc.

- Structural dynamics of exoskeletal blades, failure modes, etc.

- Containment. The rotating casing has three roles – blade support, bearing support, and containment. Their successful integration is critical.

- Bearings. Oil-free bearings are very attractive, and the use of magnetic bearings to start the engine is even more so.

- Component lives.

Aerodynamics

- Fans. In a stratified fan, the use of different blade designs is possible, with different degrees of variable pitch in inner and outer streams.

- Hub leakage characteristics. The effect of reduced blade speed in the clearance region should be investigated. Also the means of hub sealing, in the form of hub shrouds, trenches, etc is well worth studying in both compressors and turbines.

- If radius ratios should prove to be significantly different from those we currently encounter, their effect on the design of turbomachinery will become extremely important.

- The effects of the centerline flow area on the overall aerodynamics of the engine should be determined. This work would also address optimization of the exit area, mixing the three exhaust streams, and pressurizing the center stream using compressor bleed. These impact noise attenuation primarily, but also affect installation and engine/airframe integration.

Blade Design

Two activities should be undertaken to assure success in regard to blade design.

- ***Forced Vortex Designs.*** Preliminary design codes for both compressors and turbines should be modified to address non-free-vortex flow fields. It would be prudent to code a number of alternative methods. Generally, two characteristics may be pre-selected by the designer and the third characteristic or distribution of flow property then appears as a consequence of radial equilibrium or other preferred attribute. Examples of *forced vortex* flows could be

    - Linear variation of work
    - Constant reaction
    - Linear variation of exit angle

- ***Vaneless Counter-Rotating Turbomachinery.*** The free power turbine used to drive the fan in the *GE 36 (UDF)* engine is effectively an exoskeletal construction, albeit with counter-rotating stages. A review should be made of any relevant design issues in order to capitalize where possible. Successful demonstration of exoskeletal technology opens the door to full counter-rotational turbomachinery, in which, by eliminating the "non-working" stators, greater efficiencies and lower weights can be achieved.

- In the medium term, preliminary design codes for vaneless counter-rotating (VCR) compressors and turbines should be constructed, and these codes should include options to select a suitable *forced vortex* flow field.

10.2.5 Collaborative Activities

- Industrial participation should be invited as well as input from the Wright Laboratory and DARPA.

10.2.6 Costs

- The costs of exoskeletal systems should be considered.

10.2.7 The Future

- We are just scratching the surface of exoskeletal potential. The exoskeletal engine is an ideal vehicle for NASA to demonstrate its technical leadership. It has great promise for the future, and if we do not take the initiative, someone else surely will!

References

1. *"Feasibility Study of an Exoskeletal Engine Concept. Part 1. System & Component Requirements."*
   NASA Contract *NAS3-27326*.
   Ian Halliwell. December 1999.

2. *"Feasibility Study of an Exoskeletal Engine Concept. Part 2. Preliminary Design Studies."*
   NASA Contract *NAS3-27326*.
   Ian Halliwell. February 2000.

3. "*A User Guide for CDE. A Preliminary Design Code to Generate Compressor Design Envelopes*."
   NASA Contract NAS3-27377.
   Ian Halliwell. September 1997.

4. "*A User Guide for TDE. A Preliminary Design Code to Generate Turbine Design Envelopes. Volume I: The Turbine Design Code*"
   NASA Contract NAS3-27377.
   Ian Halliwell. September 1997.

5. "*A User Guide for TDE. A Preliminary Design Code to Generate Turbine Design Envelopes. Volume II: Turbine Design Envelopes*"
   NASA Contract NAS3-27377.
   Ian Halliwell. September 1997.

Figures

19. Mid-Size, Single-Spool, Exoskeletal Engine, BPR = 2.0: Design Envelope for the Fan

20. Mid-Size, Single-Spool, Exoskeletal Engine, BPR = 2.0: Design Envelope for the Final Stage of the Core Compressor

21. Mid-Size, Single-Spool, Exoskeletal Engine, BPR = 2.0: Design Envelope for the Final Stage of the Uncooled Turbine

22. A 5,000-lbf Thrust Exoskeletal Turbofan: Fan

23. A 5,000-lbf Thrust Exoskeletal Turbofan: Core Compressor

24. A 5,000-lbf Thrust Exoskeletal Turbofan: Cooled Turbine

25. A 5,000-lbf Thrust Exoskeletal Turbofan: Uncooled Turbine

26. A 2,000-lbf Thrust Exoskeletal Turbojet: Compressor

27. A 2,000-lbf Thrust Exoskeletal Turbojet: Turbine (Uncooled)

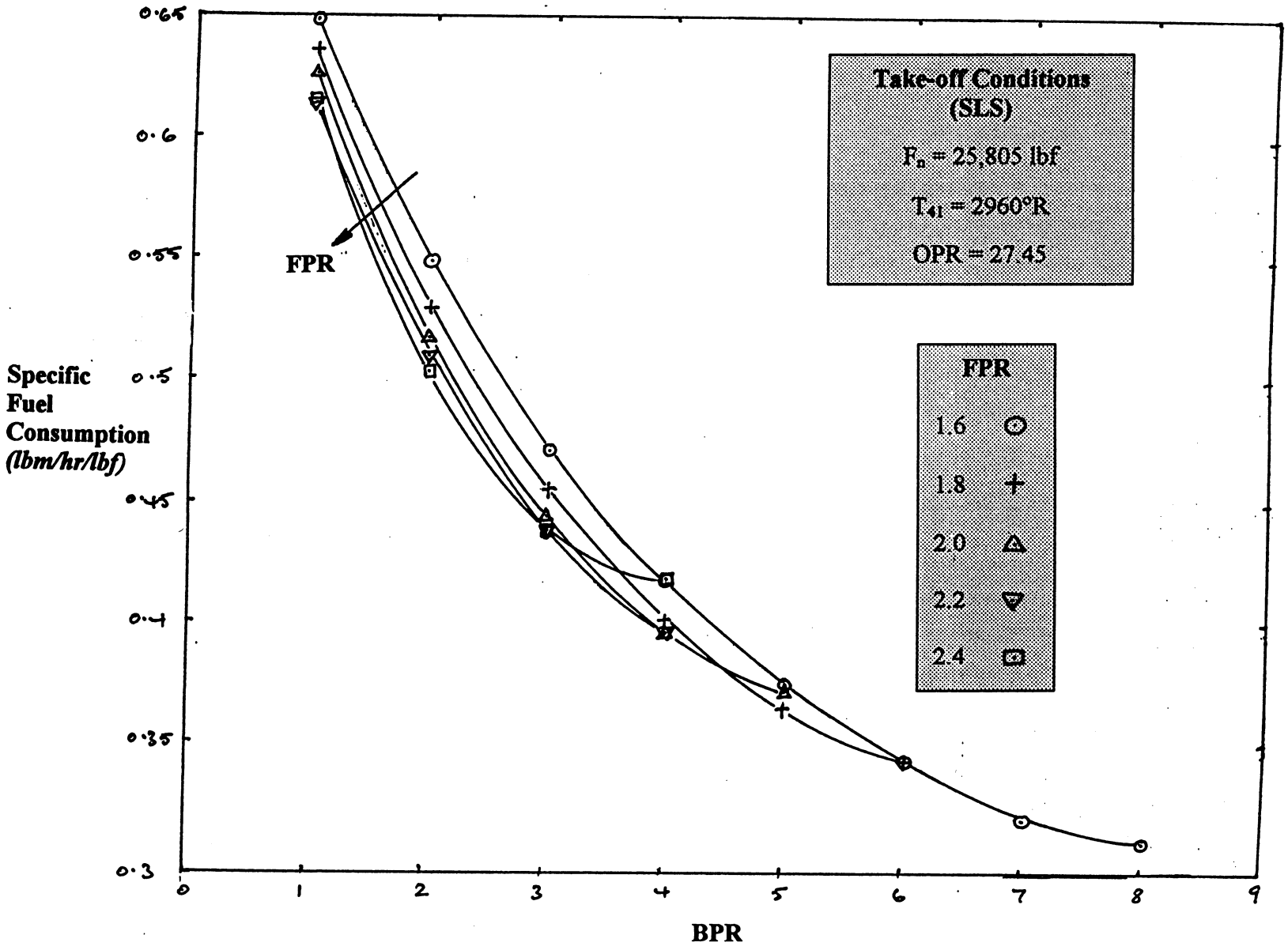

Figure 1. The Effects of Bypass Ratio and Fan Pressure Ratio on Specific Fuel Consumption for a Mid-Size Single-Spool Engine with Separate Exhaust Streams

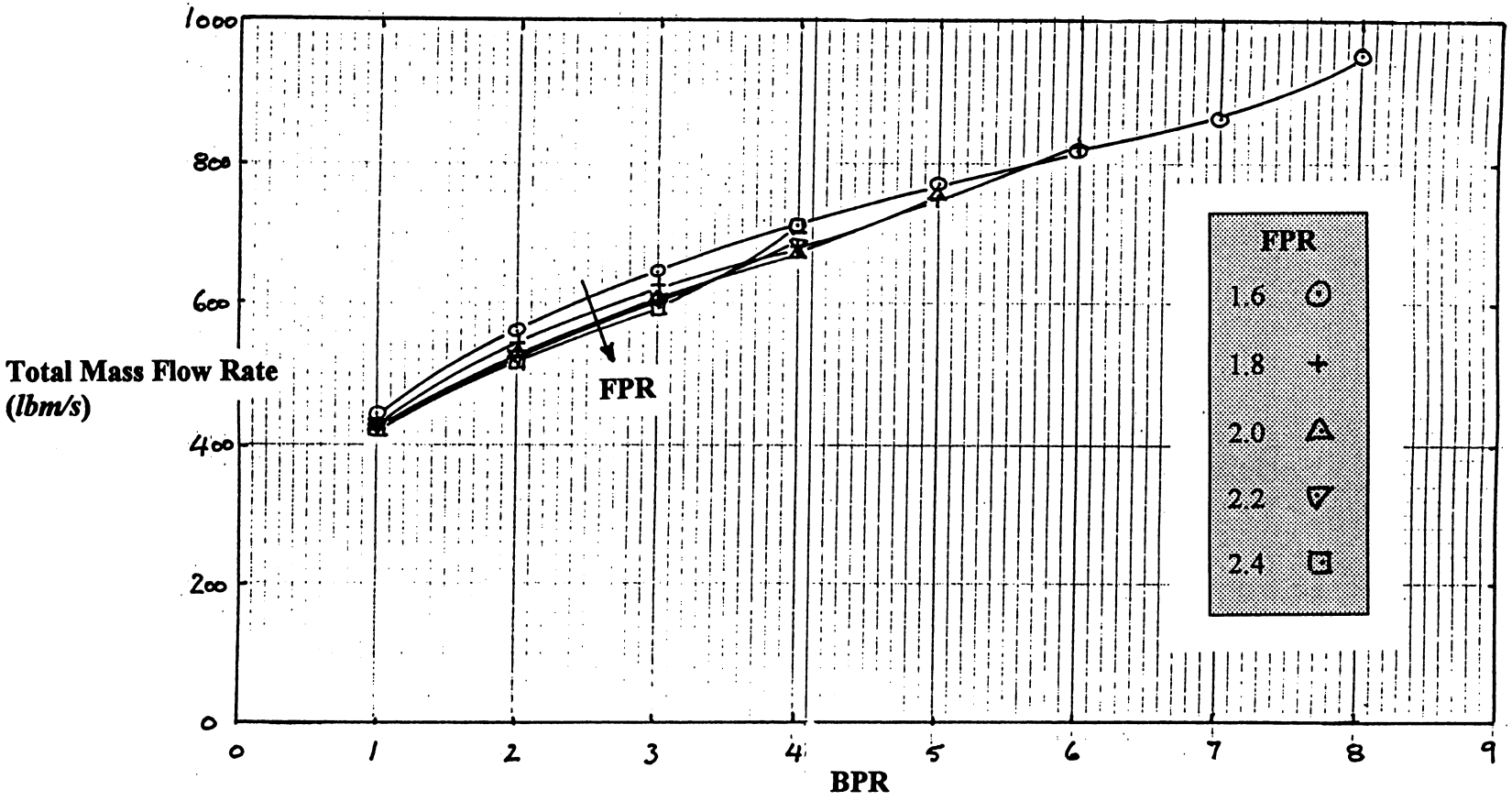

Figure 2. The Effects of Bypass Ratio and Fan Pressure Ratio on Total Mass Flow Rate Required to Produce 25,805 lbf Thrust for a Mid-Size Single-Spool Engine with Separate Exhaust Streams

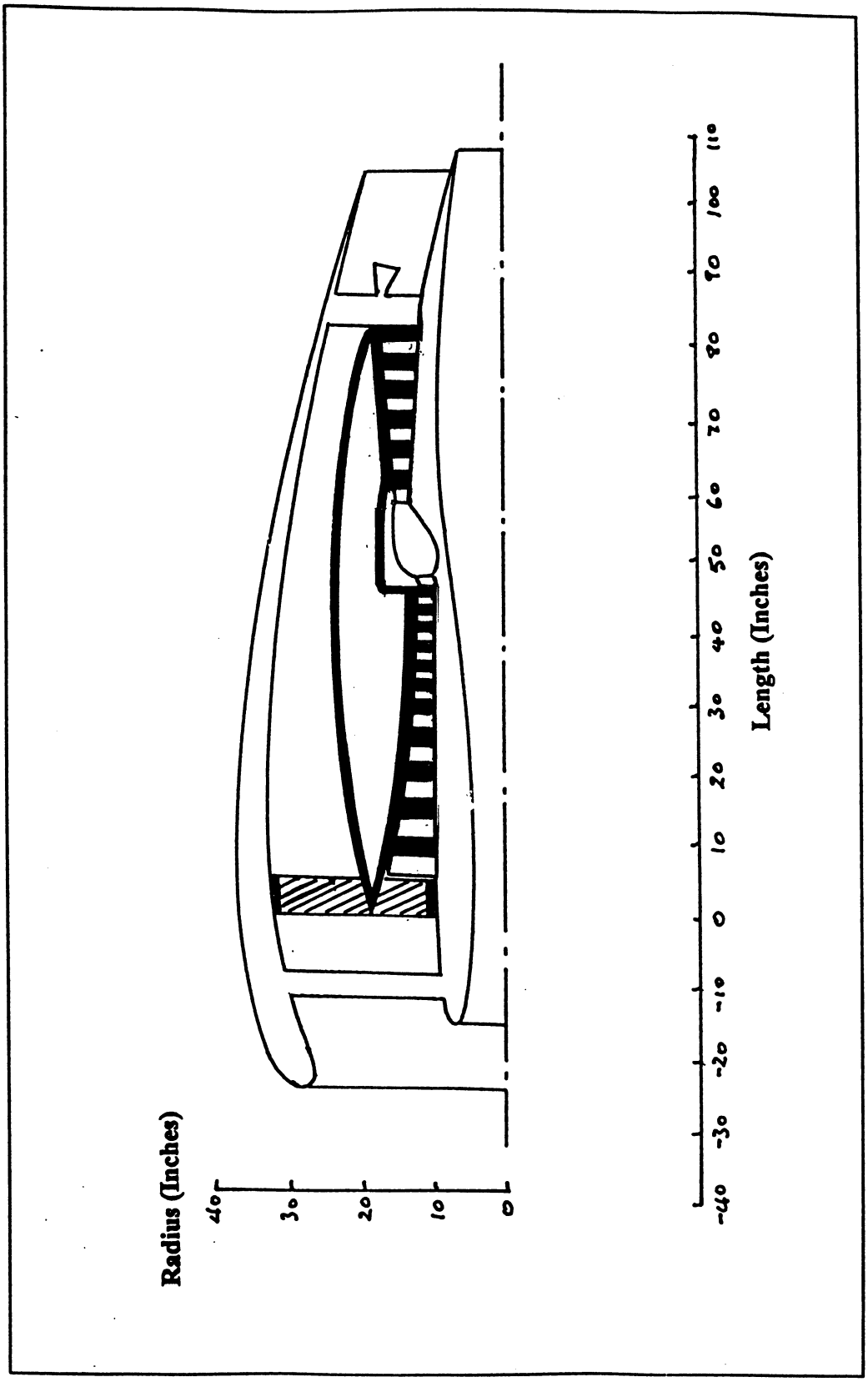

Figure 3. A Possible Single-Spool Configuration for an Exoskeletal Engine

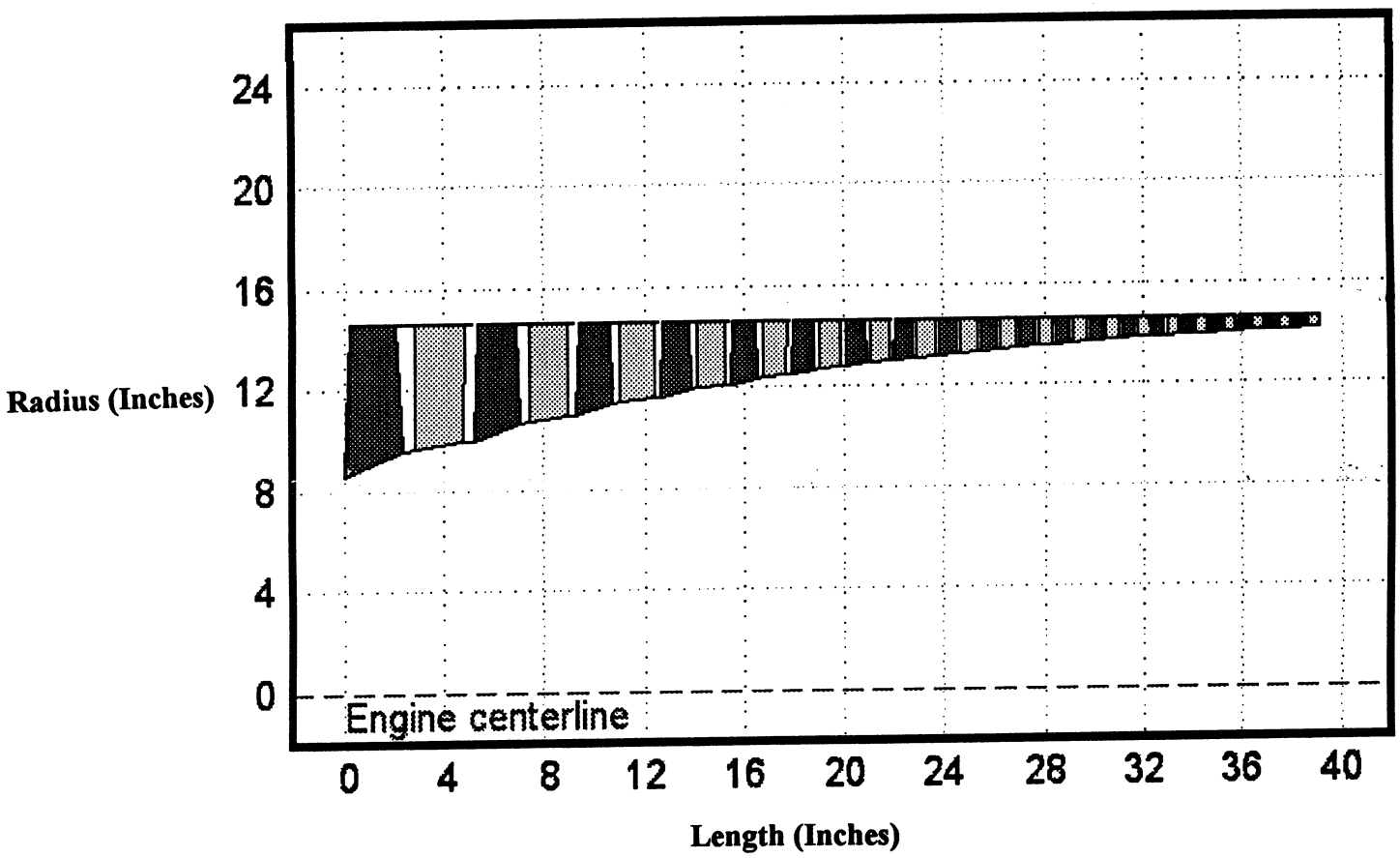

Figure 4. Mid-Size, Single-Spool, Exoskeletal Engine, BPR = 5.1 Core Compressor

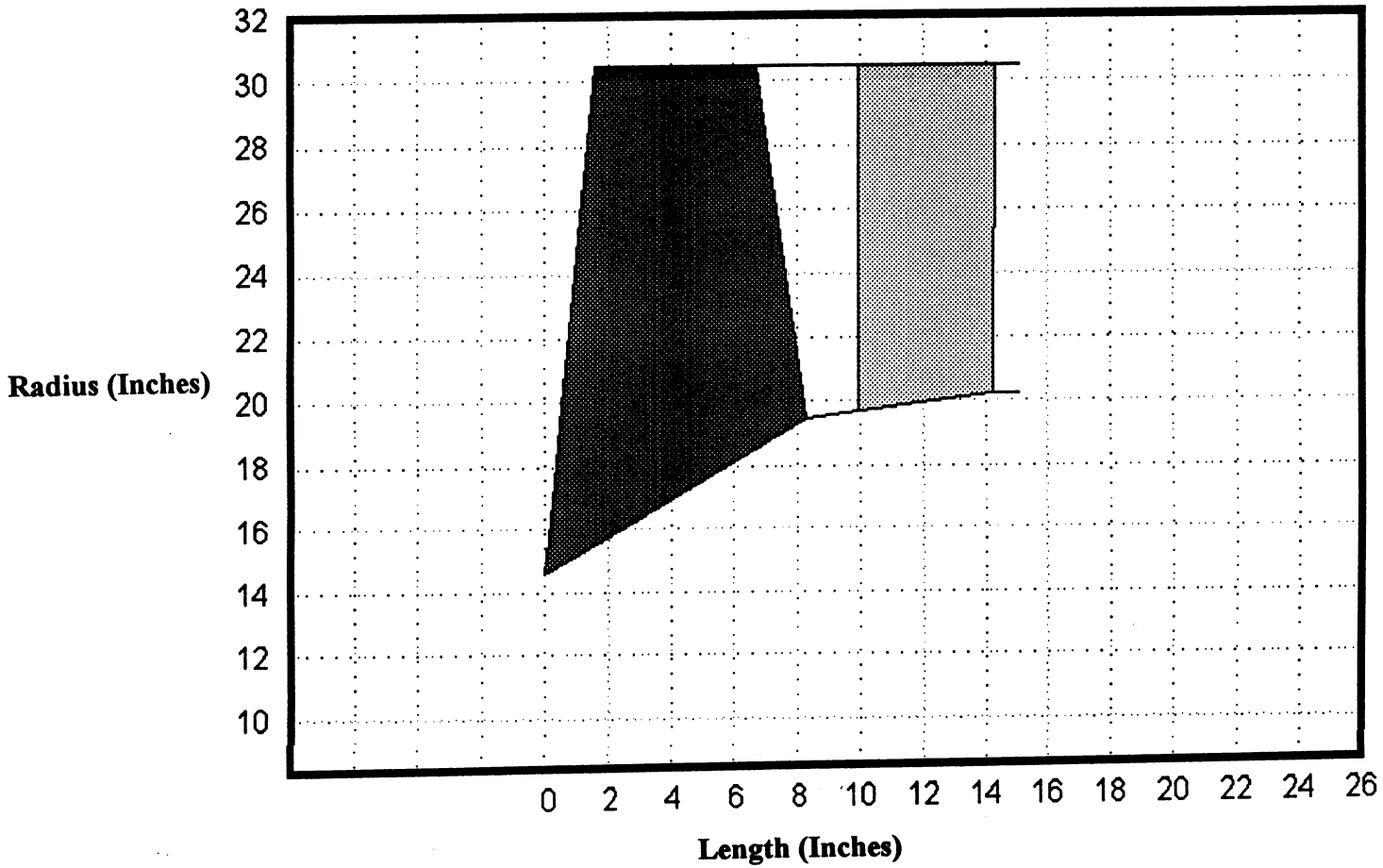

Figure 5. Mid-Size, Single-Spool, Exoskeletal Engine, BPR = 5.1 Fan

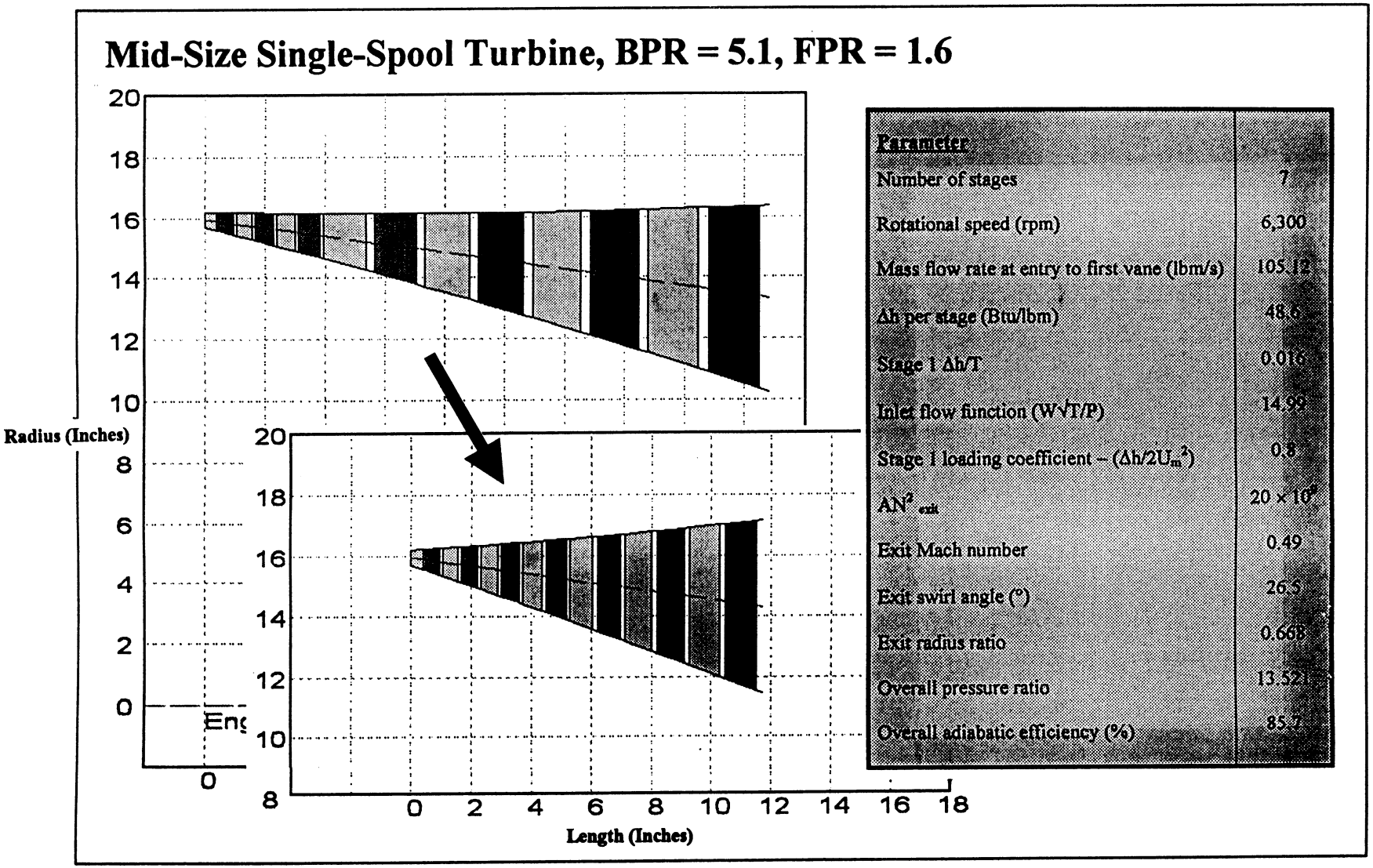

Figure 6. Mid-Size, Single-Spool, Exoskeletal Engine, BPR = 5.1 Cooled Turbine

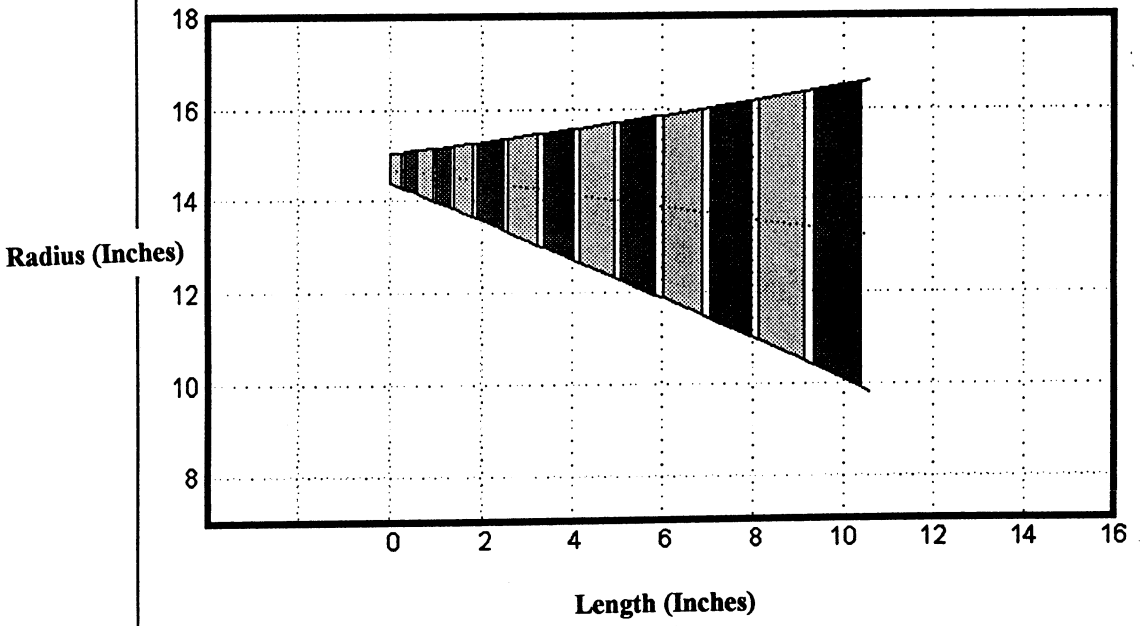

Parameter	
Number of stages	7
Rotational speed (rpm)	6,300
Mass flow rate at entry to first vane (lbm/s)	124.04
Δh per stage (Btu/lbm)	48.8
Stage 1 Δh/T	0.016
Inlet flow function ($W\sqrt{T}/P$)	17.69
Stage 1 loading coefficient – ($\Delta h/2U_m^2$)	0.94
AN^2 exit	22×10^9
Exit Mach number	0.41
Exit swirl angle (°)	37.1
Exit radius ratio	0.59
Overall pressure ratio	10.87
Overall adiabatic efficiency (%)	91.57

Figure 7. Mid-Size, Single-Spool, Exoskeletal Engine, BPR = 5.1 Uncooled Turbine

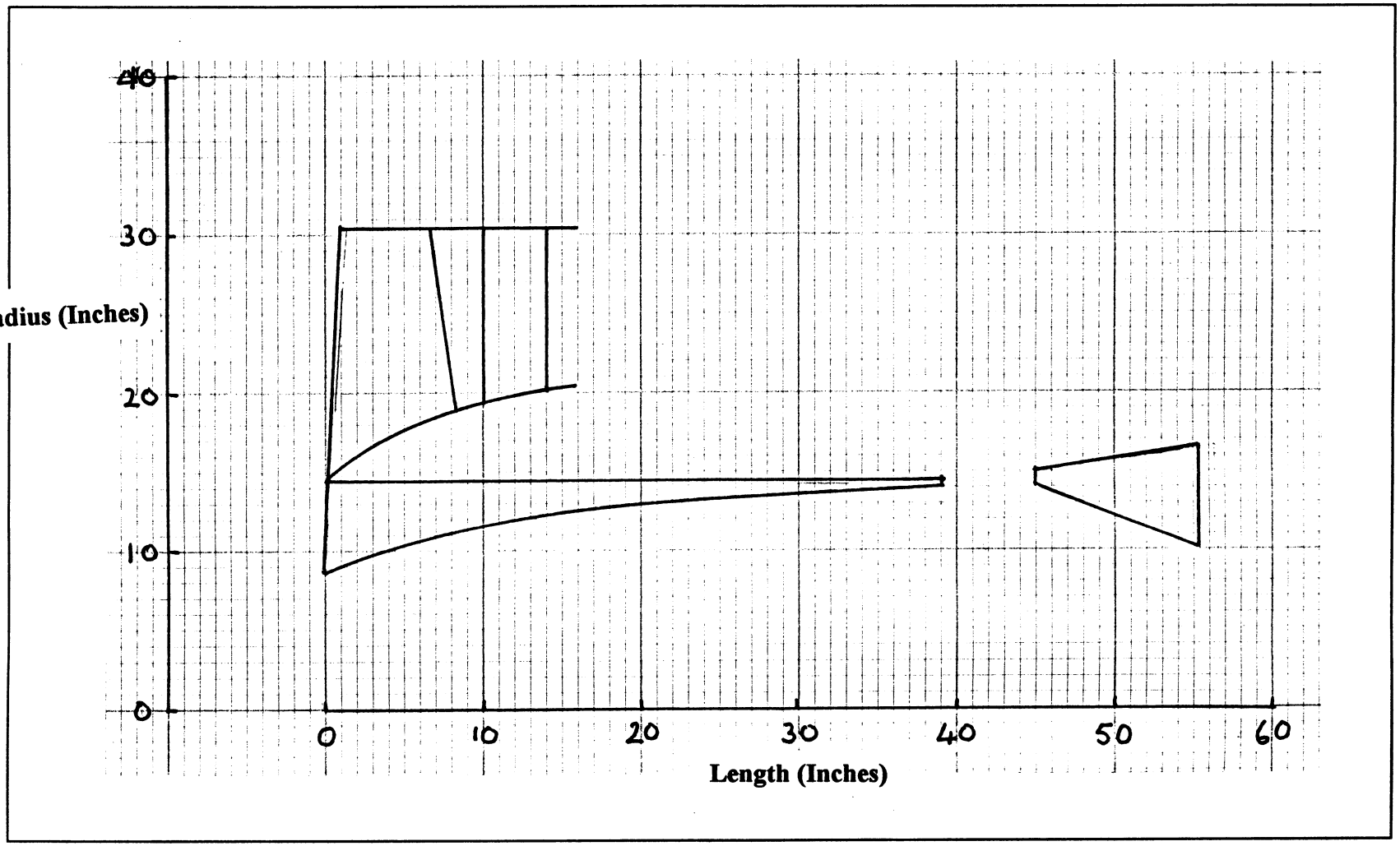

Figure 8. Mid-Size, Single-Spool, Exoskeletal Engine, BPR = 5.1
Engine Layout

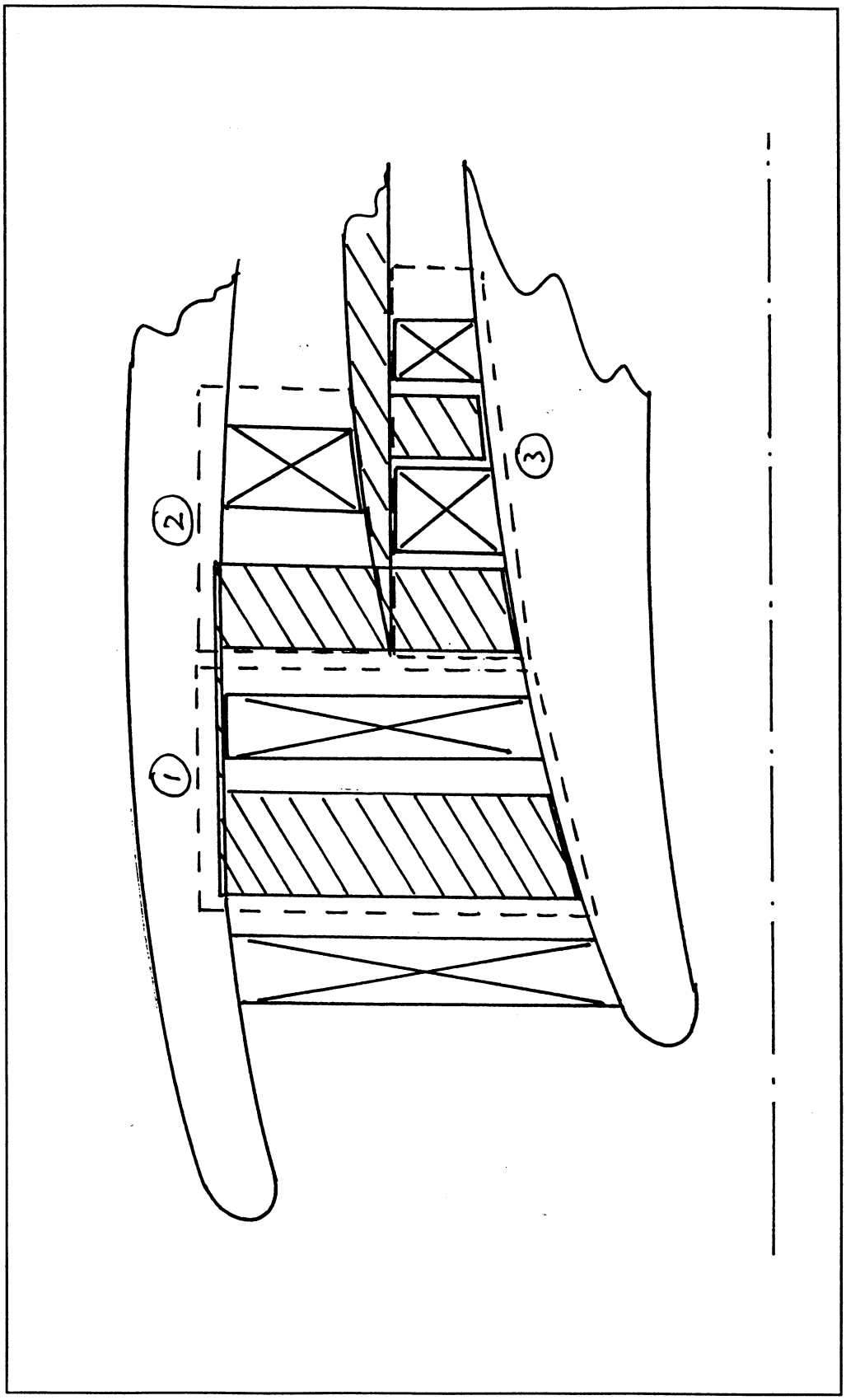

Figure 9. A Possible Split-Fan Configuration for a Low Bypass Ratio, High Fan Pressure Ratio Exoskeletal Engine

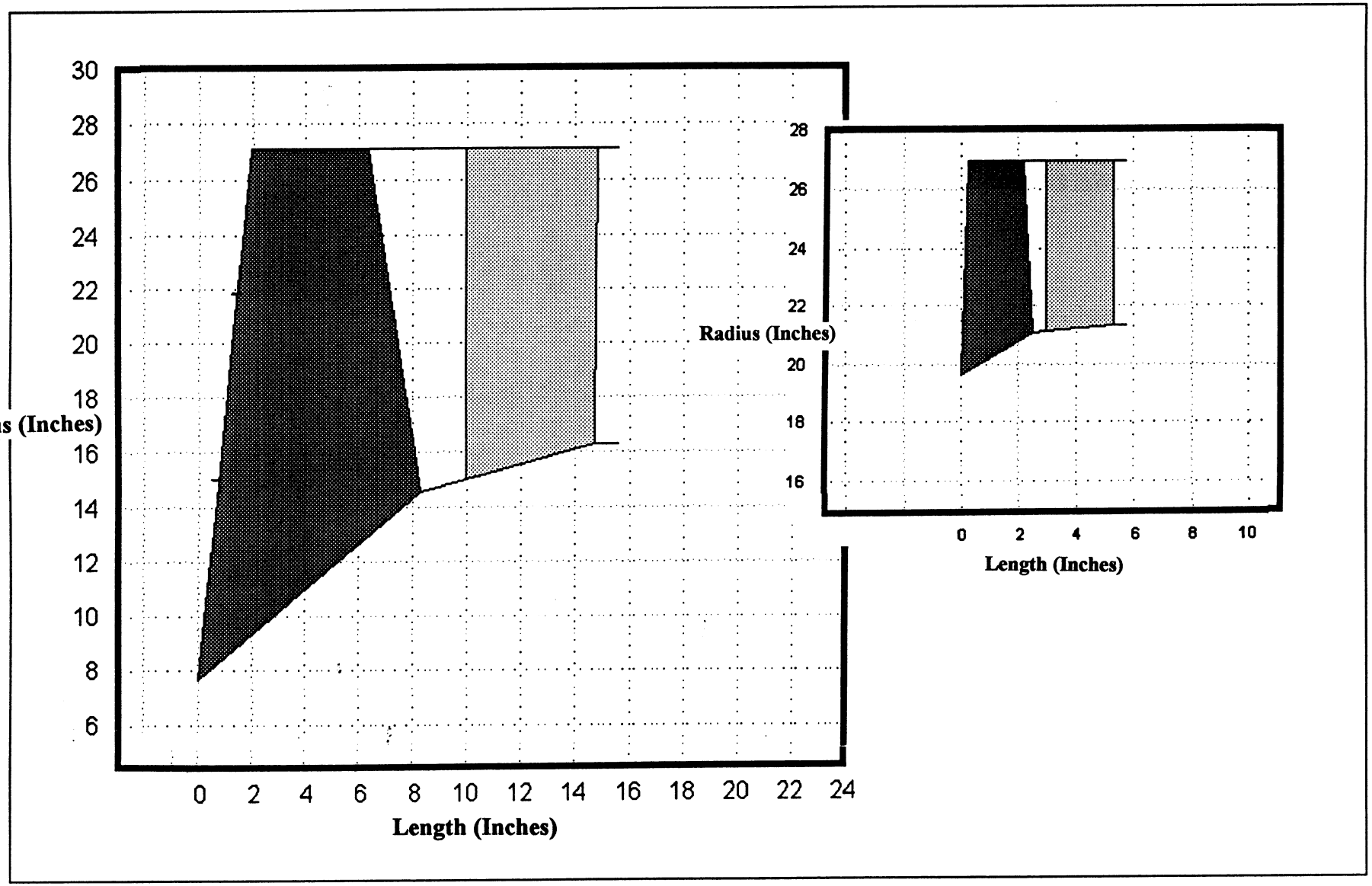

Figure 10. Mid-Size, Single-Spool, Exoskeletal Engine, BPR = 3.0 Fan – Full First Stage & Second Stage Bypass

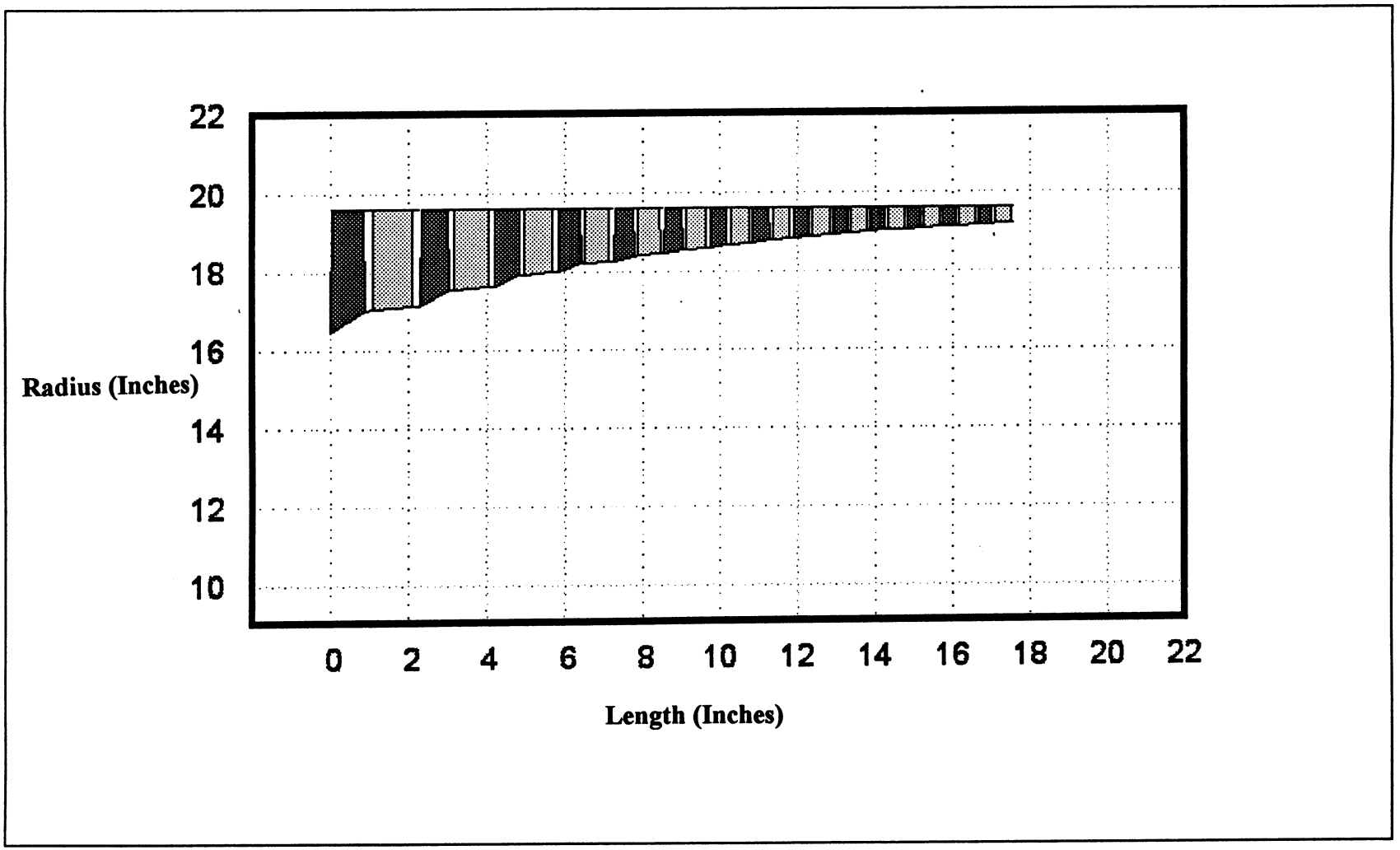

Figure 11. Mid-Size, Single-Spool, Exoskeletal Engine, BPR = 3.0 Core Compressor

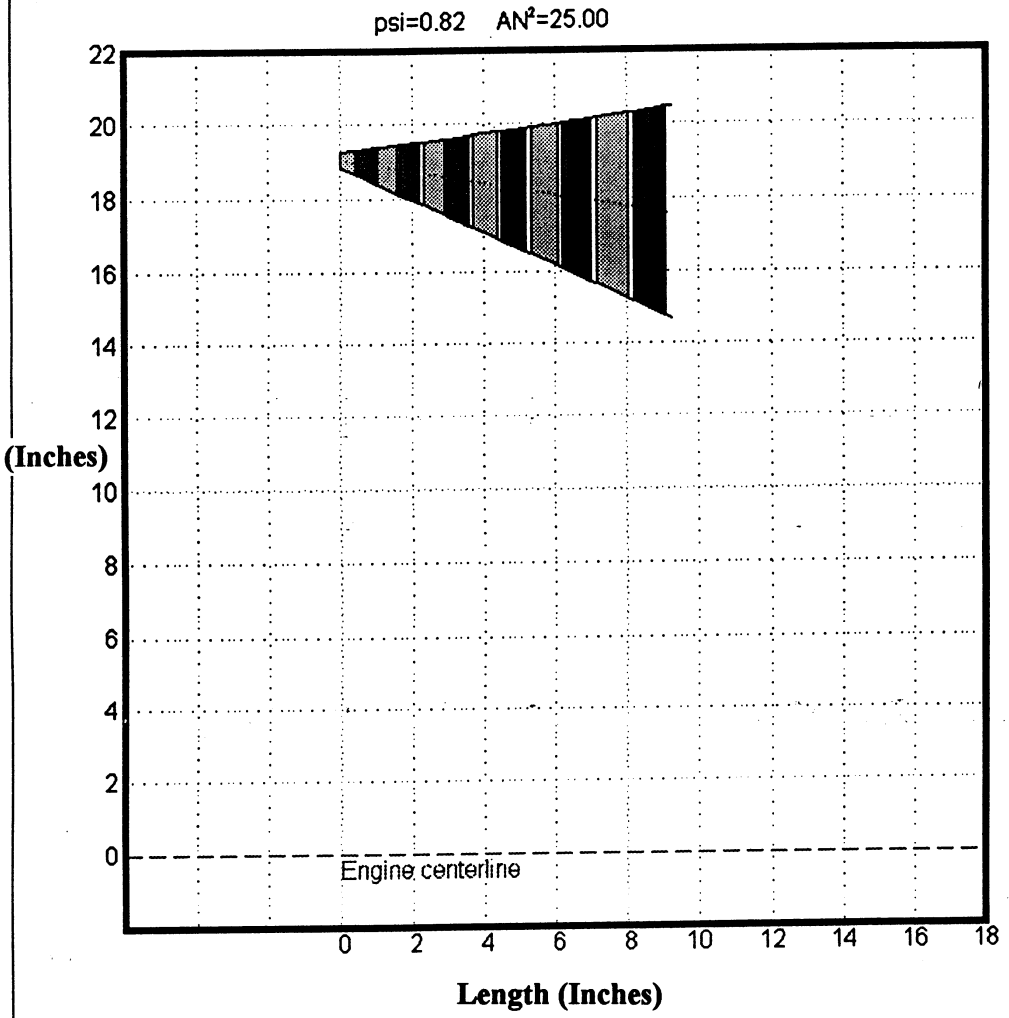

Parameter	
Number of stages	6
Rotational speed (rpm)	6,300
Mass flow rate at entry to first vane (lbm/s)	110.67
Δh per stage (Btu/lbm)	70.9
Stage 1 Δh/T	0.022
Inlet flow function ($W\sqrt{T}/P$)	16.14
Stage 1 loading coefficient – ($\Delta h/2U_m^2$)	0.82
AN^2 $_{exit}$	25×10^9
Exit Mach number	0.578
Exit swirl angle (°)	18.4
Exit radius ratio	0.716
Overall pressure ratio	17.061
Overall adiabatic efficiency (%)	88.18

Figure 12. Mid-Size, Single-Spool, Exoskeletal Engine, BPR = 3.0 Cooled Turbine

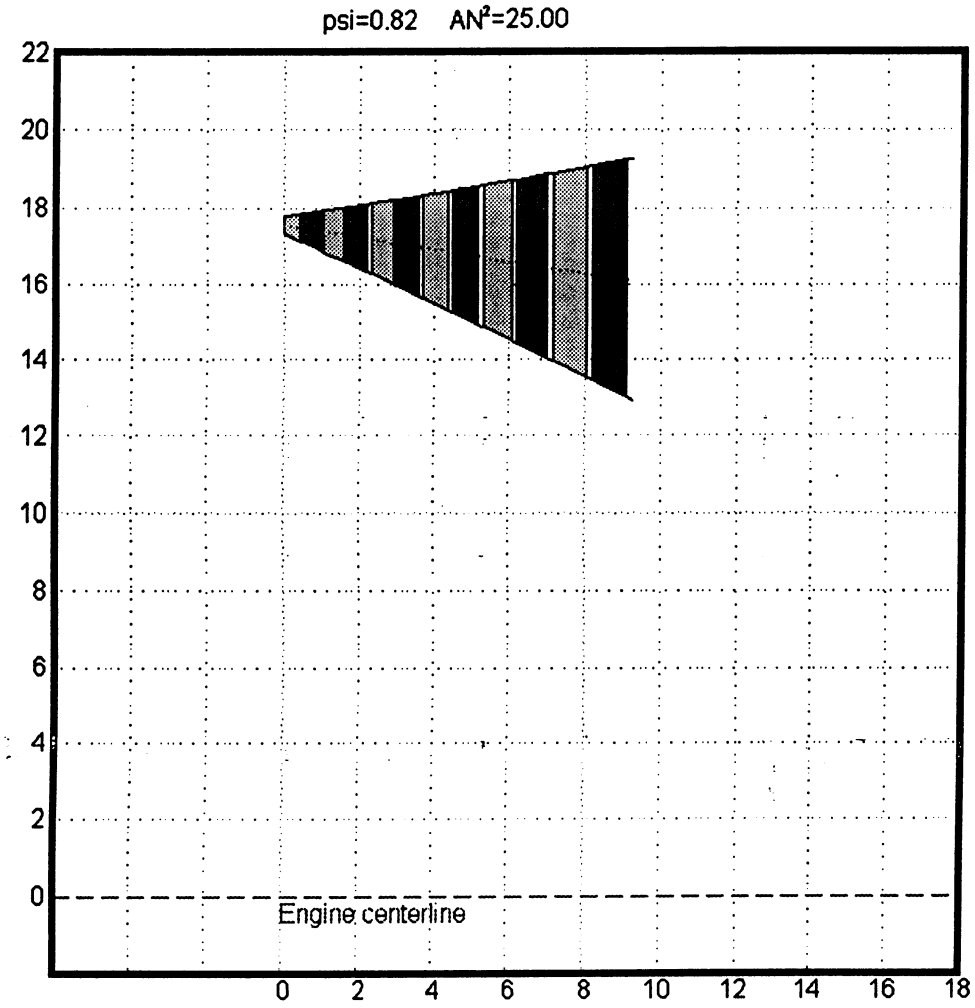

Parameter	
Number of stages	6
Rotational speed (rpm)	6,300
Mass flow rate at entry to first vane (lbm/s)	150.5
Δh per stage (Btu/lbm)	60.3
Stage 1 Δh/T	0.020
Inlet flow function ($W\sqrt{T}/P$)	21.11
Stage 1 loading coefficient – ($\Delta h/2U_m^2$)	0.82
AN^2 $_{mid}$	25×10^9
Exit Mach number	0.467
Exit swirl angle (°)	29.5
Exit radius ratio	0.671
Overall pressure ratio	12.653
Overall adiabatic efficiency (%)	92.81

Figure 13. Mid-Size, Single-Spool, Exoskeletal Engine, BPR = 3.0 Uncooled Turbine

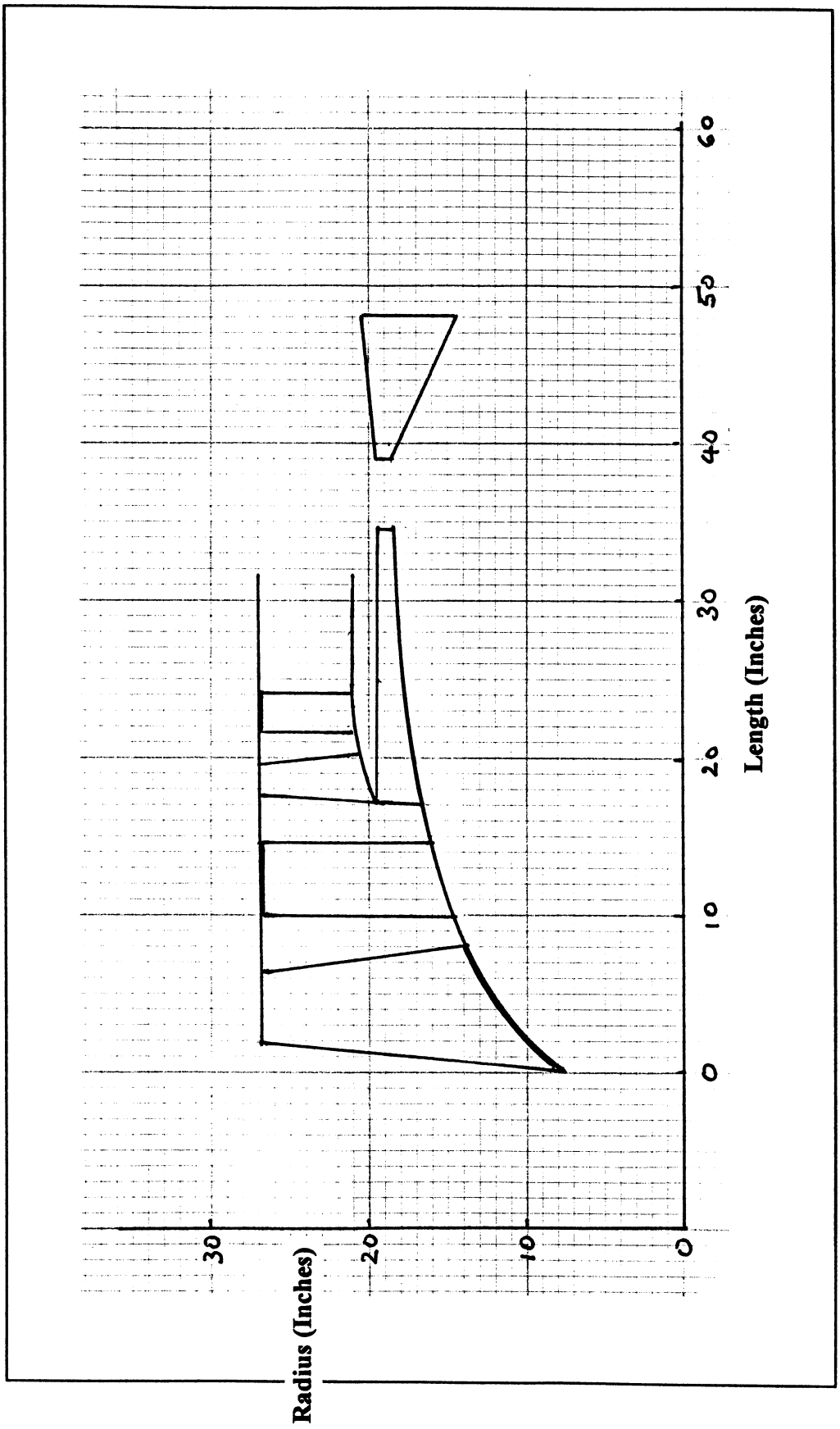

Figure 14. Mid-Size, Single-Spool, Exoskeletal Engine, BPR = 3.0 Engine Layout

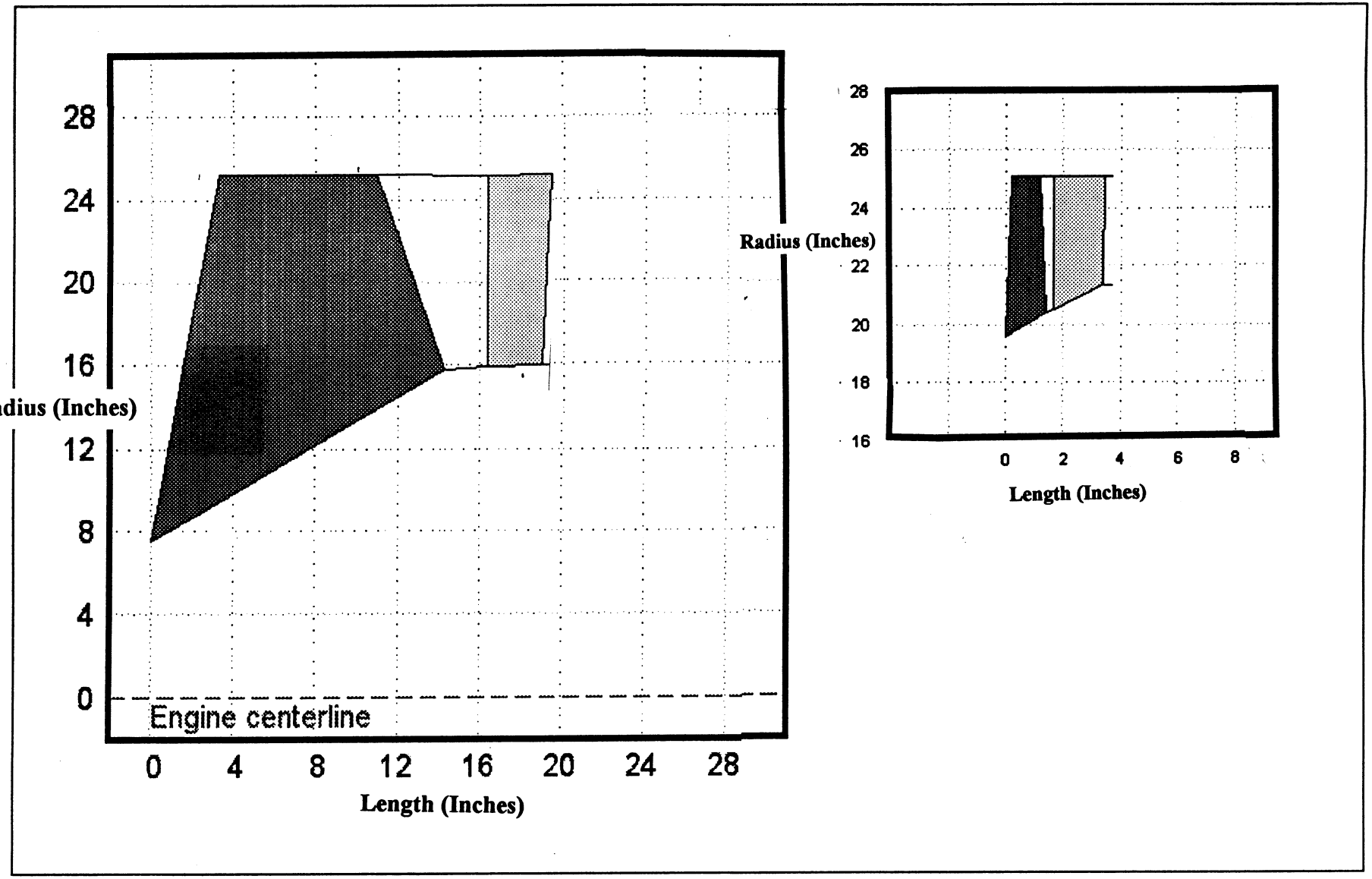

Figure 15. Mid-Size, Single-Spool, Exoskeletal Engine, BPR = 2.0
Fan – Full First Stage & Second Stage Bypass

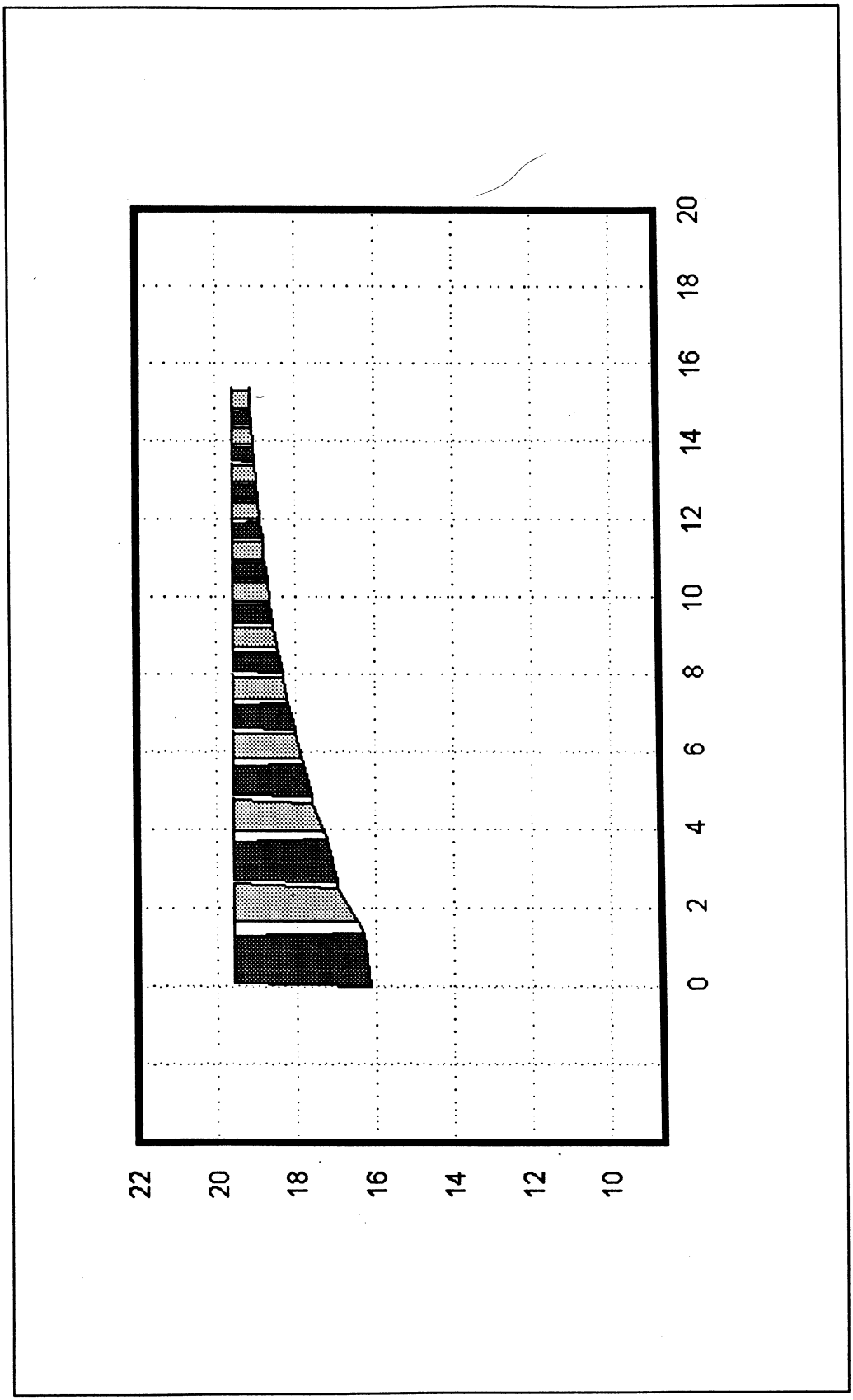

Figure 16. Mid-Size, Single-Spool, Exoskeletal Engine, BPR = 2.0 Core Compressor

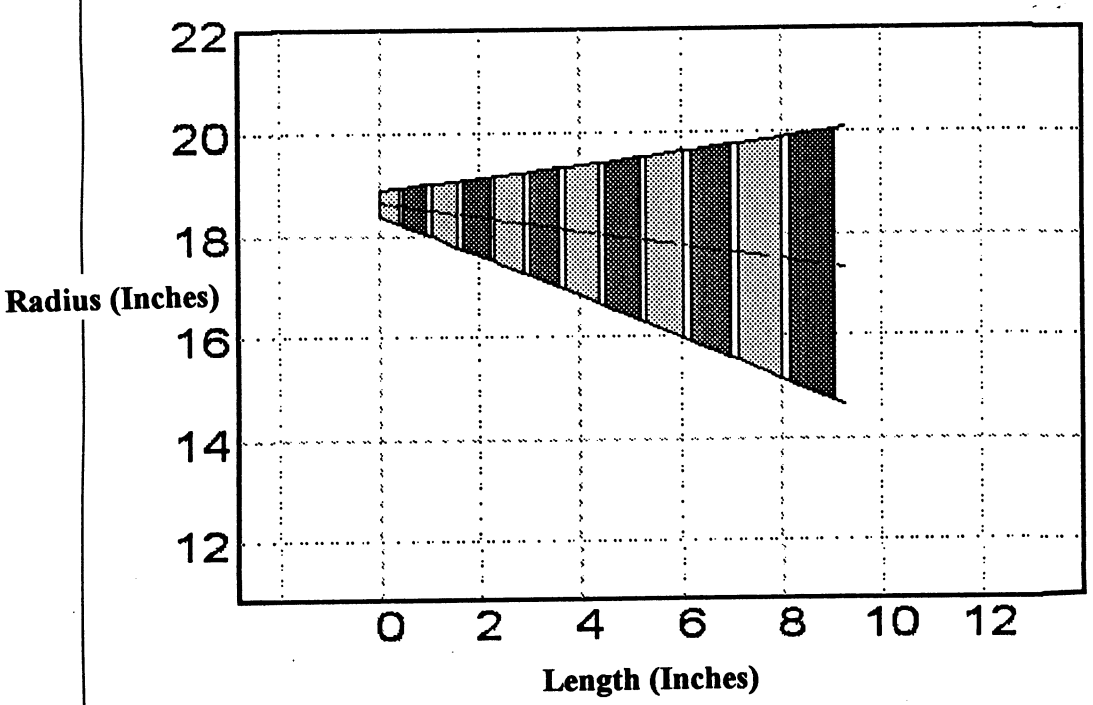

Parameter	
Number of stages	6
Rotational speed (rpm)	7400
Mass flow rate at entry to first vane (lbm/s)	126.0
Δh per stage (Btu/lbm)	68.9
Stage 1 Δh/T	0.022
Inlet flow function ($W\sqrt{T}/P$)	18.38
Stage 1 loading coefficient – ($\Delta h/2U_m^2$)	0.6
AN^2 $_{corr}$	32×10^9
Exit Mach number	0.589
Exit swirl angle (°)	6.36
Exit radius ratio	0.728
Overall pressure ratio	14.40
Overall adiabatic efficiency (%)	82.89

Figure 17. Mid-Size, Single-Spool, Exoskeletal Engine, BPR = 2.0 Cooled Turbine

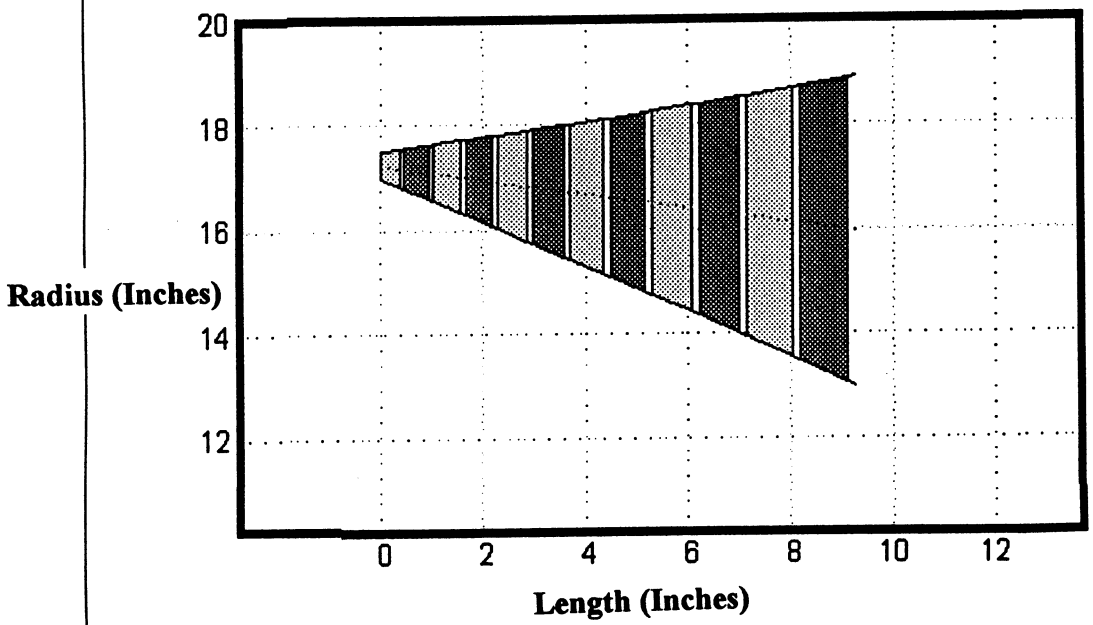

Parameter	
Number of stages	6
Rotational speed (rpm)	7400
Mass flow rate at entry to first vane (lbm/s)	171.6
Δh per stage (Btu/lbm)	58.8
Stage 1 Δh/T	0.020
Inlet flow function ($W\sqrt{T}/P$)	24.08
Stage 1 loading coefficient – ($\Delta h/2U_m^2$)	0.6
AN^2_{exit}	32×10^9
Exit Mach number	0.448
Exit swirl angle (°)	15.5
Exit radius ratio	0.686
Overall pressure ratio	10.93
Overall adiabatic efficiency (%)	94.45

Figure 18. Mid-Size, Single-Spool, Exoskeletal Engine, BPR = 2.0 Uncooled Turbine

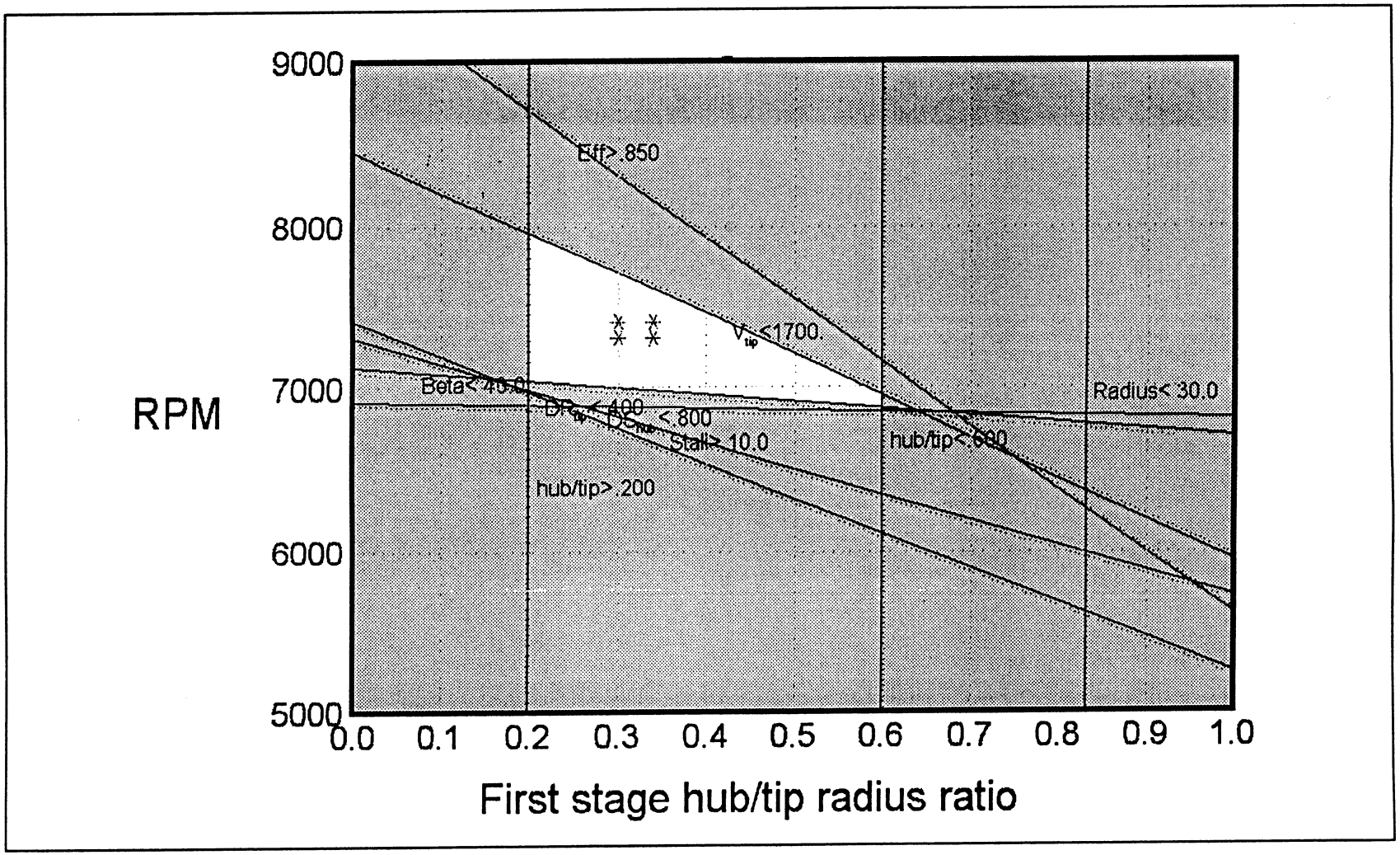

Figure 19. Mid-Size, Single-Spool, Exoskeletal Engine, BPR = 2.0 Design Envelope for the Fan

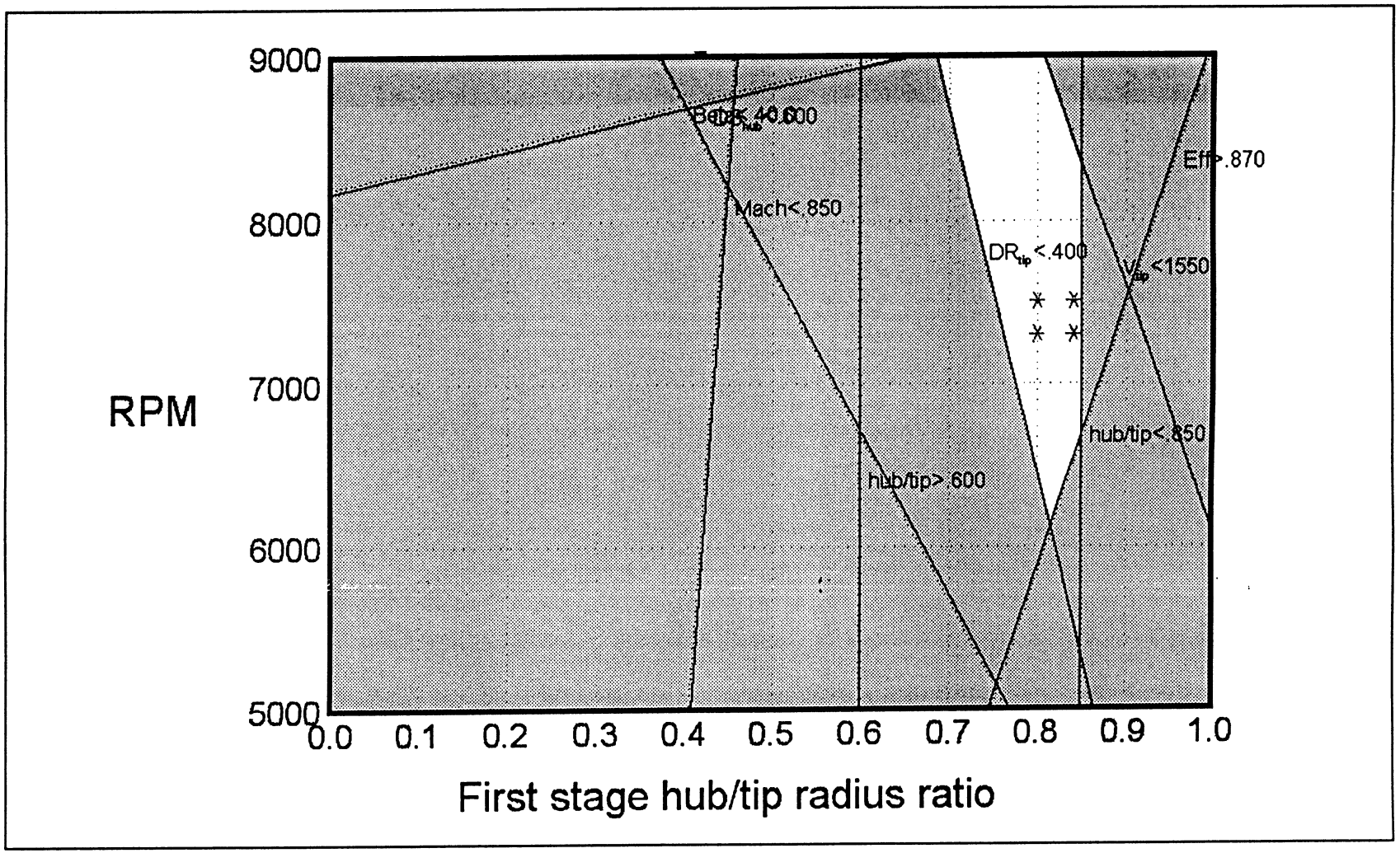

Figure 20. Mid-Size, Single-Spool, Exoskeletal Engine, BPR = 2.0
Design Envelope for the Final Stage of the Core Compressor

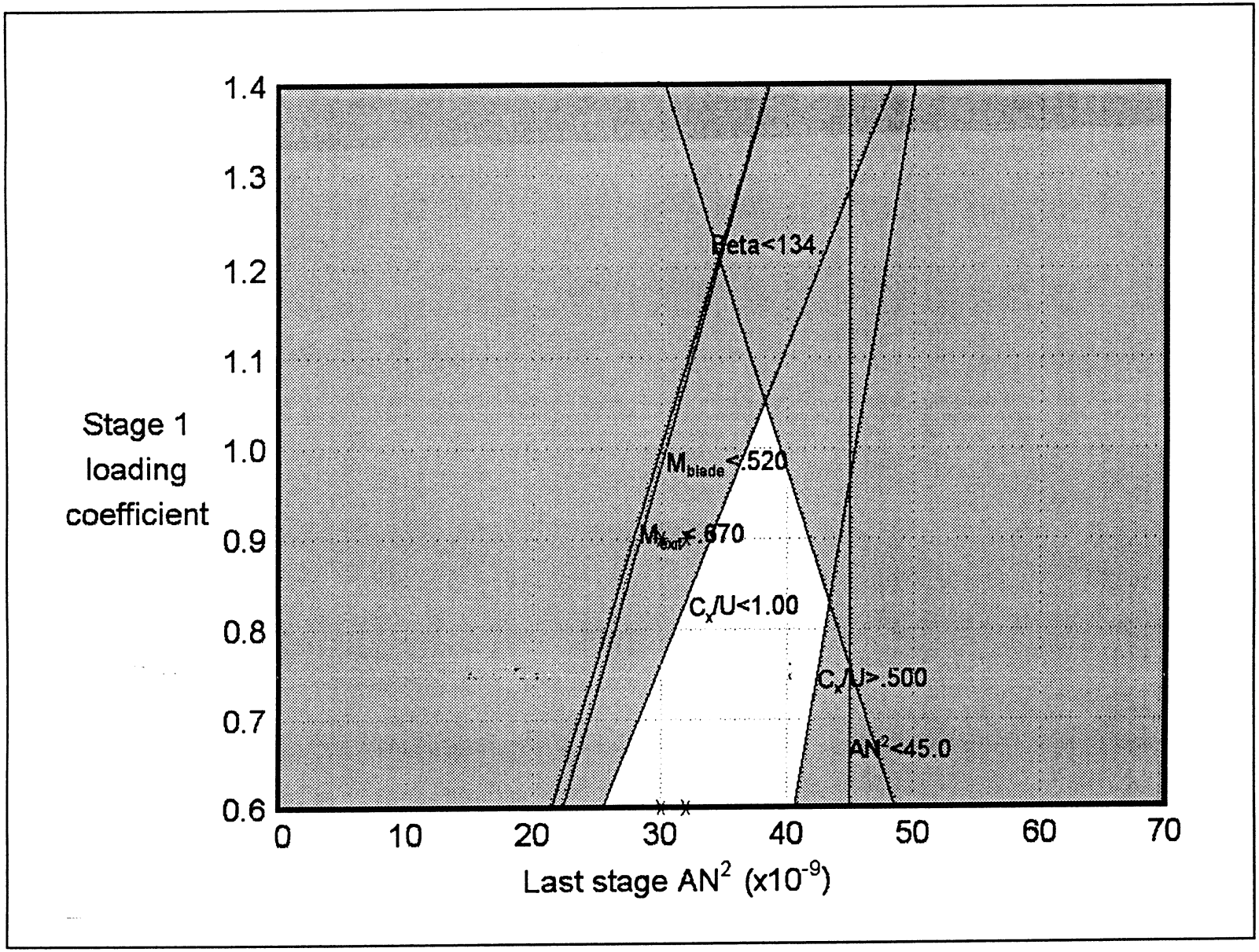

Figure 21. Mid-Size, Single-Spool, Exoskeletal Engine, BPR = 2.0 Design Envelope for the Final Stage of the Uncooled Turbine

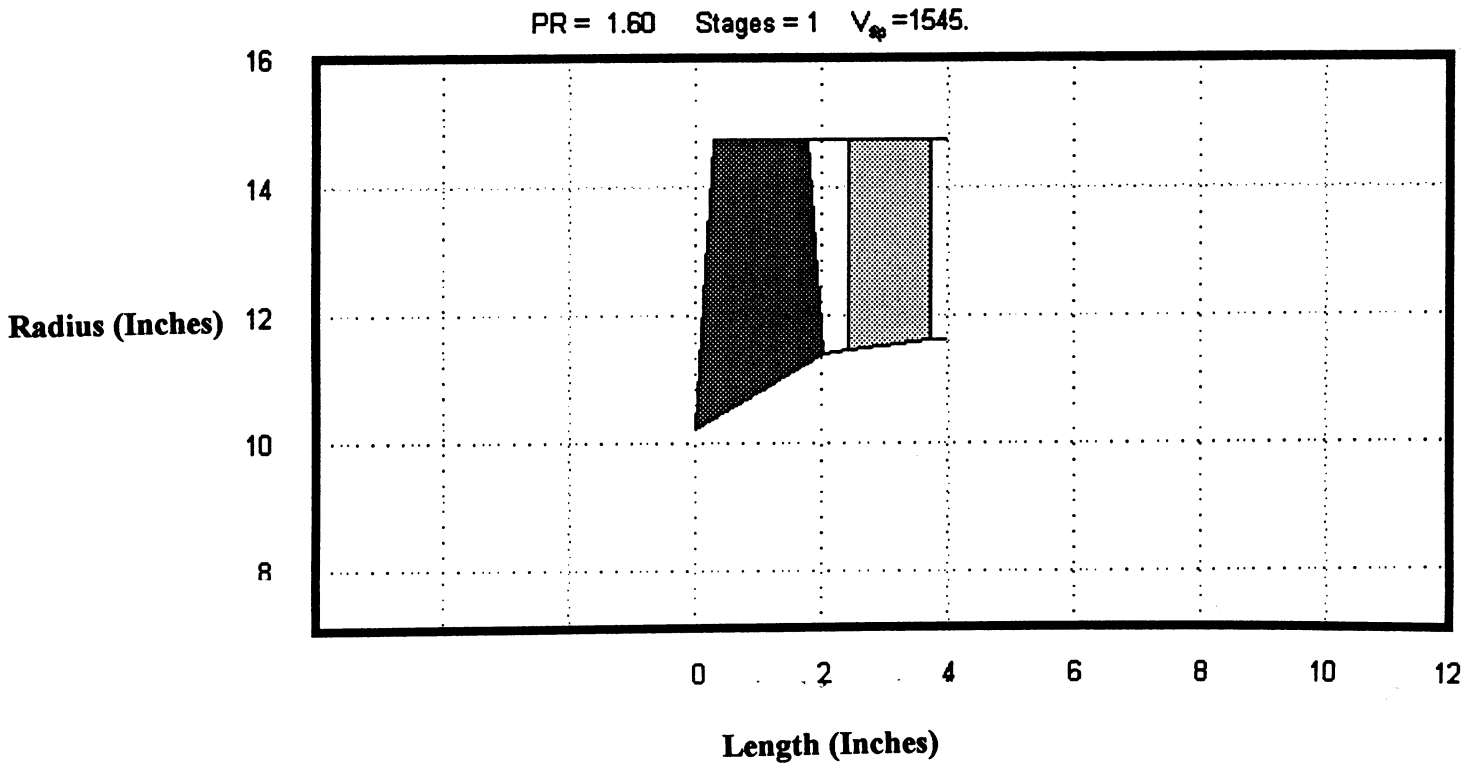

Figure 22. 5,000-lbf Thrust Exoskeletal Turbofan – Fan

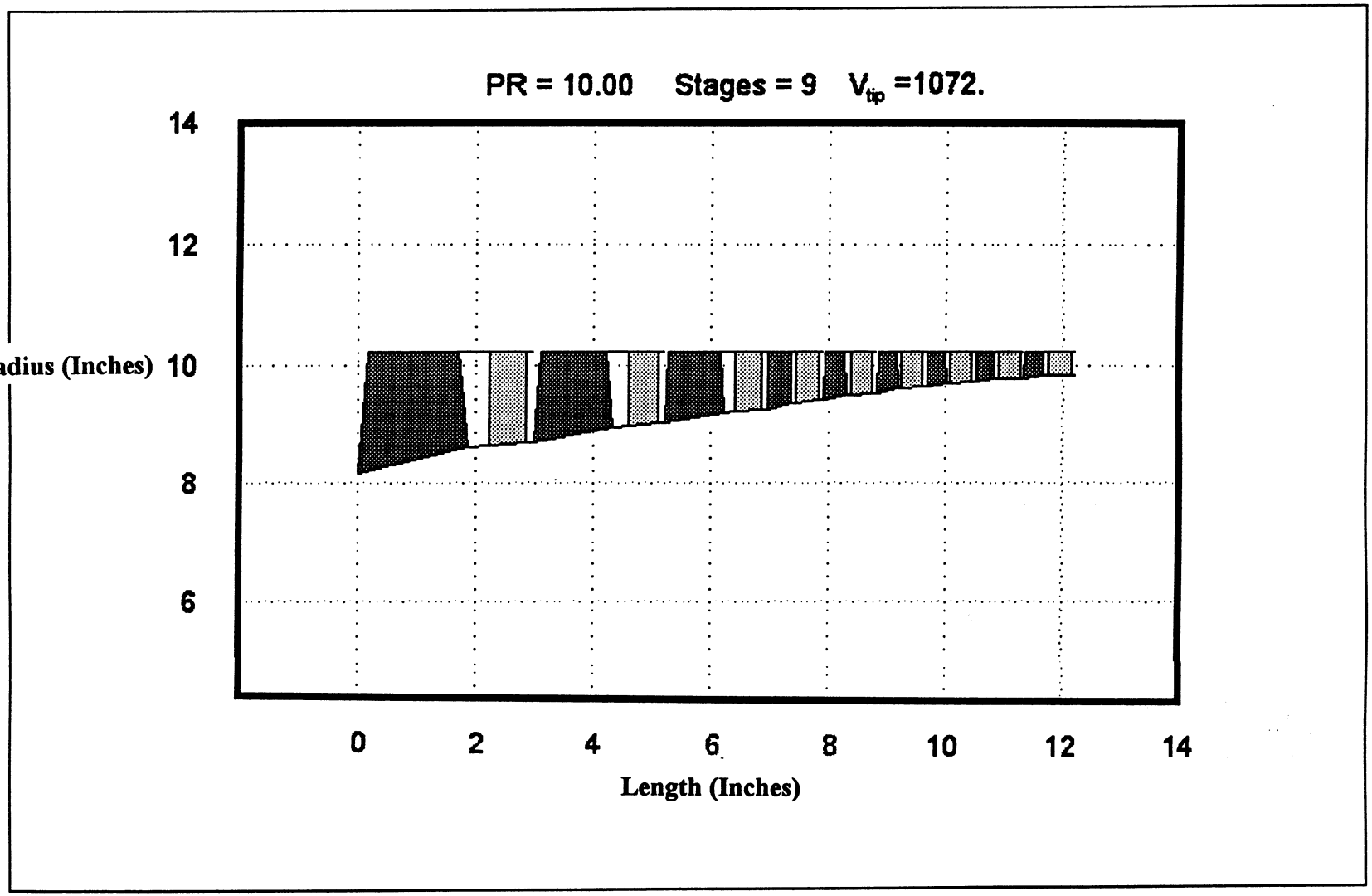

Figure 23. 5,000-lbf Thrust Exoskeletal Turbofan – Core Compressor

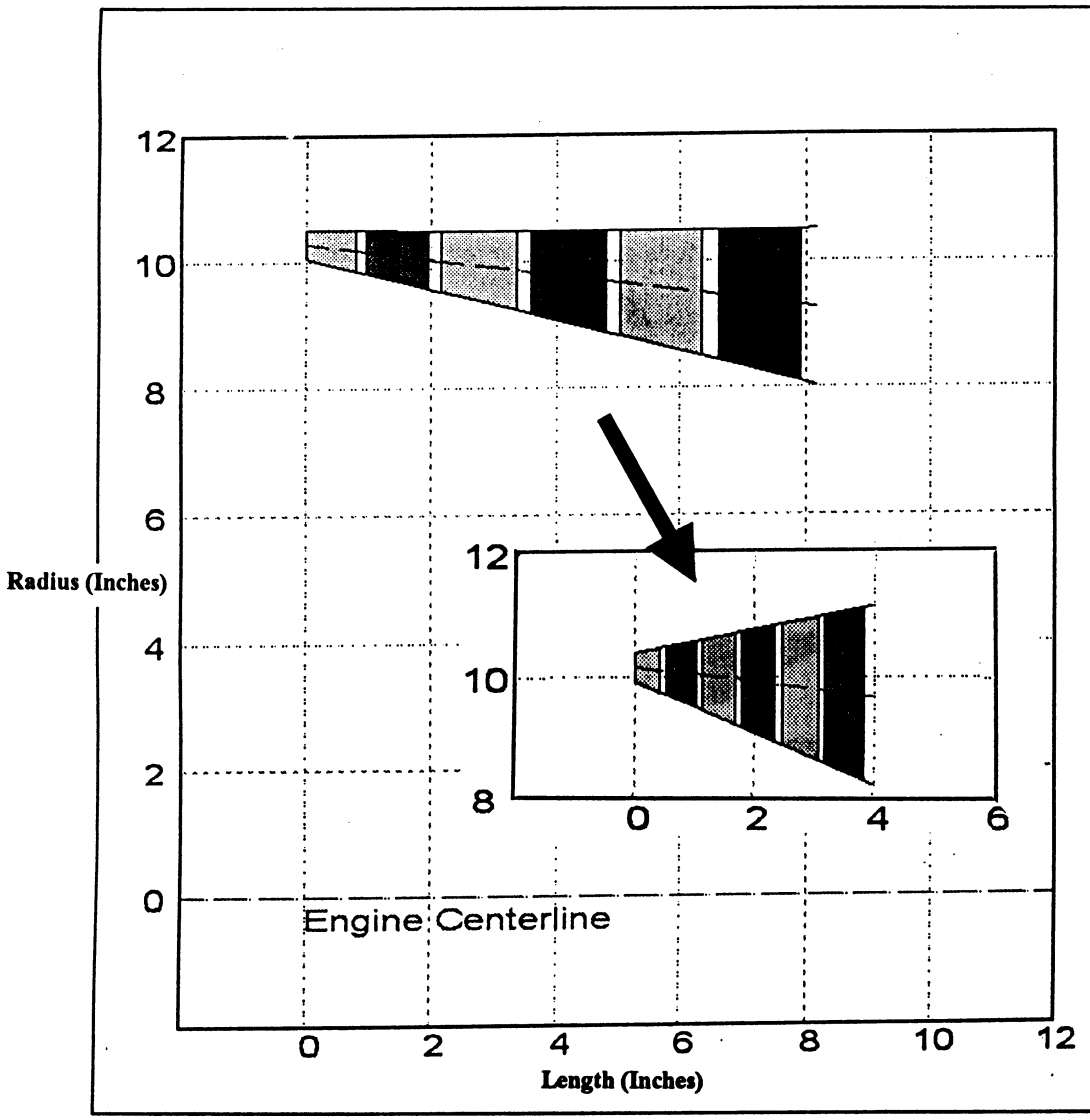

Parameter	
Number of stages	3
Rotational speed (rpm)	12000
Mass flow rate at entry to first vane (lbm/s)	29.38
Δh per stage (Btu/lbm)	80.8
Stage 1 Δh/T	0.029
Inlet flow function ($W\sqrt{T}/P$)	11.09
Stage 1 loading coefficient – ($\Delta h/2U_m^2$)	0.9
AN^2_{exit}	25×10^9
Exit Mach number	0.51
Exit swirl angle (°)	30.9
Exit radius ratio	0.74
Overall pressure ratio	6.011
Overall adiabatic efficiency (%)	90.50

Figure 24. 5,000-lbf Thrust Exoskeletal Turbofan – Cooled Turbine

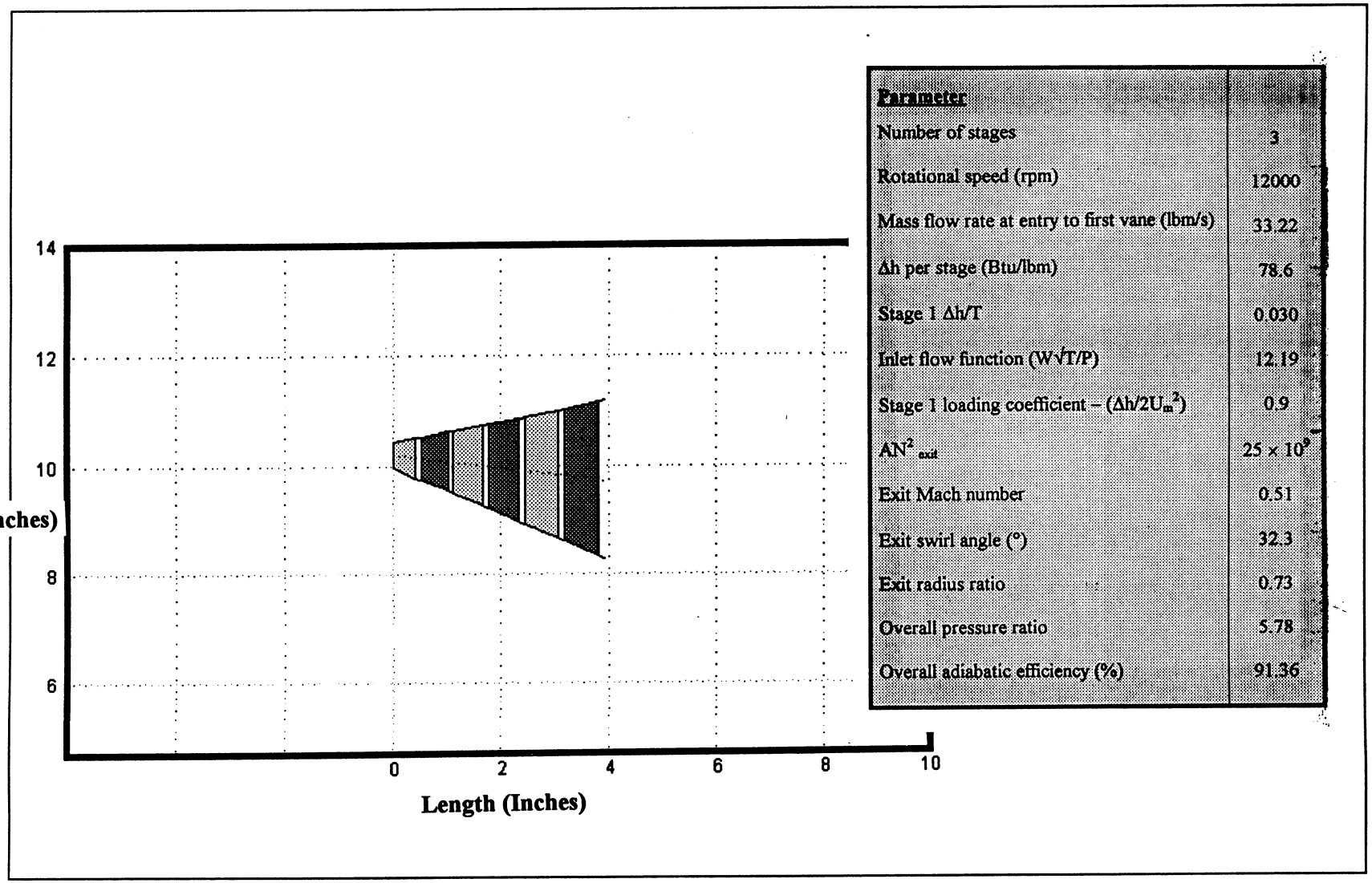

Parameter	
Number of stages	3
Rotational speed (rpm)	12000
Mass flow rate at entry to first vane (lbm/s)	33.22
Δh per stage (Btu/lbm)	78.6
Stage 1 Δh/T	0.030
Inlet flow function ($W\sqrt{T}/P$)	12.19
Stage 1 loading coefficient – ($\Delta h/2U_m^2$)	0.9
AN^2 exit	25×10^9
Exit Mach number	0.51
Exit swirl angle (°)	32.3
Exit radius ratio	0.73
Overall pressure ratio	5.78
Overall adiabatic efficiency (%)	91.36

Figure 25. 5,000-lbf Thrust Exoskeletal Turbofan – Uncooled Turbine

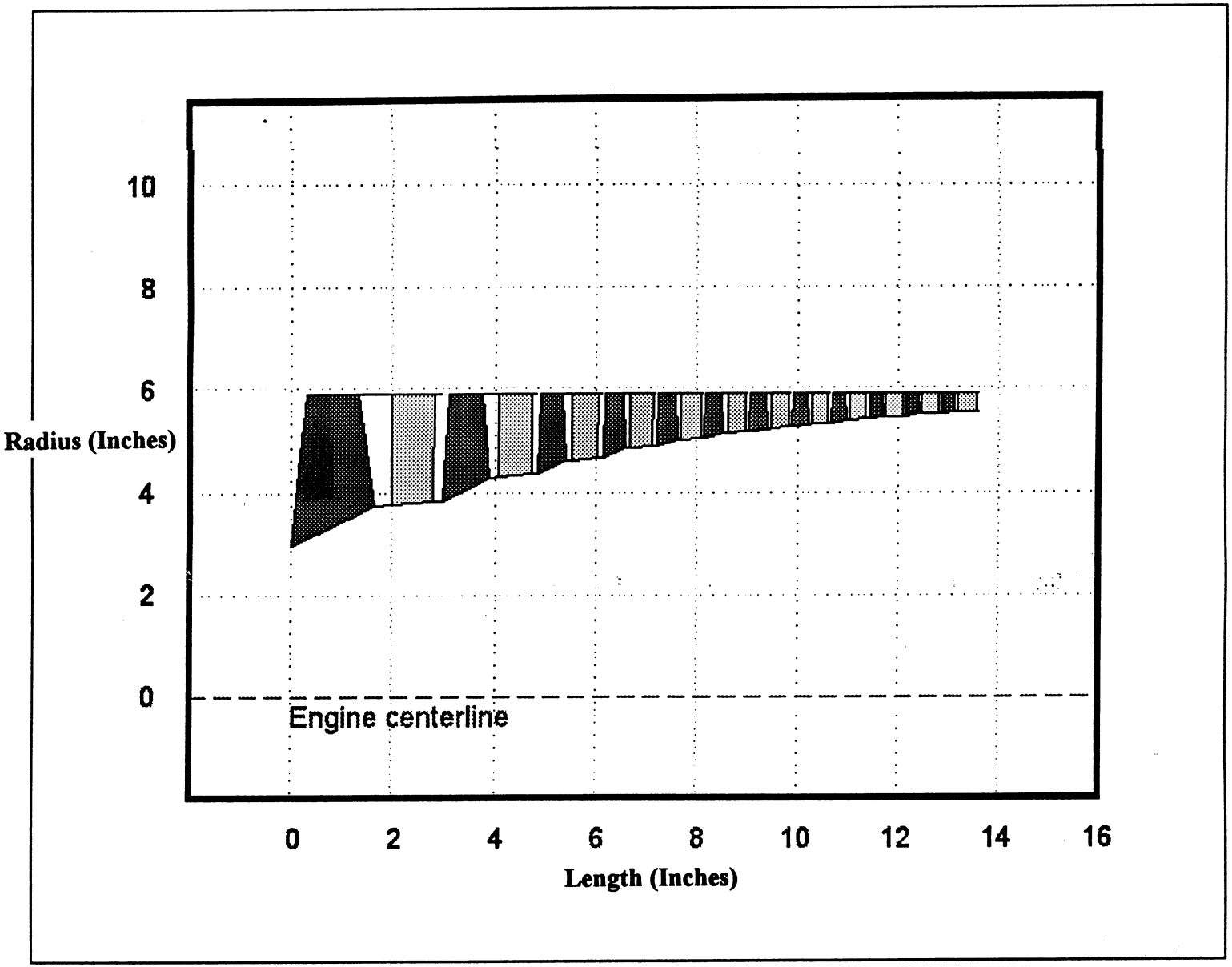

Figure 26. 2,000-lbf Thrust Exoskeletal Turbojet: Compressor

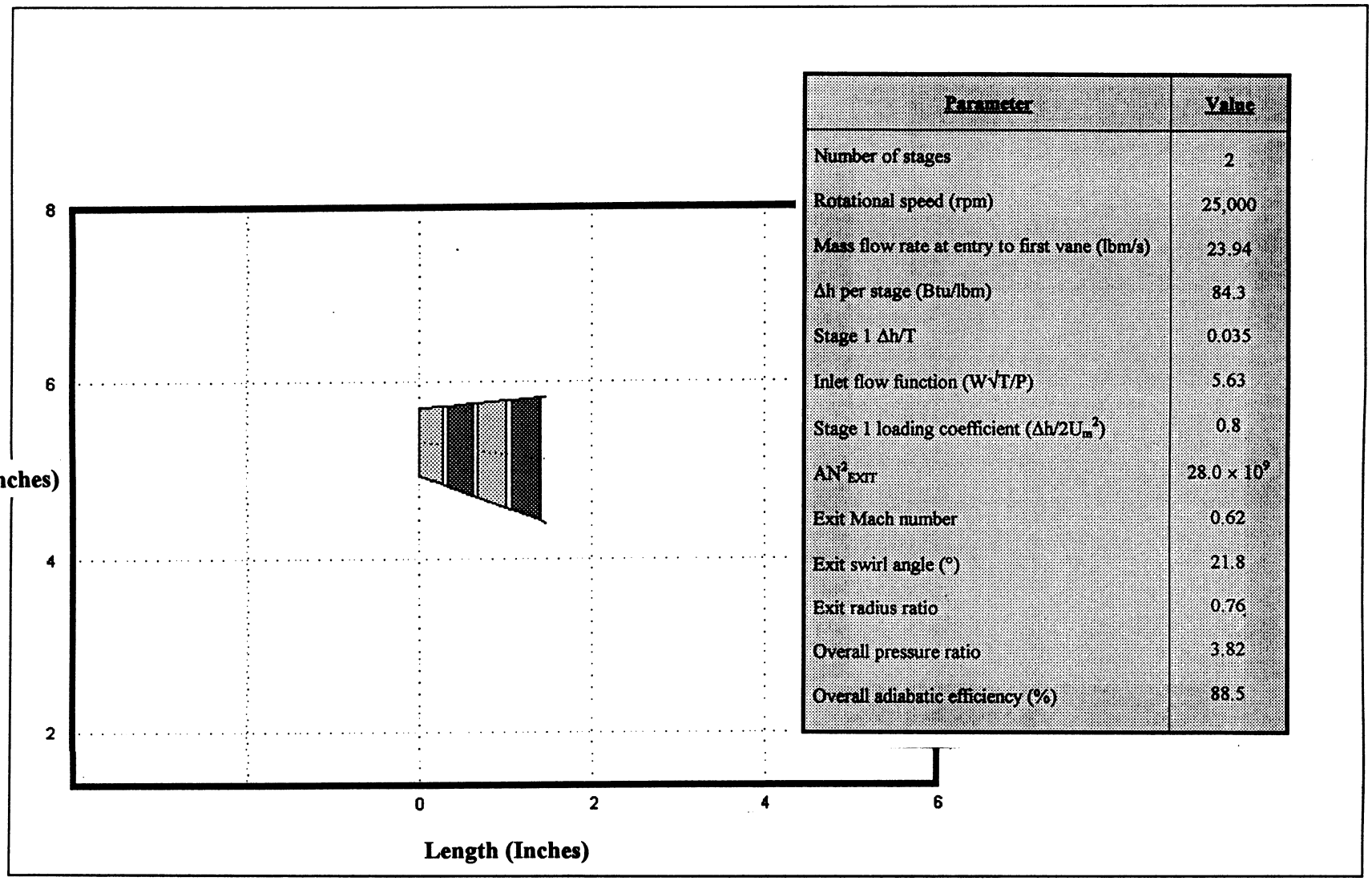

Parameter	Value
Number of stages	2
Rotational speed (rpm)	25,000
Mass flow rate at entry to first vane (lbm/s)	23.94
Δh per stage (Btu/lbm)	84.3
Stage 1 Δh/T	0.035
Inlet flow function ($W\sqrt{T}/P$)	5.63
Stage 1 loading coefficient ($\Delta h/2U_m^2$)	0.8
AN^2_{EXIT}	28.0×10^9
Exit Mach number	0.62
Exit swirl angle (°)	21.8
Exit radius ratio	0.76
Overall pressure ratio	3.82
Overall adiabatic efficiency (%)	88.5

Figure 27. 2,000-lbf Thrust Exoskeletal Turbojet: Turbine (Uncooled)

REPORT DOCUMENTATION PAGE

Form Approved
OMB No. 0704-0188

1. AGENCY USE ONLY (*Leave blank*)	2. REPORT DATE	3. REPORT TYPE AND DATES COVERED
	November 2001	Final Contractor Report

4. TITLE AND SUBTITLE

Exoskeletal Engine Concept: Feasibility Studies for Medium and Small Thrust Engines

5. FUNDING NUMBERS

WU–714–01–10–00
NAS3–27326

6. AUTHOR(S)

Ian Halliwell

7. PERFORMING ORGANIZATION NAME(S) AND ADDRESS(ES)

Modern Technologies Corporation
Propulsion Systems Group
7330 Lucerne Drive, Suite 206
Middleburg Heights, Ohio 44130

8. PERFORMING ORGANIZATION REPORT NUMBER

E–13132

9. SPONSORING/MONITORING AGENCY NAME(S) AND ADDRESS(ES)

National Aeronautics and Space Administration
Washington, DC 20546–0001

10. SPONSORING/MONITORING AGENCY REPORT NUMBER

NASA CR—2001-211322

11. SUPPLEMENTARY NOTES

Project Managers, Christos C. Chamis, 216–433–3252, and Isaiah M. Blankson, 216–433–5823, Research and Technology Directorate, NASA Glenn Research Center, organization code 5000.

12a. DISTRIBUTION/AVAILABILITY STATEMENT

Unclassified - Unlimited
Subject Categories: 07, 37, and 39 Distribution: Nonstandard

Available electronically at http://gltrs.grc.nasa.gov/GLTRS

This publication is available from the NASA Center for AeroSpace Information, 301–621–0390.

12b. DISTRIBUTION CODE

13. ABSTRACT ***(Maximum 200 words)***

The exoskeletal engine concept is one in which the shafts and disks are eliminated and are replaced by rotating casings that support the blades in spanwise compression. Omission of the shafts and disks leads to an open channel at the engine centerline. This has immense potential for reduced jet noise and for the accommodation of an alternative form of thruster for use in a combined cycle. The use of ceramic composite materials has the potential for significantly reduced weight as well as higher working temperatures without cooling air. The exoskeletal configuration is also a natural stepping-stone to complete counter-rotating turbomachinery. Ultimately this will lead to reductions in weight, length, parts count and improved efficiency. The feasibility studies are in three parts. Part 1–Systems and Component Requirements addressed the mechanical aspects of components from a functionality perspective. This effort laid the groundwork for preliminary design studies. Although important, it is not felt to be particularly original, and has therefore not been included in the current overview. Part 2–Preliminary Design Studies turned to some of the cycle and performance issues inherent in an exoskeletal configuration and some initial attempts at preliminary design of turbomachinery were described. Twin-spoon and single-spool 25,800-lbf-thrust turbofans were used as reference vehicles in a mid-size commercial subsonic category in addition to a single-spool 5,000-lbf-thrust turbofan that represented a general aviation application. The exoskeletal engine, with its open centerline, has tremendous potential for noise suppression and some preliminary analysis was done which began to quantify the benefits. Part 3–Additional Preliminary Design Studies revisited the design of single-spool 25,800-lbf-thrust turbofan configurations, but in addition to the original FPR = 1.6 and BPR = 5.1 reference engine, two additional configurations used FPR = 2.4 and BPR = 3.0 and FPR = 3.2 and BPR = 2.0 were investigated. The single-spool 5,000-lbf-thrust turbofan was refined and the small engine study was extended to include a 2,000-lbf-thrust turbojet. More attention was paid to optimizing the turbomachinery. Turbine cooling flows were eliminated, in keeping with the use of uncooled CMC materials in exoskeletal engines. The turbine performance parameters moved much closer to the nominal target values, demonstrating the great benefits to the cycle of uncooled turbines.

14. SUBJECT TERMS

Turbomachinery; Turbofan; Single-spool; Twin-spool; High bypass ratio; Radius ratio effect

15. NUMBER OF PAGES

131

16. PRICE CODE

17. SECURITY CLASSIFICATION OF REPORT	18. SECURITY CLASSIFICATION OF THIS PAGE	19. SECURITY CLASSIFICATION OF ABSTRACT	20. LIMITATION OF ABSTRACT
Unclassified	Unclassified	Unclassified	